Universidade de Aveiro Departamento de Química
2016-2017

INÊS ISABEL NUNES CARAMELO

MECHANOMODULATION OF CHONDROGENIC DIFFERENTIATION OF MESENCHYMAL STEM CELLS

MECANOMODULAÇÃO DA DIFERENCIAÇÃO CONDROGÉNICA DE CÉLULAS ESTAMINAIS MESENQUIMAIS

Universidade de Aveiro
2016-2017
Departamento de Química

INÊS ISABEL NUNES CARAMELO

MECHANOMODULATION OF CHONDROGENIC DIFFERENTIATION OF MSESENCHYMAL STEM CELLS

MECANOMODULAÇÃO DA DIFERENCIAÇÃO CONDROGÉNICA DE CÉLULAS ESTAMINAIS MESENQUIMAIS

Dissertação apresentada à Universidade de Aveiro para cumprimento dos requisitos necessários à obtenção do grau de Mestre em Bioquímica (ramo Métodos Biomoleculares), realizada sob a orientação científica do Doutor Mário Martins Rodrigues Grãos, Investigador Auxiliar da Unidade de Biologia Celular do Centro de Neurociências e Biologia Celular da Universidade de Coimbra e da Professora Doutora Maria do Rosário Gonçalves dos Reis Marques Domingues, Professora Associada com Agregação do Departamento de Química da Universidade de Aveiro.

Um agradecimento especial ao Centro de Neurociências e Biologia Celular da Universidade de Coimbra (CNC-UC) e à Unidade de Investigação de Química Orgânica, Produtos Naturais e Agroalimentares (QOPNA).

CNC
CENTER FOR NEUROSCIENCE AND CELL BIOLOGY
UNIVERSITY OF COIMBRA, PORTUGAL

qopna

Dedico esta dissertação à cidade de Aveiro,

por me ter acolhido e me ter visto crescer nestes últimos 5 anos

O júri

Presidente

Professora Doutora Rita Maria Pinho Ferreira
Professora auxiliar do Departamento de Química da Universidade de Aveiro

Doutora Helena Sofia Esmeraldo de Campos Vazão
Diretora de Laboratório na empresa HeartGenetics

Doutor Mário Martins Rodrigues Grãos
Investigador Auxiliar da Unidade de Biologia Celular do Centro de Neurociências e Biologia Celular da Universidade de Coimbra

Agradecimentos/ Acknowledgments

Em primeiro lugar, gostaria de agradecer ao meu orientador, Doutor Mário Grãos, por toda a orientação científica ao longo deste ano. Esteve sempre do meu lado não só com soluções para os problemas, bem como com novas ideias, entusiasmando-me e incentivando-me a fazer mais e melhor.

Gostaria também de agradecer à minha orientadora institucional, Doutora Rosário Domingues, pelo apoio e por nunca me ter deixado só no decorrer do ano.

Agradeço ainda ao Doutor José Lopes da Silva, professor auxiliar do Departamento de Química da Universidade de Aveiro, porque não sendo eu da área de materiais, me ter ajudado a realizar e a interpretar os ensaios de reologia descritos neste trabalho.

Um agradecimento muito especial às minhas colegas de laboratório, Catarina Domingues, Heloísa Gerardo e Tânia Lourenço. Sem elas, este trabalho não teria sido possível de realizar. Para além de terem sido o meu braço direito na parte prática, alegraram os meus dias neste último ano - fizeram-me sentir em casa e animaram todos os meus "desânimos". Obrigada, do fundo do coração.

Agradeço também à Catarina Rodrigues, Cátia Santa e Sandra Anjo pelos cafés e bons momentos passados nas horas de almoço.

Aos meus pais e irmão, não só pelo apoio durante este último ano, mas pelo apoio em toda a jornada académica. Mesmo longe, confortaram-me e fizeram-me sentir sempre em casa. Agradeço também aos meus avós, tios e padrinhos por toda a preocupação. Com vocês aprendi o significado de família.

Ao meu namorado, Leonardo da Silva, por ser o meu porto de abrigo, em todas as horas, todos os dias. "E soube que era amor para a vida toda"

Às minhas "ex-amigas", por me conseguirem por sempre a rir em todos os momentos com as suas macaquices. Levo-vos para a vida. Ao meu primo João Ana, por me ouvir sempre que preciso. Atura-me desde que nasci e é como um irmão. À minha companheira de boleias, Cláudia Gomes, por tornar as viagens até Cantanhede uma animação. À Sara Moura, por ser uma companheira de estudo e de "desenrascansos".

Quero agradecer ainda aos restantes colegas e amigos que sempre me estenderam uma mão amiga. É bom saber que "ninguém separa o que Aveiro uniu".

A todos estes aqui mencionados, novamente, uma grande obrigada. Se não vos tivesse comigo, nada disto seria possível.

Key words

Mesenchymal Stem Cells; Differentiation; Chondrogenesis; Chondrocytes; Mechanotransduction; Extracellular Matrix; Matrix stiffness

Abstract

Hyaline cartilage is composed by specialized cells named chondrocytes. It is mainly present on joints. Its degeneration is associated not only with ageing, but also with diseases like osteoarthritis and rheumatoid arthritis. Cell therapy is an emerging concept for these diseases. Mesenchymal stem cells (MSCs) can differentiate into various cell lineages, including chondrocytes. Recent studies indicate the significance of how cells are capable of sensing mechanical stimuli and initiate signaling cascades – mechanotransduction. Although the mechanisms are not totally understood, it is known that mechanotransduction plays a significant role during chondrogenesis. "Mechanical memory" is an emerging concept: it has been demonstrated that cells lose their multipotency if cultured on stiff substrates for more than 10 days. Distinct studies using primary cells or MSCs indicate that optimal matrix stiffness for chondrogenic differentiation is between 1 kPa and 320 MPa, depending on cell type and platform used. On the present study, we aimed to elucidate the optimal stiffness for chondrogenic differentiation of MSCs. Various PDMS substrates were produced and characterized by rheology, presenting Young's modulus between 21 kPa and 0.9 kPa. We verified a decreasing tendency on the nucleus area along with substrate softening, suggesting that MSCs were responding to substrate stiffness. To reduce the influence of "mechanical memory", only naïve cells were induced to differentiate. Safranin O (SO) staining revealed that 1 kPa substrate favored cell agglomeration, typical of chondrogenesis. Using fluorescence of this dye, we established a semi-quantitative assay to evaluate chondrogenic differentiation of MSCs. This assay suggests that 1 kPa substrate potentiates chondrogenic differentiation of MSCs. Despite SO assay results need further validation by RT-PCR, preliminary data indicates 1 kPa as the optimal stiffness for chondrogenic differentiation.

Palavras-chave **Células estaminais; Diferenciação; Condrogénese; Condrócitos; Mecanotransdução; Matriz Extracelular; Ridigez da Matriz**

Resumo

A cartilagem hialina, cujas células especializadas são os condrócitos, encontra-se maioritariamente presente nas articulações. A degeneração deste tecido está associada a envelhecimento e a diversas doenças como artrite reumatóide e osteoartrite. Recentemente, tem sido investigada a possibilidade de desenvolver terapias celulares para o tratamento destas patologias, utilizando células estaminais mesenquimais (MSCs). As MSCs têm capacidade para se diferenciar em várias linhagens, incluindo condrócitos, apresentando-se como um dos mais promissores tipos celulares em medicina regenerativa. Nos últimos anos as vias de sinalização iniciadas pelos estímulos mecânicos do meio envolvente – mecanotransdução - tem sido alvo de estudo. Apesar dos mecanismos de diferenciação condrogénica não serem completamente conhecidos, tem-se tornado evidente que a mecanotransdução desempenha um papel crucial neste processo. Foi recentemente demonstrado que as MSCs têm "memória mecânica" e que, se cultivadas por mais de 10 dias num substrato rígido perdem a multipotência. Vários estudos utilizando células primárias ou MSCs apontam a rigidez ótima para diferenciação condrogénica deste 1 kPa até 320 MPa, dependendo do tipo de células e plataforma utilizados. Este estudo propôs-se então a clarificar qual a rigidez ótima para diferenciação condrogénica de MSCs. No presente estudo, foram preparados vários substratos de PDMS e caracterizados por reologia, apresentando módulos de Young que variam entre 21 kPa e 0.9 kPa. A diminuição da área nuclear nos substratos menos rígidos permitiu validar que estes substratos são capazes de induzir um estímulo mecânico. Somente células de baixa passagem foram induzidas a diferenciar diminuir o impacto da memória mecânica. A coloração de Safranin O (SO) permitiu evidenciar que a formação de aglomerados celulares – típica da condrogénese – é favorecida pelo substrato de 1 kPa. Recorrendo à fluorescência deste corante, foi possível estabelecer um método semi-quantitativo para avaliar diferenciação condrogénica de MSCs. Este ensaio indica que o substrato de 1 kPa potencia a diferenciação condrogénica de MSCs. Apesar dos resultados de SO requererem uma validação mais exaustiva por RT-PCR, os resultados preliminares apontam o que a rigidez ótima para diferenciação condrogénica de MSCs é de 1 kPa.

Index

Abbreviations list

A	ACAN	Aggrecan
	AMH	Anti-Muelletian hormone
	3-APTES	3-Aminopropyltriethoxylsilane
	AT	Adipose Tissue
	ATCD5	Chondrogenic cell line derived from teratocarcinoma AT805
B	BM	Bone Marrow
	BMP	Bone morphogenetic protein
C	C/EBPα	CCAAT/enhancer-binding protein alpha
	CBP/p300	cAMP response element-binding protein binding protein and its paralog p300
	CDK	Cyclase-dependent kinases
	CDM	Chondrogenic differentiation medium
	cDNA	Complementary DNA
	CFU-F	Colony forming unit-fibroblast
	CILIP	Cartilage Intermidiate Zone Matrix Protein
	Col2a1	Collagen type II
	Col9a1	Collagen type IX
	Col11a	Collagen type XI
	CSPC	Cartilage stem/progenitor cells
	CZ	Calcified Zone
D	ddH_2O	Double-distillated water
	DMSO	Dimethylsulfoxide
	DZ	Deep zone

E	E	Young's Modulus
	ECM	Extra Cellular Matrix
	ERK	extracellular signal–regulated kinases
F	F-actin	Filamentous actin
	FA	Focal adhesions
	FAK	Focal adhesion kinase
	FBS	Fetal Bovine Serum
	FN	Fibronectin
G	G′	Elastic/storage modulus
	G′′	Viscous/loss modulus
	GAG	Glycosaminoglycans
	GDFs	Growth and differentiation factors
	GF	Growth factor
	GSK3β	Glycogen synthase kinase 3
	GT	Generation time
	GTP	Hydrolyze guanosine triphosphate
H	HA	Hyaloronic acid
	HC	Hyaline Cartilage
	HS	Heparan sulfate
	hMSC	Human Mesenchymal Stem cells
I	ICAP1	Integrin beta-1-binding protein 1
	IGF-1	Insulin-like growth factor 1
	ILK	Integrin-linked kinase

M	MAPK	Mitogen-activated protein kinase
	MEM	Minimum Essential Medium
	MZ	Middle zone
	MLC	Myosin light chain
	MLCK	Myosin light-chain kinase
	MMP	Matrix metalloproteinases
	MPCs	Bone marrow mesenchymal progenitor cells
	MRE	Magnetic resonance elastography
	MSCs	Mesenchymal Stem Cells
L	LPL	Lipoprotein lipase
O	OA	Osteoarthritis
P	PBS	Phosphate buffered saline
	PCR	Polymerase chain reaction
	PD	Population doubling
	PDMS	Polydimethylsiloxane
	PPAR	Peroxisome proliferator-activated receptor gamma
	PM	Proliferation Medium
	PRG4	Lubricin
R	RA	Rheumatoid Arthritis
	Rac1	Ras-related C3 botulinum toxin substrate 1
	RhoA	Ras homolog gene family, member A
	ROCK	Rho-associated protein kinase
	RT-PCR	Real time - Polymerase chain reaction
	Runx2	Runt-related transcription factor 2

S	SB	Subchondral bone
	sGF	Soluble growth factor
	SMC	Smooth muscle cell
	SO	Safranin O
	Sox	SRY-type high-mobility-group
	SZ	Superficial zone
	SZP	Superficial zone protein
T	TAK1	Transforming growth factor beta-activated kinase 1
	TAZ	Transcriptional coactivator with PDZ-binding motif
	TCPs	Tissue culture polystyrene
	TGFβ	Transforming growth factor beta
	TNC	Total number of cells
U	UC	Umbilical cord
	UCT	Umbilical Cord Tissue
V	Vav1	Vav guanine nucleotide exchange factor 1
Y	YAP	Yes-associated protein

1. Introduction

1. Introduction

1.1 Cartilage characteristics and associated diseases

Cartilage is a specialized tissue that can be divided into three types: hyaline, fibrous and elastic [1]. Fibrous cartilage is the less elastic, usually related to zones where forces applied are harder, such as the knee or vertebral joints. Elastic cartilage has more flexible properties and it is often present in specific zones, like the external ear. Hyaline cartilage (HC) is mainly associated to bone development, growth, repair and articular joints. Here, HC coats the edges of coupled bones, creating a slot filled with synovial fluid facilitating transmission of loads and diminishing friction [2]. In addition, HC lacks blood, lymphatic vessels, or nerves.

Chondrocytes are specialized cartilage cells, confined in lacunae and encircled by the extracellular matrix (ECM), responsible for maintaining and repairing the ECM [1,3]. Water, collagen, and proteoglycans predominantly compose cartilaginous ECM. Together, these elements distribute chondrocytes sparsely and retain water. Water is mainly present between collagen fibers and contributes to its gel-like properties, enabling HC to retake its shape after compression. Collagen type II constitutes 90-95% of all cartilaginous ECM collagen and is responsible for maintaining the sturdy structure. Collagen types I, IV, V, VI, IX, and XI are also present, but in a minor fraction. Despite constituting only 10-15% of the ECM, proteoglycans are essential for a healthy joint function, since they provide HC both endurance and flexibility characteristics. Aggrecan (ACAN) is the most abundant proteoglycan. Proteoglycans are stabilized on the ECM by hyaluronan [4]. This complex is responsible to maintain cartilage osmotic properties (Figure 1).

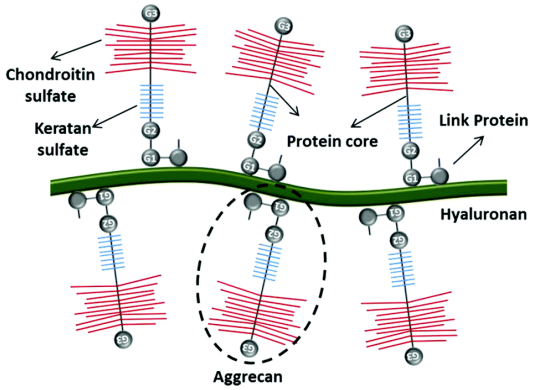

Figure 1 – **Organization of hyaluronan on cartilage ECM**. Hyaluronan forms a complex, mediated by adapter proteins, with proteoglycans to stabilize these proteins on the ECM and maintain homeostasis [4].

HC is organized into three distinct zones with different functions: superficial, middle and deep zones (Figure 2) [5]. The superficial zone (10-20% of total volume) is composed by parallel to surface collagen type I fibers and flattened chondrocytes at high density. It is responsible for lubrication and protection of deeper zones [2,5]. The middle zone (40-60% of total volume) has thicker obliquely organized collagen fibers, proteoglycans and spherical chondrocytes. It is responsible to resist deformation. Finally, the deep zone (30% of total volume) endures compressive forces caused by movements of the body and transmit it to the bone. Here, chondrocytes are hypertrophic, exhibit large diameters [6], collagen fibers are oriented perpendicular to the surface and are thicker than in the middle zone [2,5]. Moreover, middle and deep zones express prominent levels of proteoglycans enabling it to bear compressive forces. Also, collagen types II and IX are more prevalent on these zones. The subsequent zone is a calcified layer responsible for connecting cartilage to the bone. These characteristics grant specific zone stiffness [7]. Stiffness increases with profundity: superficial zone has low matrix stiffness,

around 80 kPa; middle zone stiffness is near 2.1 MPa, deep zone is estimated to be 320 MPa and calcified zone is about 5.6GPa.

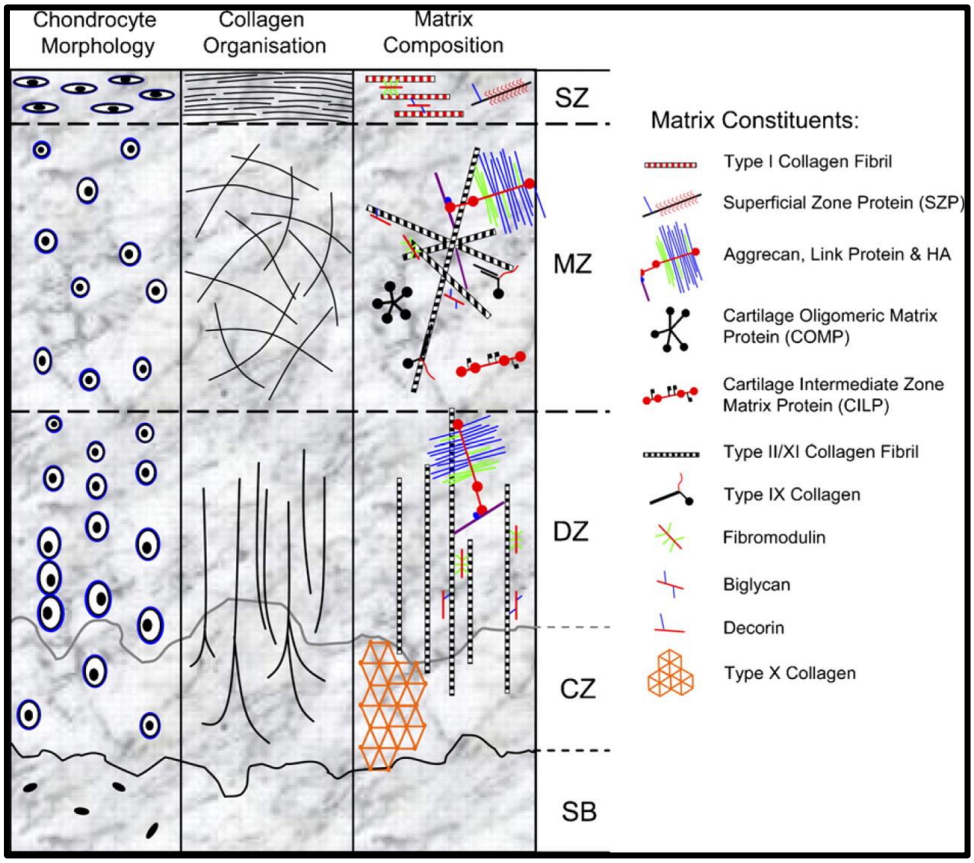

Figure 2 – **Articular cartilage schematic cross-sectional representation [5]**. Superficial zone (SZ) is predominantly composed by flattened chondrocytes and collagen type I, whose fibrils are parallel to the surface [2,5]. These fibrils are parallel to the surface. On the middle zone (MZ), spherical chondrocytes are dispersed between the oblique collagen fibers. Additionally, collagen is thicker and perpendicular to the surface on the deep zone (DZ). Here, chondrocytes are hypertrophic. Middle and deep zones express higher levels of collagen type II and IX and proteoglycans. Calcified zone (CZ) connects cartilage and the bone (SB).

Zonal organization is achieved by differential secretion of specific biomolecules to the extracellular matrix by chondrocytes [8,9]. Superficial zone is maintained by the presence of transforming growth factor (TGF)-β1 and bone morphogenetic protein (BMP)-7, whereas middle and deep zones are maintained by TGF-β1 and insulin-like growth factor (IGF)-1. This leads to differences on intracellular signaling, and consequently differential expression of zone-specific chondrogenic

markers. Particularly, chondrocytes of superficial zone secrete superficial zone protein (SZP), also known as lubricin, a mucinous protein present on synovial fluid [8]. On middle and deep zones chondrocytes express higher levels of aggrecan (ACAN), glycosaminoglycans (GAG) and collagen type II (Col2a1), when compared to superficial zone [9,10]. Middle zone chondrocytes express Cartilage Intermediate Zone Matrix Protein (CILP) [5]. Also, deep zone chondrocytes express runx2, a transcription factor needed for endochondral ossification during bone repair [6]. The zonal differential secretion and/or expression described agrees with the characteristics of the cartilaginous zones — chondrocytes of superficial zones maintain lubrication, while chondrocytes of deeper zones synthetize proteoglycans to tolerate stronger forces.

Ageing alters ECM characteristics [11]. Hydration of the ECM and proteoglycan aggregates decreases with age, diminishing joint lubrication. Besides, chondrocytes migrate into inner layers and concentrate on the deep zone. Together, these modifications reduce HC ability to resist to compressive forces and movements between bones are hampered.

There are innumerous diseases that affect articular cartilage [12,13]. Osteoarthritis (OA) and rheumatoid arthritis (RA) are good examples of diseases that impair the homeostasis of joints. OA is characterized by a progressive degeneration of articular cartilage whose mechanisms and causes are not completely understood [12]. Remodeling and sclerosis are usually associated. It can be idiopathic or secondary (triggered by other diseases, such as neurologic or metabolic disorders). RA is an autoimmune disease that results in chronic inflammation [14]. This disease is associated with the destruction of cartilage, mainly mediated by “aggressive” fibroblast-like synoviocytes [13]. Physiologically, these cells are responsible for maintaining synovial fluid and ECM. In case of disease, they activate innate and adaptive immune system, attracting immune cells to the synovial fluid. Thus, the

balance between proteases and their inhibitors is impaired, which stimulates cartilage erosion and promotes chondrocyte catabolism, resulting in joint injury [14].

Cartilage regenerative capacity is currently an important biomedical challenge and a goal that will have a high impact on patient's quality of life. Hence, several strategies are currently being pursued with that objective in mind. Recently, a cartilage stem/progenitor cells (CSPCs) population was identified on cartilage [15]. These cells show a great chondrogenic potential, suggesting at least some regenerative capacity. Possibly in the future, a more exhaustive study of these cells will help to develop a more effective cell therapy. Currently, injection of autologous chondrocytes is an innovative treatment option for RA, OA and other cartilage diseases [16]. However, the literature indicates that when cultured in monolayer, chondrocytes de-differentiate, hampering cell expansion [17]. Recent studies indicate a promising future for cell therapy using mesenchymal stem/stromal cells (MSCs) for RA and OA, since they have the ability to modulate inflammation while undifferentiated cells [18,19] and have been documented to have the ability of differentiating along the chondrogenic lineage [20]. Therefore, MSC therapy is a promising alternative with these two distinct targets, which could possibly increase treatment efficiency. In fact, there are already ongoing clinical trials with MSCs for OA [19]. Despite preliminary promising results, studies point that efficiency of treatment could probably increase if cells where guided toward a specific cell lineage. Matrices, scaffolds and/or adequate adjuvants, such as appropriate growth factors administered along with MSCs, might be the key to increase treatment success rate.

Hence, optimizing culture conditions for the proliferation and subsequent chondrogenic differentiation of MSCs is a present-day need, allowing in the future that MSCs could be used for regenerative therapy in cartilage diseases, ageing,

degeneration and possibly bone repair. In this present study, we aim to define an optimal substrate for chondrogenic differentiation of MSCs *in vitro*.

1.2. Mesenchymal stem cells can differentiate into chondrocytes

Human mesenchymal stem (or stromal) cells (hMSC) are multipotent cells present not only in extra-embryonic tissues, like the umbilical cord tissue — UCT (also known as Wharton's jelly (Figure 3)) — and placenta, but also in adult tissues like the bone marrow (BM) - where MSCs were first identified - or adipose tissue (AT) [21]. These cells have colony forming unit-fibroblast (CFU-F) capacity, suggesting that they are capable of proliferating and forming colonies, similar to fibroblasts behavior [22].

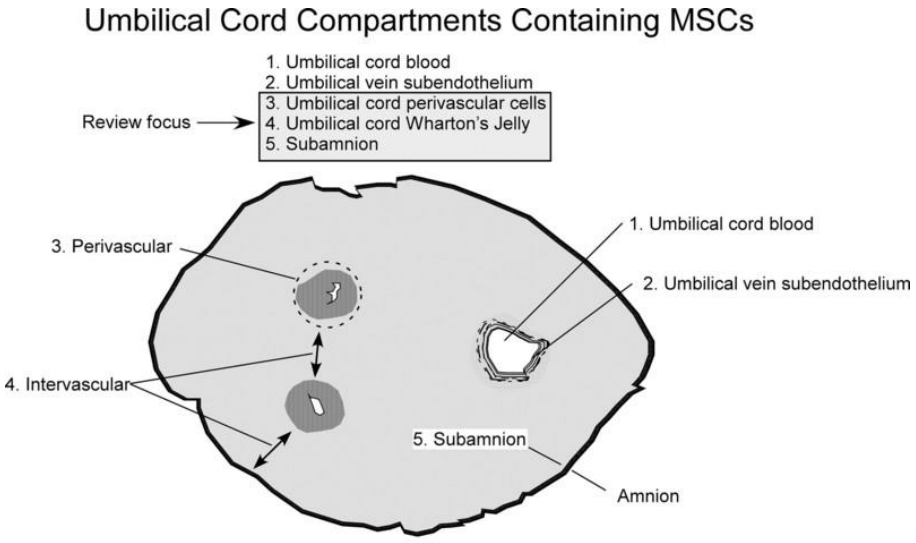

Figure 3 - **Umbilical cord schematic representation.** MSCs can be isolated from the Wharton's Jelly (zone 4) [21]

MSCs present a set of obligatory surface markers (CD73, CD90 and CD105) and lack the expression of others (CD45, CD34 and CD14 or CD19 and HLA-DR) [20]. Moreover, they have the ability not only to proliferate extensively but also to differentiate *in vitro* into osteocytes (bone cells), chondrocytes (cartilage cells) and adipocytes (fat cells). MSCs can also differentiate into other cellular types like cardiomyocytes (heart muscle cells) and hepatocytes (liver cells) [23,24]. Although the differentiation mechanisms are not completely understood, during the past years it has become clear that apart from soluble biomolecules (like growth/differentiation factors), the matrix elasticity, cell adhesion and cell shape are also able to trigger different signaling cascades and modulate differentiation towards distinct lineages [25,26].

Soluble growth factors (sGFs) play a key role in initiating differentiation signaling cascades in mesenchymal stem cells (MSCs). Transforming growth factor β (TGFβ) has three isoforms (1, 2 and 3) and it is involved in many cellular processes, like proliferation, apoptosis, cell migration and adhesion [27]. Recent studies asserted that TGFβ3 as an essential element on chondrogenesis and myogenesis [28,29]. Binding of TGFβ3 to receptor type I recruits type II receptor, which phosphorylates GS-domain of receptor I and activates the dimer (Figure 4) [30]. This dimer recruits and phosphorylates SMAD2 and SMAD3 complex. Instead, binding of BMPs (bone morphogenetic proteins), GDFs (growth and differentiation factors) or AMH (anti-Muellerian hormone) to the receptor recruits SMAD1, SMAD5 and SMAD8. Both pathways induce the formation of a complex with SMAD4, which is capable of binding DNA and regulate the expression of transcription factors. Furthermore, it has also been documented that phosphorylated SMAD3, specifically MH2 domain, forms a complex with SOX9 (SRY-type high mobility group box 9). Also, this complex requires CBP/p300 (cAMP response element-binding protein binding protein and its paralog p300), a protein with histone acetyltransferase

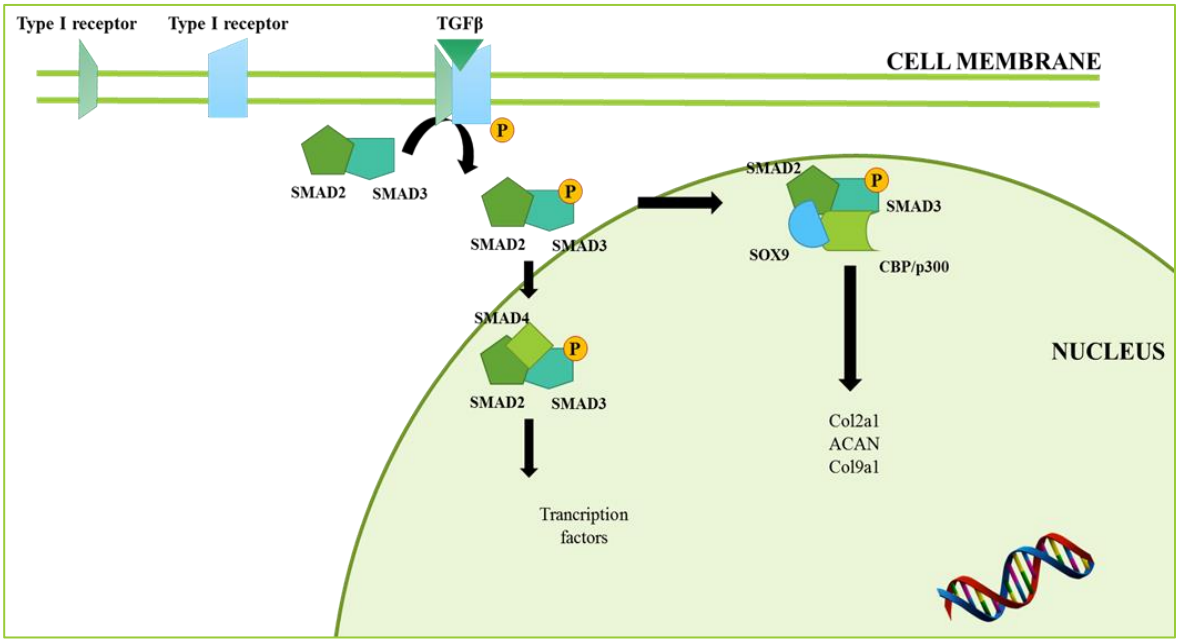

Figure 4 - **Signaling pathway of TGFβ during chondrogenesis, mediated by the Smad2/3 complex**. Binding of TGF activates the dimer, which phosphorylates Smad2/3 complex [30]. Then, this complex can bind to Smad4 and target different transcription factors – generic pathway. On chondrogenic pathway, Smad2/3 forms a complex with Sox9 and CBP/p300 [31], enabling it to move into the nucleus and target specific chondrogenic genes, as Col2a1, ACAN and Col9a1 [33-35].

activity, as a co-activator [31]. Sox9 cooperates with L-SOX5 and SOX6 to activate target genes [32]. Particularly, SOX9 has a DNA-binding domain that targets *Col2a1* gene, a gene that encodes type II collagen, one of the most abundant component of cartilaginous matrix [33,34]. It also binds to other cartilaginous specific genes, such as collagen type IX and XI (*Col9A1, Col11A*) and aggrecan [35].

Moreover, TGFβ also primes MAPK signaling pathway [36]. It can be subdivided into p38 and ERK-1 pathways that promote and repress chondrogenesis, respectively. Although p38 signaling during chondrogenesis is widely accepted, ERK1/2 is controversial, since its inhibition has different effects on distinct cell lines: on MSCs does not influence differentiation while on ATCD5 cells— a mouse teratocarcinoma chondrogenic cell line that is widely use to study chondrogenic differentiation — it positively influences differentiation [37,38]. Possibly, these differences are due to the coordinated and differential activity of p38 and ERK1/2

signaling pathways during chondrogenesis, documented on bone marrow mesenchymal progenitor cells (MPCs) [36]. Besides, MAPK pathway also modulates cell adhesion molecules expression, as N-cadherin and integrin α5β1, known to be important during chondrogenesis. As a conclusion, TGFβ3 is an essential factor for triggering chondrogenic differentiation of MSCs.

MSCs respond to a large variety of biomolecules of the ECM. Various combinations of materials have been tested to induce chondrocyte differentiation [39]. In fact, a study revealed that pellet cultures – 3D cultures - of MSCs express higher levels of chondrogenic markers (*Col2A1*, *Sox9* and *ACAN*) when differentiated in the presence of TGFβ3 and heparan sulfate (HS) [40]. In fact, it was shown that HS enhanced TGFβ3 signaling and Smad2/3 expression when compared to control conditions. This study also documented that there were no differences on the expression of TGFβ receptors, suggesting that HS possibly favors the binding ratio of TGFβ to receptors. Another study stated that hyaluronic acid (HA) 3D hydrogel is the one that most potentiates chondrogenesis of adipose stromal derived cells, when compared to heparan-sulfate and chondroitin-sulfate hydrogels [41]. These data suggest that composition of the extracellular matrix influence chondrogenic differentiation of MSCs.

Despite the fact that TGFβ3 plays a central role on chondrogenesis, other molecules are also documented as differentiation enhancers [42]. For example, insulin and glucose have been pointed as stimulators of DNA synthesis by facilitating the availably of a source of energy to various cell processes [43]. Ascorbic acid facilitates collagen-I and -II deposition. Furthermore, GDF-5 stimulates cell condensation during early stages, and increases collagen II expression, by phosphorylation of Smad1/5/8 complexes [44]. IGF-1 also enhances chondrogenesis, but is less studied [37].

Although chondrogenic differentiation mechanisms are not fully understood, some proteins have been identified as mediators. One example is Vav1, a protein involved on defining between chondrogenic or adipogenic fate [45]. Vav1 is known to increase Sirt1 expression, a deacetylase that targets Sox9 (a chondrogenic marker) and PPARγ, required for adipogenesis. It was documented that Sirt1 deacetylates Sox9, activating it and inducing chondrogenesis. Losing Vav1 inactivates Sox9 and activates PPARγ, promoting adipogenesis. Therefore, Vav1 absence has a negative effect on chondrogenesis. MicroRNAs have also been identified as chondrogenic mediators, particularly miR-335-5p, which is highly expressed during chondrogenesis [46]. This micro RNA inhibits two Sox9 inhibitors, Daam1 and Rock1, potentiating chondrogenesis on MSCs. In the future, the interplay between all these mediators need to be elucidated.

1.2.1. The interplay between N-cadherin, integrins and the Extracellular Matrix plays a key role on chondrogenic differentiation

The ECM is a non-cellular component that exists in all tissues (although with distinct compositions), that provides structural support to cells [47,48]. Various fibrous proteins compose ECM - collagen type I and III, fibronectin, elastin, laminins, tenascin - and proteoglycans – decorin, perlecan, aggrecan and hyaluronic acid. These proteins form a compliant meshwork that is responsible for the mechanical characteristics of the ECM. Each protein plays specific roles to maintain ECM homeostasis. Proteoglycans buffer, hydrate and facilitate force-resistance properties [49]. Collagens regulate tensile strength, cell adhesion and migration and direct tissue development [50]. They are usually associated with elastin, a molecule that enables the tissue to stretch. Fibronectin is mainly involved on ECM internal organization and mediates cell attachment [47]. ECM is a dynamic structure,

preserved by a balance between matrix metalloproteinases (MMPs) and MMP inhibitors [48]. Cells adhere to ECM, mediated by specific receptors, such as integrins, that transduce signals and initiate signaling cascades. The reciprocal interaction between ECM and cells is crucial to trigger various biochemical and biophysical signals that sustain cell survival, proliferation, growth and differentiation. Succinctly, ECM is essential to maintain cell homeostasis.

Chondrogenesis is modulated, *in vivo*, during development by the 3D structure that regulates cell shape [51]. Firstly, mesenchymal cells are condensed on pre-cartilage zones. This condensation is mediated by cell-cell adhesion molecules, especially N-cadherin and N-CAM [52]. During differentiation, expression of these receptors decreases, enabling a more spherical morphology, and initiates a reorganization of the cytoskeleton [53]. Cell shape can also be altered by biophysical interactions between integrins and collagen and proteoglycans, with the former being also connected to the cytoskeleton. Changes on polymerization of cytoskeletal filaments is transmitted to the nucleus, leading to upregulation of chondrogenic factors, such as Sox9, which are capable of initiating synthesis of cartilage-specific ECM molecules [54]. Then, the fate of these pre-cartilaginous cells can diverge: they can undergo an articular hyaline tissue pathway or an endochondral bone development pathway [42]. Cells on the articular path start to express doublecortin and growth/differentiation factor-5 (GDF-5) and are malitrin-1 negative. Additionally, they maintain high expression of *ACAN* and *PRG4* (lubricin) and low *Col2a1* and do not proliferate extensively or acquire a hypertrophic phenotype.

Cell shape has also been documented as an essential regulator of cell fate in several contexts [55]. Cells are capable of altering their morphology, namely through N-cadherin expression, in order to facilitate cell-cell interactions that are known to promote actin polymerization [56]. Moreover, RhoA (a Rho GTPase family protein) and its downstream effector, Rho-associated protein kinase (ROCK), have been

identified as cell shape mediators. They are known to be involved on focal adhesion-initiated signaling, myosin phosphorylation, regulation of actin contractility and promote formation of stress fibers [25]. ROCK activity was documented to be higher on spread cells than on round cells, the former known to exhibit stress fibers and be more contractile [57]. In addition, RhoA activity is modulated by cell density [25]. RhoA activity was proven to be higher on low-density cultures when compared to high-density cultures. Likewise, MSCs express more stress fibers on low-density cultures. RhoA and ROCK are proteins of interest since they have been documented as relevant factors on lineage commitment of MSCs between osteogenic and adipogenic fates [25]. Namely, RhoA downregulation is associated to unspread and spherical cells, which promotes adipogenesis. No significant differences were found on RhoA activity during chondrogenic/myogenic differentiation of MSCs [58,59]. If RhoA plays any key role during chondrogenesis, it is still unknown.

Likewise, Rac1 - a Rho GTPase - activity was found to be modulated by cell shape [59]. This protein is known to be activated by integrins and stimulate cell spreading [60] promoting actin meshwork and increasing N-cadherin cell adhesion [61]. A recent study identified Rac1 as the "cell shape sensor" that regulates myogenic or chondrogenic lineage commitment [59]. Results indicate that in the presence of TGFβ3, cells cultured on a substrate that favors acquisition of a non-spread spherical morphology (due to the presence of small islands that provide cell attachment only on those confined areas), express higher levels of Sox9 (a chondrogenic marker), when compared to unconstrained spread cells. This study hypothesizes that the "round shape" can inhibit Rac1—a protein necessary and sufficient to commit MSCs to a myogenic lineage (Figure 5). Also, it was suggested that a spread shape activates Rac1, which increases N-cadherin expression and leads to the expression of smooth muscle cell (SMC) genes. Also, this protein is involved on late skeletal myotube fusion. Concluding, Rac1 inhibition is required during chondrogenic differentiation.

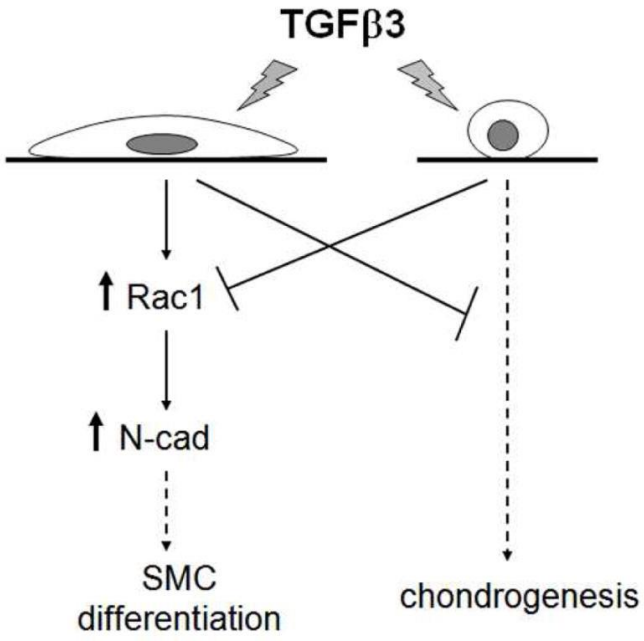

Figure 5 - **Cell shape modulates MSCs chondrogenic and myogenic fate** [59]. If cell acquires a spread shape, Rac1 activity increases leading to an increased expression of N-cadherin. This protein is needed to commit cells to myogenesis. When cells acquire a round shape, Rac1 activity is inhibited, committing cells to chondrogenesis.

Specific receptors on the cell surface are responsible for recognizing ECM proteins, initiating signaling cascades. It is important to understand how the expression of adhesion receptors is modulated during chondrogenesis. Particularly, integrin expression pattern during chondrogenic differentiation has been investigated [62,63]. Results suggest that fibronectin receptor (integrin α5ß1) and fibrinogen and fibronectin receptor (GPIIb/GPIIIa) downregulation may assist chondrogenic differentiation. These studies also proposed that downregulation of ILK, CD47 and ICAP1 might be involved in transducing the signal intracellularly. Possibly, downregulation of these specific integrins may assist cells to acquire a round shape, triggering chondrogenic differentiation signaling. Furthermore, a

study confirmed that binding of integrin ß1 to collagen type I is essential to alter cell morphology and facilitate cell-cell adhesion is essential during cell condensation typical of chondrogenesis [64]. In summary, interactions between MSCs and ECM are essential to trigger chondrogenesis.

1.2.2. hMSCs signaling pathways can be mechanomodulated

Stiffness is a structural property of an object that can be defined as the internal resistance to deformation (change of size or shape) when a force is applied, that depends on the organization, size and shape of the material [65]. Tensile modulus is a normalized metric, independent of geometric properties, that defines the material tendency to undergo elastic strain (unitless normalization of deformation), when experiences stress (force per unit of area). Young's modulus (or tensile modulus) (E) is a measure of stiffness and can be determined by the following formula: $E = \frac{stress}{strain}$. It is usually presented on units of pressure, as Pascal. Also, shear modulus (G) defines the material resistance to shear stress.

Several techniques, as magnetic resonance elastography (MRE) have provided information about each organ stiffness [66]. Therefore, various studies put an effort on understanding of how cells are capable of sensing microenvironment stiffness and activate mechanical intracellular pathways and modulate gene expression - mechanotransduction [67].

The significance of mechanotransduction has become clearer on the past few years. Consequently, several studies have tried to explain how cells sensed the matrix elasticity, and how it was transduced through signaling pathways (Figure 6) [26,68–70]. Focal adhesions (FA), which involve integrins—transmembrane receptors that bind to ECM elements on the extracellular side—, were identified as mediators to transmit tension forces. These structures are connected (on the

intracellular side) to actomyosin cytoskeleton—composed by filamentous actin (F-actin) and myosin-II, a motor protein that mediates contractility of the actin filaments through adapter proteins. Integrins can transmit signaling bidirectionally. FA are responsible to initiate a cascade signaling in response to substrate stiffness. First, a stiff substrate induces stress fibers - contractile actin and non-contractile myosin II filaments - contraction and microtubules compression, creating a traction force that initiates integrin signaling: adapter proteins bind cytoplasmic domains of integrins and activate integrin binding to the ECM [70]. Mechanical force on integrins, particularly on talin – a FA component – expose vinculin binding sites and recruit other proteins that bind to actin [71]. Consequently, actin polymerization is further stimulated and stress fibers contractility is altered [70]. Thus, contractility of actin cytoskeleton increases, which fosters focal adhesions growth, elongation and increase expression levels of focal adhesion components, as filamin, talin or focal adhesion kinase (FAK) [26]. Particularly, $\alpha 5\beta 1$ integrin can switch between relaxed and tensioned state in response to myosin II cytoskeletal tension in response to substrate stiffness [68]. This conformational change promotes FAK phosphorylation, initiating several signaling cascades, promoting further activation of integrins and enhancing cell adhesion to ECM and increasing intracellular tension [70]. These alterations lead to modifications on cell shape – namely, cells growing on stiff substrates exhibit a spread shape.

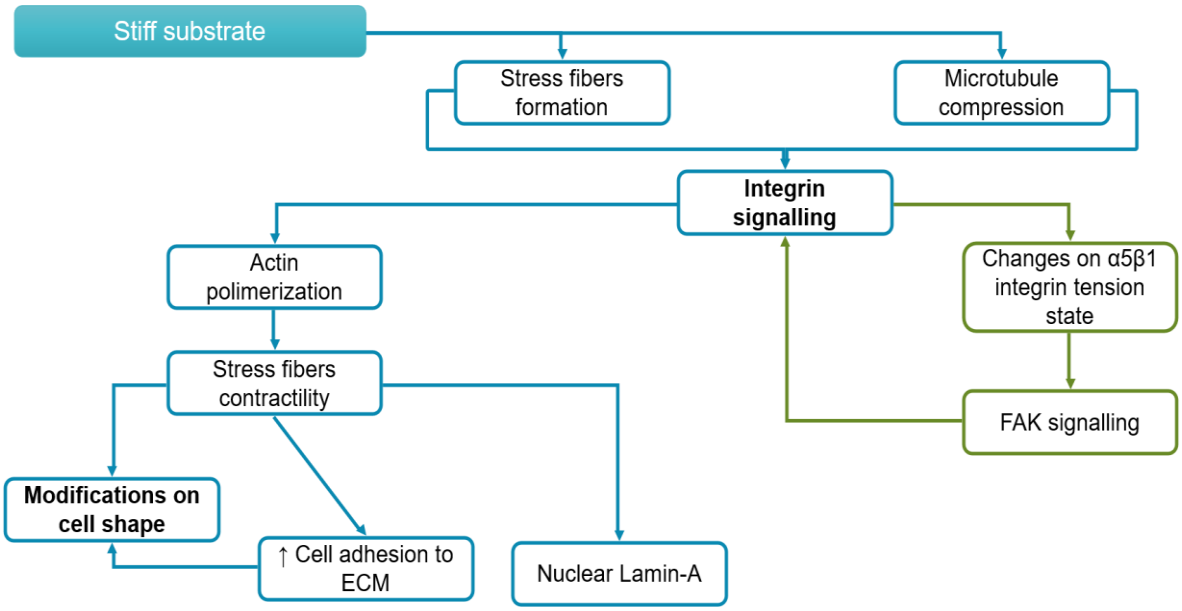

Figure 6 – **Substrate stiffness can modulate intracellular signaling pathways.** Mediated by focal adhesions, cells are capable on sensing the stiffness of the microenvironment, and initiate specific signaling cascades that modify their cytoskeleton, and consequently their shape and gene expression [26,68–70]. Stress fibers and microtubule compression activate integrin binding [70]. Moreover, changes on tension state on integrin activates integrin signaling pathways, mediated by FAK [68]. Together, this increases actin polymerization and stress fibers contractility, which leads to an increase on cell adhesion to the ECM, mediated by focal adhesion. These alterations modify cell shape - cells growing on a stiff substrate exhibit a spread shape. Also, intracellular tension can be transmitted to the nucleus, modulating gene expression. Particularly, nuclear lamin-A is more expressed on stiff substrates [80].

RhoA/ROCK signaling pathway was found to play a key role on mechanotransduction [70,72]. Mechanical tension activates RhoA, and consequently its effector, ROCK. ROCK activates LIMK1, which phosphorylates and inactivates cofilin, a actin-depolymerizing protein [72]. Cofilin binding to actin leads to depolymerization while phosphorylation of this protein enables actin polymerization and stabilization and stress fiber formation [73]. Also, ROCK also phosphorylates and activates myosin light chains of myosin II (MLC) [74,75].

Activated MLC can interact with actin, modulate cytoskeleton contractility and form stress fibers. Accordingly, RhoA/ROCK signaling pathway can modulate the cytoskeleton in response to substrate stiffness. The actin cytoskeleton-focal adhesion interplay is essential to transduce mechanical signals – forces generated by actin polymerization affect the activity of mechanoresponsive proteins, such as integrins; these proteins activate small G proteins, as Rho, capable of regulating cytoskeleton proteins [76]. Changes on actomyosin contractibility and actin polymerization modulate the resulting force machinery, forming an actin–integrin feedback network.

Furthermore, actomyosin contractility and resistive forces of microtubules transmit the balance of tensions to the nucleus, modulating genetic expression. The nucleus is a mechanoresponsive structure, since it is strictly connected to the cytoskeleton (Figure 7) [77]. LINC complex (SUN2 and nesprins) proteins connect nucleoskeleton to the cytoskeleton [78]. Particularly, it connects lamin A/C, fibrillar proteins present on the inner layer of the nuclear envelope to extra-nuclear actin and transmit intracellular tension to the nucleus. On a stressed nucleus, conformational changes are induced in lamin A and B, hindering access to kinases, such as cyclase-dependent kinases (CDK) [77,79]. Consequently, lamin A/C are not degraded and are stabilized on the nucleus. Also, it has been described that culturing cells on a stiff substrate not only stabilizes lamin-A but also increases its expression (Figure 6) [80]. On soft substrates, low-stress conditions do not impair interaction between kinases and lamin A/C, resulting on their degradation [77]. Evidences also indicate that cells growing on a stiff substrate exhibit a stretched nucleus while cells growing on a soft matrix exhibit a relaxed nucleus [79]. Therefore, it is possible to conclude that nucleoskeleton can be mechanomodulated.

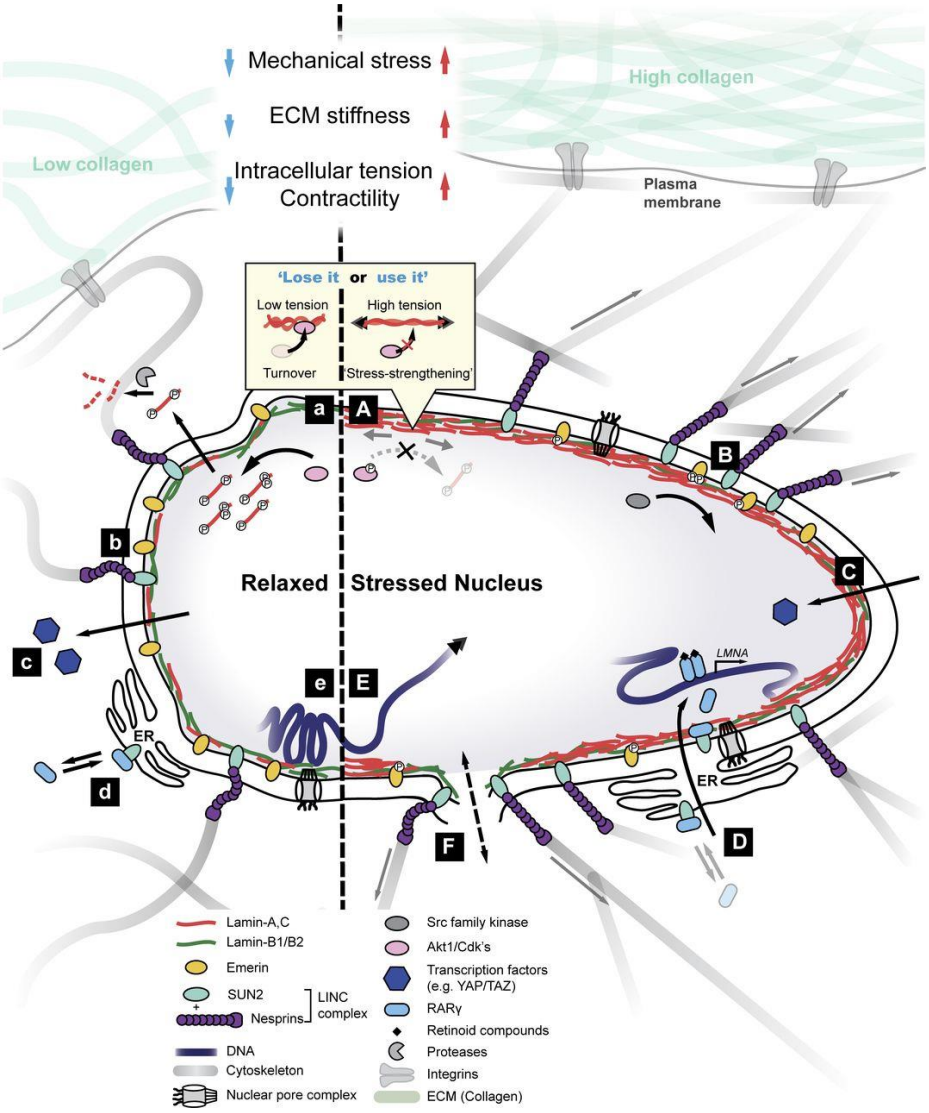

Figure 7 - **Nucleus is a mechanoresponsive structure** [78]. LINC complex proteins are responsible to connect cytoskeleton to the nucleoskeleton. Cells growing on a stiff substrate show high intracellular tension. LINC complex transmits this tension to the nucleus, inhibiting lamin-A degradation and stabilizing it on the nucleus. On a relaxed nucleus, lamin-A is degraded.

MSCs are capable of sensing the stiffness of the microenvironment in which they are cultured, triggering different signaling pathways that modulates their fate [81,82], similar to what was described above for cell shape. A stiff ECM leads to the development of focal adhesions, which increases stress fibers and intracellular stress

because of enhanced phosphorylation (and activation) of myosin light chain (MLC). This intracellular tension regulates cell shape: well-defined and aligned stress fibers and enhanced focal adhesions increase cell spreading area (Figure 8) [70,81]. Conversely, cells growing on soft matrix internalize (possibly by endocytosis) integrins, limiting ECM-integrins connection [70]. This impairs the formation of focal adhesions, stress fibers and consequently intracellular tension decreases. As a result, MSCs show a poorly defined cytoskeleton and acquire a round shape. A study demonstrated that when cultured on collagen I coated acrylamide gels with distinct degrees of stiffness, cells start to modify shape: on softer substrates (0,1 - 1 kPa), they start to develop branches, while on stiffer substrates (25 kPa - 40 kPa) the acquire polygonal shape [26]. Hence, MSCs modulate their shape in response to stiffness of the environment in which are being cultured. Moreover, in response to stiffness, MSCs activate distinct integrins: cells growing on soft substrates activate preferentially β1 integrins, but decrease their distribution on cell surface, enhancing ECM detachment [83]; in turn, MSCs growing on substrates with moderate stiffness (10 kPa) recruit preferentially β3 integrins, develop focal adhesions [70].

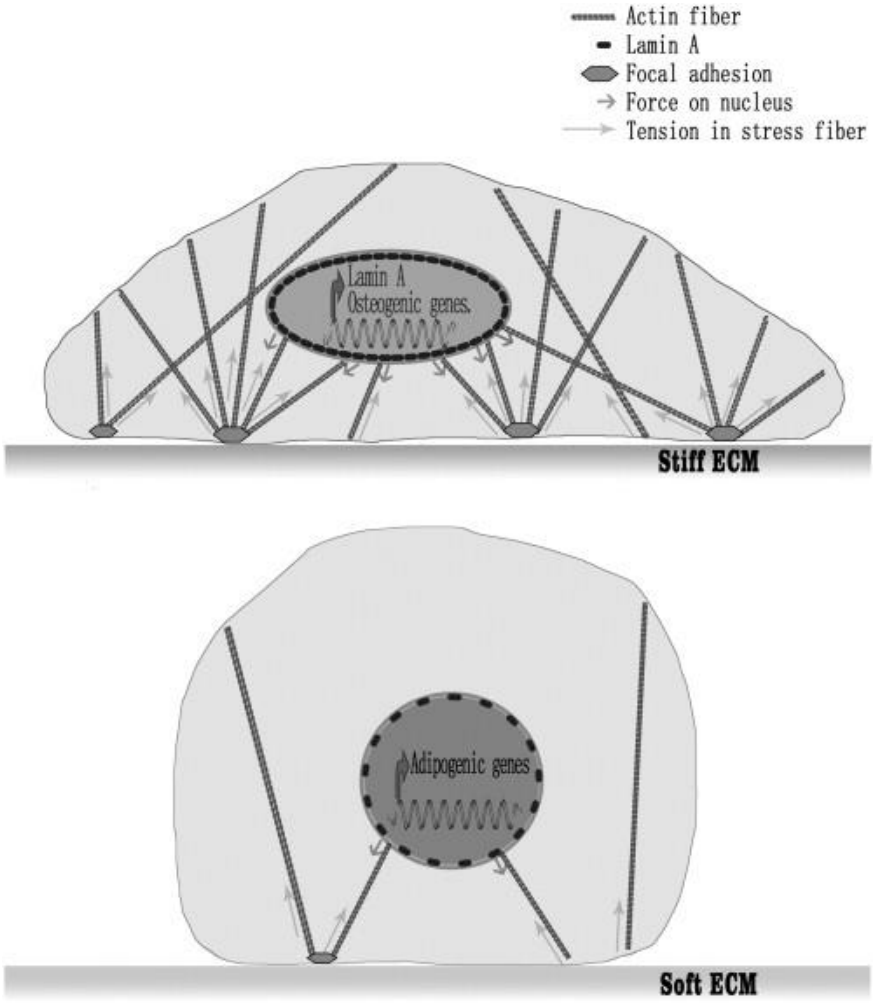

Figure 8 - **Cells are capable of modifying their shape in response to ECM stiffness** [81]. If cells are growing on a stiff substrate, intracellular tension increases, which leads to an increase on focal adhesions and formation of aligned stress fibers, spreading cell area [70,81]. On a soft substrate, intracellular tension and expression of focal adhesions components decreases, stress fibers are not prominent which enables cells to acquire a round shape.

1.2.2.1. Mechanotransduction signals are involved during chondrogenic differentiation

Efforts have been made to culture chondrocytes *in vitro*. The literature shows that when cultured on 2D systems in presence of TGFβ3, primary chondrocytes dedifferentiate and acquire a fibroblastic phenotype, impairing proliferation [84]. However, another study indicates that both primary chondrocytes and ATCD5 (a chondrogenic cell line ATDC5 derived from teratocarcinoma AT80) can mature and acquire characteristics of distinct cartilage zones [85]. In fact, this study demonstrated that primary chondrocytes cultured in the presence of TGFβ on acrylamide gels of 0,5MPa express higher levels of chondrogenic markers (*Sox9*, *Col2a1* and *ACAN*) when compared to 0.2 MPa and 1.1 MPa gels. This data enhances the significance of mechanotransduction during cell growth, since in the absence of optimal stiffness, chondrocytes are not able to preserve their phenotype. In terms of signaling pathways, no differences were found on Smad3 activity on different stiffness. However, cells cultured on 0.5 MPa gels showed that Smad3 was more prevalent on the nucleus and that p38 pathway through MAPK kinase TAK1 was also targeted chondrogenic markers. ROCK activity increases with stiffness. It was suggested that reduced ROCK activity on soft substrates induced autocrine TGFβ expression [85]. Hence, mechanical stimulus is essential to maintain a chondrogenic phenotype.

Optimal culture stiffness has been identified for differentiation of MSCs on various lineages: soft substrates promote adipogenesis (2.5-5 kPa), while intermediate matrices (8-17 kPa) promote myogenesis and stiff matrices (100 kPa) promote osteogenesis [26,86]. Several efforts have been made trying to define optimal 2D and 3D culture conditions for the differentiation of MSC into chondrocytes [51,58,87]. 3D structures, such as pellet or micromass culture, are more

like *in vivo* models than 2D cultures. Nevertheless, these systems are more difficult to control and to analyze, and more susceptible to mechanical loadings, like hydrostatic pressure or uniaxial compression (reviewed in [51]). 2D models are somehow farther from what occurs *in vivo* and are typically easier to control and analyze, specifically in what concerns the effect of matrix stiffness on chondrogenic differentiation.

Initially, naïve MSCs do not express basal levels of lineage specific markers, and are round and small. Although matrix stiffness is not sufficient to determine cell lineage it is now clear that it plays a significant role. It has been investigated how stiffness can modulate chondrogenic differentiation [58,88]. In the presence of TGFβ3, bone marrow hMSCs adherent to stiffer substrates (2D culture) (15 kPa and stiffer) expressed higher levels of smooth muscle markers (calponin-1 and α-actin), while cells differentiating on a soft gel (1 kPa) expressed higher levels of collagen II (chondrogenic marker) and lipoprotein lipase (LPL) (adipogenesis marker) [58]. Research groups developed 3D scaffolds to study chondrogenic differentiation. Using 3D methacrylate hyaluronic acid (HA) hydrogels with different stiffness, it was found that low crosslinking hydrogels (3.5-3.6 kPa) favored cartilage matrix synthesis and deposition, while high density crosslinking hydrogels hypertrophic cartilage differentiation [88]. Additionally, a different study indicates that 3 kPa HA-hydrogel upregulates aggrecan and collagen type II expression when compared to stiffer hydrogels, as 90 kPa [41]. In conclusion, these studies point that, for on both 2D and 3D culture, a soft matrix favors chondrogenesis.

In the absence of soluble growth factors, substrate composition and stiffness are still capable of modulating chondrogenic differentiation of MSCs [87]. Sulfonated proteoglycans are a component of the ECM [2]. A study indicates that polyacrylamide gels coated with sulfonated groups, even in the absence of specific chondrogenic growth factors can induce chondrogenic differentiation [87]. This

same study specifies that murine MSCs cultured on low stiffness hydrogels (1 kPa) express higher levels of chondrogenic markers, such as *Col2a1* and *Sox9*, when compared to stiffer substrates.

A different study also shows that MSCs are capable of differentiating into chondrocytes with specific characteristics if grown encapsulated in hydrogels – 3D culture - with optimal specific matrix stiffness and with fibers oriented according to specific cartilage zones and in the presence of specific zone biomolecules [89]. Specifically, this study proves that of all variables tested, matrix modulus has a leading effect on differentiation of MSCs into superficial and deep zone chondrocytes (80 kPa and 320 MPa, respectively), while TGFβ1 has a major effect in driving differentiation into middle zone chondrocytes. Despite cells were growing on a 3D environment, this writes down that possibly stiffness can guide cells to acquire zonal characteristics.

As described above, RhoA is plays a key role on lineage commitment. In order to investigate how its activity is modulated by mechanotransduction, in the presence of TGFβ, a study acknowledged that no significant differences were found on RhoA activity between soft and stiff substrates on MSCs [58]. Conversely, RhoA/ROCK are well characterized mechanotransducers [70,72]. Substrate stiffness should alter their activity, which surprisingly does not occur in this study. Yet, if transfected with RhoA vector, expression of both chondrogenic and adipogenic markers on soft substrates, and smooth muscle markers on stiffer substrates increases [58]. Perchance, RhoA is thought to be involved on the expression of various lineage markers, despite that lineage commitment needs another stimulus. Moreover, it was documented that matrix stiffness did not modulate Smad2/3 activity, suggesting that TGFβ signaling is independent of mechanical stimulus. Contrary, on chondrocytes and ATCD5 cells literature shows inconsistent results showing

RhoA/ROCK pathway represses chondrogenesis [90]. Interestingly, no evidences were found that ROCK targets Sox9. Thus, it is not possible to establish a clear role of RhoA and its effector, ROCK, during chondrogenesis.

It has been described that stress fibers activation by β1 integrin—through FAK and ERK signaling, possibly mediated by small GTPases - has an inhibitory effect on chondrogenesis [91]. Moreover, when submitted to dynamic compression during chondrogenic differentiation, integrin expression was downregulated, suppressing signaling though the ß1/FAK/ERK pathway, consequently up-regulating Smad2,3-mediated signaling, enhancing chondrogenesis [92]. These results are concordant with the previously described pattern of integrin α5β1 expression during chondrogenesis, which becomes downregulated [63]. Possibly, downregulation of this receptor suppresses the pathway formerly described and enhances chondrogenesis.

Together, this data suggests that when cultured on a specific microenvironment, with optimal stiffness and suitable biomolecules MSCs can differentiate into chondrocytes. Interestingly, there is a large discrepancy between the stiffness pointed by these studies, since both soft and stiff substrates (to acquire zonal specific characteristics) are shown as optimal for chondrogenic differentiation. Even though it needs to be taken under consideration that 2D and 3D models create distinct environment for the cells, stiffness is still the mutual variable. Thus, future investigations need to clarify which stiffness most favors chondrogenesis.

1.2.2.2. Cells have "mechanical memory"

Several proteins have been identified as mechanotransducers [55]. Focal adhesions are an important mechanosensor that can trigger diverse pathways and modulate the cytoskeleton and nucleoskeleton. Yes-associated protein (YAP) and TAZ were identified as important mechanotransducers, that change localization in response to cytoskeleton tension [93]. YAP localization is predominantly nuclear if cells are grown on stiff substrates and on cytoplasmic if cells are cultured on soft substrates. It was documented that YAP/TAZ localization was modulated by intracellular tension – particularly, increased Rho activity, actin polymerization and stress fibers are responsible for its accumulation in the nucleus [93]. Phosphorylated YAP can not be translocated into the nucleus and is retained on the cytoplasm. In response to increased intracellular tension, mediated by an unknown kinase, Rho GTPases reduce inhibitory phosphorylation of YAP, enabling it to translocate into the nucleus [94], favoring cell proliferation. Also, inhibition of Rho activity prevented nuclear localization [93]. The Hippo pathway, mediated by LATS1/2, also modulates YAP localization [95]. LATS1/2 phosphorylates YAP and relocalizes it on the cytoplasm. Rho inhibition is responsible to activate LATS1/2, excluding YAP from the nucleus. In summary, YAP localization is a balance between pathways formerly described. Moreover, lamin-A is more expressed on stiffer substrates [80]. This study suggested that this protein was responsible to stabilize YAP/TAZ complex on the nucleus. Furthermore, YAP/TAZ localization can be modulated by cell density: YAP has low activity on high cell density culture [96], possibility due to less spreading of the cells.

YAP has been found to be the key to the "mechanical memory" of stem cells [97]. YAP endures permanently activated on MSCs cultured on a hard substrate (TCPs), even if cells are moved to a softer substrate. Therefore, these evidences suggest that

expansion conditions of MSCs can influence their differentiation fate. It was documented that MSCs cultured on soft substrates more than 10 days, and then moved to a stiff substrate decreased neurogenic markers and increased osteogenic markers expression, equaling cells grown exclusively on stiff substrates [98]. Also, MSCs cultured on stiff substrates and then transposed to soft substrates reduced *runx2* (osteogenic marker) expression; nonetheless, it persisted active. Neurogenic markers increased but its expression was lower when compared to cells cultured exclusively on soft substrates. It was also documented that MSCs cultured on TCPs (1 GPa) for 1 and 7 days could totally and partially, respectively, reverse nuclear localization of YAP and runx2 if transferred to a soft substrate (2 kPa) [97]. On cells cultured on 10 kPa substrates, these differences were not evidenced. Longer periods on TCPs biased MSCs differentiation into osteogenesis. This suggests that expanding MSCs on a stiff substrate "primes" stem cell fate.

Substrate topography – substrates with specific topography that modulate cell shape - and fluid shear stress – stress induced by fluid flow – can modulate cell contractibility [57]. This study states that cells can preserve their multipotency if a low optimal intracellular contractibility is achieved, allowing proliferation, but not committing to adipogenesis. Hypothetically, if cells are expanded on an optimal soft substrate, with low intracellular tension, YAP/TAZ complex can not translocate into the nucleus and differentiation will not be biased.

Recently, YAP has been associated with regulation of stem cell fate, including chondrogenesis [96,99]. YAP was found to inhibit MSC differentiation into chondrocytes [96]. Additionally, YAP expression is mostly responsible for suppressing Smad signaling, decreasing target genes of this pathway. Both studies are concordant, since it has been previously described that softer gels promote chondrogenesis, and consequently YAP is not present in the nucleus [58,96]. Therefore, this reveals the relevance of mechanical memory during chondrogenesis.

However, there are currently no studies showing how this "memory" can possibly influence MSCs during chondrogenesis.

"Mechanical memory" highlights the need to use low passages cells. Cell therapy applications usually require a high number of cells. Expansion of cells on substrates with the optimal stiffness could be an alternative to maintain multipotency and/or to prime a specific lineage. Therefore, a high number of cells could be available without loss of multipotency and perchance a higher potency to differentiate. Since it has become clear that MSCs lose their multipotency if cultured more than 10 days on stiff substrates, results can be biased if high passages MSCs are induced to differentiate. On the study mentioned before, where no differences were found on RhoA expression between substrates with different stiffness [58], it was possibly because cells were used at passage 8-11 and they no longer had the ability to respond to cell stiffness.

All taken together, data shows the ability of MSCs to differentiate on chondrocytes. Literature highlights the relevance of mechanical memory, enhancing the need to induce only naïve MSCs to differentiate. Although mechanisms involved during chondrogenesis are not totally understood, improving culture conditions for cell proliferation and differentiation could be a step closer to develop a future cell therapy to cartilage diseases and clarify the role of specific proteins during chondrogenesis, as for example RhoA, whose role during chondrogenesis is still not consensual.

1.3. Polydimethylsiloxane (PDMS) is a suitable substrate for cell culture

As previously described, MSCs trigger different signaling pathways when cultured on substrates with distinct rigidity. As a result, there has been an effort to develop biocompatible materials whose stiffness can be modulated. Polydimethylsiloxane (PDMS) as emerged as an interesting solution for a suitable substrate for cell culture [100–102]. The literature comprises different Young's modulus (E) to the same elastomer:curing agent ratio (Table 1), since differences on the temperature and curing time can influence polymerization - the higher curing time or temperature, the higher the polymerization reaction extension. Also, it is possible to infer that increasing curing agent proportion creates a more dense network of PDMS, and consequently stiffness increases [103]. Therefore, to replicate the exact same conditions, it is necessary to choose the more adequate protocol for the aims of the study. Distinct stiffness measurement techniques may also introduce some variability.

Table 1 - PDMS stiffness with different base:curing agent ratio

PDMS (base:curing)	Young's Modulus	Curing temperature	Reference
10:1	1783 kPa	60 °C (18h-20h)	[100]
	1300 kPa	80 °C (4h)	[104]
	750 kPa	60 °C (1h)	[102]
30:1	259 kPa	60 °C (18h-20h)	[100]
	100 kPa	80 °C (4h)	[104]
40:1	45 kPa	80 °C (4h)	[104]
50:1	48 kPa	60 °C (18h-20h)	[100]
	38 kPa	60 °C (1h)	[102]
	8 kPa	80 °C (4h)	[104]
60:1	3 kPa	80 °C (4h)	[104]

PDMS seems to be a very a good material to study the effects of stiffness during chondrogenesis, since it can comprise a wide range of stiffness. Additionally, it is possible to functionalize its surface enabling an efficient protein coating of PDMS surface facilitating cell adhesion [105,106]. Therefore, PDMS is pointed as a promising option to help to comprehend the mechanisms involved during chondrogenesis.

1.3.1. Rheological testing to determine viscoelastic properties of PDMS

Materials have specific mechanical properties, such as viscosity and elasticity [107]. A material purely elastic can return to its original shape after a force is applied. Specifically, the work force induced to deform is stored and after its removal, energy can be recovered. However, many materials are not ideal elastics, exhibiting viscous and elastic properties – viscoelastic materials. After compression, shape and volume can be altered. Deformation can be associated to volume modifications, which is usually determined by Poisson ratio (v). PDMS Poisson ratio is around 0,5, suggesting that it does not change its volume significantly under compression [108]. Additionally, volume can remain unaltered macroscopically, but there will be a shape modification [107]. Therefore, elasticity and viscosity can be measured if deformations and forces are quantified.

Rheology is the study of how materials deform when forces of a certain magnitude are applied to the structure. G is called the shear modulus, and describes the resistance to deformation [109]. It is related to G' modulus (storage modulus) - the elastic component - and G'' modulus (loss modulus) - the viscous component. Both can be determined by rheometric studies. Namely, G' can be related to the Young's modulus (E) via Poisson ratio, trough the following formula: $E = 2 \times G' \times (1 + v)$. A frequency sweep analysis can give information about structure

and dynamics of a specific material [107]. For elastic hydrogels, storage and loss modulus are independent of the frequency applied, and G' modulus is higher than G'' [107,109]. In contrast, viscoelastic hydrogels are frequency depend and G'' is predominant at low frequencies. At higher frequencies, G' can dominate if the substrate is not able to relax.

$Tan\ \delta$ correlates G' and G'' trough the following formula:

$$Tan\ \delta = \frac{G''}{G'}$$

This formula elucidates about the prevalent behavior of the material [110]. Values smaller than one indicate that elastic properties are dominating.

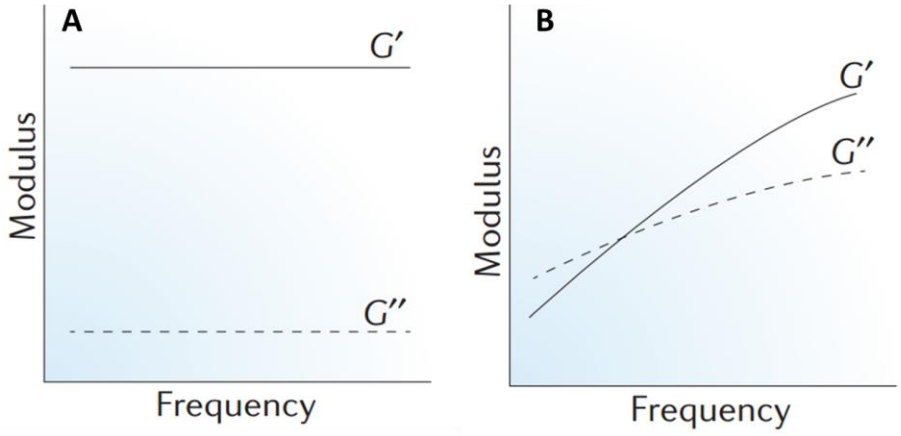

Figure 9 - **Frequency sweep of elastic and viscoelastic hydrogels [109].** Elastic materials (left) are frequency independent and G' predominates. Viscoelastic materials (right) are frequency dependent and G'' predominates at low frequencies.

Studies described above point towards a large discrepancy of putative optimal substrate stiffness (between 1 kPa and 1783 kPa) (Table 1). Since PDMS is a promisor substrate candidate for this study, a rheological study will help us understand not only elastic but also viscous properties of this material. Different formulations will be synthetized to create substrates with specific elastic and viscous behaviors. Culturing cells on PDMS substrates with different stiffness will help us to define optimal viscoelastic characteristics for chondrogenic differentiation and MSCs proliferation.

1.4. Objectives

As formerly described, MSCs can trigger signaling pathways in response to substrate stiffness. Therefore, we postulated that chondrogenesis can be mechanomodulated.

On the present study, we aimed to define an optimal stiffness for chondrogenic differentiation. For that, we characterized viscoelastic properties of distinct PDMS formulations by rheology and validated that these substrates were capable of triggering a mechanical stimulus on MSCs. To reduce the impact of mechanical memory, only low passages MSCs (P2) were induced to differentiate. We evaluated the influence of a range of stiffness on chondrogenic differentiation of MSCs, performing a glycosaminoglycan semi-quantitative assay and assessing the expression of chondrogenic markers by RT-PCR. Moreover, we studied MSCs kinetics proliferation on PMDS substrates.

2. Materials & methods

2. Materials & methods

2.1. Cell culture of hMSCs

All cell culture procedures were performed under aseptic conditions, on a class II vertical laminar air flow cabinet (HeraSafe HS-18, Heraeus). Cells were cultured on an incubator (Shel Lab), at 37 °C, with 5% CO_2 and 95% humidity. Culture mediums and sterile 1x phosphate buffered saline (PBS) were stored at 4 °C. Before use, both were pre-warmed in a water bath at 37 °C.

2.1.1. Isolation, expansion and cryopreservation of hMSCs

For isolation procedure of hMSCs, fragments of the human umbilical cord (UC) were washed with serum-free Minimum Essential Media (MEM) α medium (Life Technologies) supplemented with Penicillin (10 U/ml), Streptomycin (10 μg/ml) and Amphotericin B (2.5 μg/mL) (all from Life Technologies). Fragments were placed on a tissue culture polystyrene (TCPs) (Corning-star) 21cm² dish, and left to dry around 20 minutes. Then, a glass coverslip was placed on top of the fragments. Both steps aimed to increase the contact between the fragments and the surface of culture, since hMSCs are adherent cells. Proliferation medium (PM) – MEM α medium supplemented with 10% (v/v) MSCs qualified Fetal Bovine Serum (FBS) (Hyclone), Penicillin (10 U/ml), Streptomycin (10 μg/ml) and Amphotericin B (2.5 μg/mL) (all from Life Technologies) was added and fragments were placed on an incubator. After 12 days of culture, fragments were checked for cell migration to the dish and colonies formation, up to 25 days. If after this period no colonies were formed, the sample was considered negative and discarded. When colonies formed were

compact, fragments were discarded. Adherent cells were washed with sterile 1x PBS twice and detached with 0.05% (v/v) trypsin-EDTA (Life Technologies) for 5 minutes at 37 °C. Trypsin was inactivated by adding DMEM high glucose medium (Hyclone) supplemented with 10% (v/v) FBS (Gibco, Life Technologies), Penicillin (10 U/ml), Streptomycin (10 µg/ml) and Amphotericin B (2.5 µg/mL) (all from Life Technologies). MSCs were resuspended for complete cell dissociation. Then, cell suspension was centrifuged at $290 \times g$ for 5 minutes at RT (Eppendorf Centrifuge 5810R), on a conical tube (Sarstedt). Supernatant was discarded and the pellet was resuspended on PM. MSCs were seeded on new 21cm² or 55cm² TCPs plate (Corning star) and expanded with PM – passage 1 (P1). Fresh medium was added every 2/3 days until 80-90% confluence was achieved. This procedure was repeated at each cell passage.

To calculate the total number of harvested cells, 10 µl of the resuspended cell solution was added to a hemocytometer. The average of the four corners was calculated and multiplied by 10^4. Subsequently, when needed, an exact number of cells could be seeded.

For cryopreservation, after centrifugation step previously described, cells were resuspended on FBS (Gibco) supplemented 10% dimethylsulfoxide (DMSO), to prevent the formation of crystals. Resuspended cells were placed on a cryovial (Nunc) and stored during 24h at -80 °C refrigerator on a Mr. Frosty™ Isopropanol Freezing Container. This cryovial was then transferred to liquid nitrogen. When needed, cells were thawed on a water bath at 37 °C. Cell suspension was transferred to a conical tube (Sarstedt) and DMEM high glucose medium (Hyclone) supplemented with 10% FBS (Gibco, Life Technologies), Penicillin (10 U/ml), Streptomycin (10 µg/ml) and Amphotericin B (2.5 µg/mL) (all from Life Technologies) was added. Cell suspension was centrifuged at $290\ x\ g$ for 5 minutes at RT (Eppendorf Centrifuge 5810R). The pellet was resuspended on PM and cells

were seeded on a TCPs plate considering the information described on the cryovial label.

2.1.2. Chondrogenic differentiation of hMSCs

To evaluate the impact of substrate stiffness during chondrogenesis, MSCs were induced to differentiate on functionalized (according to section 2.6.) PDMS substrates – 21 kPa, 18 kPa, 4 kPa, 1 kPa and 0.93 kPa and glass. Only naïve MSCs – passage 2 cells – were induced to differentiate into chondrocytes. Near confluence P1 MSCs were harvested and resuspended on 1 ml of PM. For chondrogenic differentiation, MSCs were seeded at 10.000/cm², according to the protocol described on section 2.1.1. After 24h, cells were washed with sterile 1x PBS twice and chondrogenic differentiation medium (StemPro® Chondrogenesis Differentiation Kit, Life Technologies) (CDM) was provided. Fresh CDM was added every three days. Cells were maintained in culture for 9 days. For control experiments, hMSCs were seeded at 8.000/cm² and cultured with PM for 9 days. Control cells cultured on glass were seeded at 3.000/cm².

Cells in culture were monitored on a contrast phase microscope (Axiovert 40C).

2.2. Safranin O assay to assess chondrogenic differentiation

2.2.1. Giemsa staining and spectrophotometric assay

Giemsa azure-eosin-methylene blue solution is a mixture of Azure-B and Eosin Y and methylene blue. Methylene blue has affinity to DNA. Also, azure and eosin form a complex and intercalate DNA, producing a purple coloration on the nucleus

(Romanowsky effect) [111,112]. Despite Giemsa absorbance has already been described to infer about the number of attached cells [113], it has not been verified if this method was reliable after dye extraction. For that, cells were seeded at 3.000/cm², 10.000/cm², 20.000/cm² and 30.000/cm². After 24h, culture medium was removed and cells were washed twice on 1x PBS. Cells were fixed with 4% (w/v) paraformaldehyde (Sigma) for 20 minutes, washed 3 times with 1x PBS and stained with Giemsa solution (diluted in 1x PBS in the ratio 1:20, according to the manufacturer's instructions) for 15 minutes. This step was followed by 4 washes with ddH_2O water to remove unbounded dye. Bounded dye was extracted with the addition of 5% (v/v) tricloroacetic acid (TCA) (diluted in ddH_2O) for 10 minutes. Absorbance of extracted dye was measured at 550 nm on 96-well white microplate, using a Microplate Spectrophotometer (PowerWave XS, BioTek).

A calibration curve correlating Giemsa absorbance and the total number of seeded cells was elaborated, performing a linear regression on GraphPad Prism 7 software.

2.2.2. Safranin O staining and fluorescence assay

Safranin O (SO) is a dye that has affinity to glycosaminoglycans (GAG), a protein of cartilaginous ECM. Since SO is a cation, one molecule of dye binds each of the negatively charged groups of GAG [114,115]. Fluorescence of this dye is proportional do GAG content [116]. To analyze GAG synthesis by measuring SO fluorescence, cells were induced to differentiate on all PDMS substrates (21 kPa, 17 kPa, 3 kPa, 1 kPa and 0.93 kPa) and glass for 9 days (see details on section 2.1.2). At day 9, differentiated and control cells grown on all PDMS substrates and glass were stained with SO. For that, culture medium was removed and cells were wash twice on 1x PBS. Cells were fixed with 4% (w/v) paraformaldehyde (Sigma) for 20 minutes,

and washed 3 times with double-distillated water (ddH_2O). To acidify the environment and favor the impairment with a cation, cells were rinsed on 1% (v/v) acetic acid [117]. Then, samples were stained with 0.1% (w/v) Safranin O (Alfa Aesar) solution (diluted in ddH_2O), at RT, for 5 minutes [118]. To remove unbounded dye, cells were washed 4 times, for 5 minutes each, with 1x PBS. Stained cultures were observed on a contrast phase microscope (Axiovert 40C). Images were acquired by a AxioCam, with the support of Axiovision Microscope Software (both from Carl Zeiss). For SO extraction and removal of bounded dye, 75% ethanol was added for 5 minutes. Fluorescence was read on a fluorescence plate reader (SpectraMax – Gemini) – Ex_{530nm}/Em_{570nm}, using a 96-well black microplate.

To quantify the background of SO staining, we performed replicates of blank samples. For that, all PDMS substrates and glass were functionalized and PM medium without cells was added. The substrates were kept on the incubator for 9 days. Then, the protocol formerly described was performed. The mean of the three replicates was subtracted to SO fluorescence of cultured cells.

After SO extraction, cells were washed twice with 1x PBS, and stained with Giemsa, according to section 2.2.1. Due to discrepancies on value range of SO assay and Giemsa assay results, SO fluorescence and Giemsa absorbance values were normalized to a 1 to 10 range using the following formula [119]:

$$z = 1 + \frac{(\mathrm{x} - \min(\mathrm{x})) \times (10 - 1))}{\max(\mathrm{x}) - \min(\mathrm{x})}$$

Finally, normalized GAG values were calculated using Safranin O fluorescence/Giemsa absorbance ratio.

2.3. RNA isolation, purification, reverse transcription and real time – polymerase chain reaction (RT-PCR) analysis of chondrogenic markers expression

To study chondrogenic genes expression by RT-PCR, cells were induced to differentiate on glass, 17 kPa and 1 kPa substrates for 9 days (see details on section 2.1.2). At day 9, total RNA was extracted from control and differentiated cells. On all the procedures described on this section, only RNAse free tips (VWR) were used. The first step is RNA isolation and purification. For that, at day 9, culture medium was removed and cells were washed once with cold 1X PBS. Cold TRIzol (Invitrogen) was added and, using a scrapper, cells were harvested and lysed. Cell lysate was collected to a microtube and vortexed and frozen at -80 °C, if needed to be stored. The mixture was then centrifuged at $12000 \times g$ for 10 minutes at 4 °C and supernatant was transferred to a new microtube. To promote organic/aqueous phase separation, chloroform was added to the sample and left at RT for 3 minutes. Then, the mixture was centrifuged at $12000 \times g$, for 15minutes at 4 °C. Aqueous phase – the upper layer - was transferred to a new microtube and 70% (v/v) ethanol was added. Ethanol addition is important because it has a low dieletric constant, facilitating the neutralization of nucleic acids backbone charges, making it less hydrophilic and easing the binding of this molecule to the column [120].

Purification protocol was followed according to the manufacturer's instructions. RNA/ethanol solution was added to a RNA purification column (RNeasy Mini Kit – Qiagen) and centrifuged at $7.378 \times g$ at RT. RNA binding to the column was followed by washing steps. These steps required the sequential addition of cleaning buffers (RW1 and RPE) to the purification column followed by short centrifugations at $7.378 \times g$ at RT. The addition of these buffers aimed to remove any contaminants.

Composition of RW1 and RPE (reconstituted in ethanol 100%) buffers is not known. However, ethanol is important to remove any salts that might still be present. Finally, RNAse free water was added to the RNA purification column, to dilute purified RNA, and the column was centrifuged one last time at $7.378 \times g$ for 1 minute.

The total amount of RNA was quantified on a spectrophotometer (Nanodrop™ 1000 Spectrophotometer). Absorbance was measured at 260nm, since nucleic acids absorb at this wavelength. RNA content of each sample was quantified three times and total amount was calculate using the average of three measurements. To evaluate quality of samples, absorbance at 230nm (contaminants absorb at this wavelength) and 280nm (proteins, phenol and other contaminants absorb at this wavelength) were also measured. Samples with 260nm/280nm ratio near 2 and 260nm/230nm near 2-2.2 were considered pure. Purified RNA was frozen at -80 °C.

Polymerase chain reaction (PCR) requires DNA templates. Catalyzed by a reverse transcriptase, complementary DNA (cDNA) was synthetized from a RNA template. For that, a mix composed by Taqman buffer, $MgCl_2$ (cofactor for the enzyme), dNTPs, random hexamers, water, RNAse inhibitors, MultiScribe Reverse Transcriptase and RNA template was prepared. The reaction was performed on a thermal cycler (BioRad MyCycler™): 10 minutes at 25 °C (incubation) followed by 30 minutes at 48 °C (DNA polymerization) and finally 5 minutes at 95 °C (enzyme deactivation). cDNA was stored at -20 °C. During this reaction, first, random hexamers bind RNA strands; then, MultiScribe enzyme synthetizes cDNA.

Target genes studied were, as follow: GAPDH (used as a housekeeping gene), Sox9, Aggrecan, Collagen type II and runx2. For each pair of primer (Table 2), a mix of SYBR® Green Real-Time PCR Master Mix (includes SYBR® Green I dye, AmpliTaq Gold® DNA Polymerase and dNTPs), forward and reverse primers, RNAse free water and cDNA template was prepared. Primers used had already

been described [121]. Additionally, a blast primer (NCBI) (https://www.ncbi.nlm.nih.gov/tools/primer-blast/) was performed to be certain of its specificity. Amplification was performed on an Applied Biosystems 7500 Real Time PCR System. PCR reactions were prepared in duplicate. First, samples were heated and held during 10 minutes at 95 °C, followed by 40 cycles of denaturation (95 °C, 15 seconds), annealing (60 °C, 1 minute) and extension (72 °C, 20 seconds).

SYBR® Green I dye has affinity to DNA double strands and emits fluorescence proportionally to the total amount of PCR generated products [122]. When the number of copies reaches detection limit, there is an exponential increase of fluorescence, suggesting that DNA is being replicated exponentially. C_T is the number of the cycle that signal reaches the threshold; it is inversely proportional to the amount of the product amplified. Samples were analysed using the $2^{-\Delta\Delta C_T}$ method. The fold change of each target gene was calculated using the following formula:

$$Fold\ change = 2^{-((C_{T,target\ gene\ DG} - C_{T,GAPDH\ DG}) - (C_{T\ target\ gene,CG} - C_{T\ GAPDH,CG}))}$$

where *DG* is the differentiation group and *CG* is the control group.

Primers concentrations were optimized. All combination of primer concentrations (50 nM, 300 nM and 900 nM) of forward and reverse primers were tested. Concentrations of primers chosen were shown to have a precise melt curve and did not form primer-dimers (Figure S6 and S7).

Table 2 - **Primers sequences used for RT-PCR**. Genes under study were collagen type II, aggrecan, Sox9 and runx2. GAPDH was used as a housekeeping gene.

TARGET GENE	**SEQUENCE**
GADPH F′	5′-CTCTGCTCCTCCTGTTCGACA-3′
GADPH R′	5′-ACGACCAAATCCGTTGACTC-3′
SOX9 F′	5′-GACTTCCGCGACGTGGAC-3′
SOX9 R′	5′-GTTGGGCGGCAGGTACTG-3′
ACAN F′	5′-TCGAGGACAGCGAGGCC-3′
ACAN R′	5′-TCGAGGGTGTAGCGTGTAGAGA-3′
COL2A1 F′	5′-GGCAATAGCAGGTTCACGTACA-3′
COL2A1 R′	5′-CGATAACAGTCTTGCCCCACTT-3′
RUNX2 F′	5′-GGAGTGGACGAGGCAAGAGTTT-3′
RUNX2 R′	5′-AGCTTCTGTCTGTGCCTTCTGG-3′

2.4. Nuclear staining and immunofluorescence

DAPI is a fluorescent dye that has affinity to DNA [123]. To evaluate effective number of cells attached and nucleus area, cells were stained with this dye. For that, MSCs were cultured on all PDMS substrates (21 kPa, 18 kPa, 3 kPa, 1 kPa and 0.93 kPa) and TCPs. After 24, cells were fixed with 4% (w/v) paraformaldehyde (Sigma), as described before (section 2.2). Then, cells were permeabilized with PBS-0.1% Triton-X 100 (v/v) for 20 minutes. After being washed twice with 1x PBS, cells were incubated for 5 minutes with PBS-0.1% Tween (v/v). Finally, cells were incubated in the dark with a DAPI solution (0.8 μg/μl) for 5 minutes and washed 3 times with 1x PBS.

Images were collected on a fluorescence microscope (Zeiss Axiovert 200M), using AxioVision release 4.8 software (Zeiss). For each PDMS substrate, twelve images were randomly acquired and analyzed on Fiji/ImageJ software. Images were converted to a binary scale. Watershed tool was applied to identify nucleus merged

together. The software automatically counted the number of cells on each field (particles smaller than 100 μm² were considered background). Since the area of each field acquired was known, real cell density could be calculated. Moreover, Fiji/ImageJ automatically calculated nucleus area.

2.5. Proliferation kinetics of MSCs on PDMS substrates

Cell therapy requires a high number of cells [19]. Thus, MSCs need to be previously expanded *in vitro*. Therefore, we evaluated MSCs capacity to proliferate on PDMS substrates - 18 kPa and 1 kPa and TCPs. First, we expanded P1 cells on TCPs. Then, at P2, cells were seeded at 10.000/cm² on TCPs, 18 kPa and 1 kPa substrates. For the following passages, MSCs were seeded at 8.000/cm². MSCs were proliferated until passage 6 and stiffness was kept constant. Passages procedures were performed according to what was previously described on section 2.1. For each passage on PDMS substrates, PDMS was functionalized according to section 2.6.1.

To evaluate kinetics of MSCs on different substrates, population doubling (PD) – the number of times that a population has doubled - and generation time (GT) – the period of time that a population needs to double its size - was calculated according to the following formulas [124]:

$$PD = \frac{log_{10}(N_H) - log_{10}(N_I)}{log_{10}2}$$

$$GT = \frac{log_{10}2 \times \Delta t}{log_{10}(N_H) - log_{10}(N_I)}$$

where N_H is the number of harvested cells, N_I is the number of seeded cells, and Δt is the number of days of cells in culture.

Total number of cells (TNC) was determined by accumulative counting of the number of cells on each passage [125]. TNC is calculated using the following formula, where B represents the total number of cells in the previous passage:

$$TNC = \frac{N_H \times B}{N_I}$$

TNC accounts for the theoretical number of cells that could be obtained if no cells were discarded between each passage.

2.6. Synthesis and functionalization of PDMS substrates

PDMS is an elastomer that polymerizes in the presence of a curing agent, at moderately high temperatures and in the presence of platinium (Figure 10) [126,127]. Elastomer has ethylene groups while curing agent are shorter chains and methyl groups. Crosslinking reaction is a platinum-catalyzed hydrosilylation. Initially, Pt(ii) is coordinated by two ethylene groups. Then, Pt(ii) is oxidized to Pt(iv) and becomes coordinated to the curing agent instead. At this moment, a hydrogen binds to ethylene group and Pt(iv) is reduced to Pt(ii), enabling it to be coordinated with two ethylene elastomers again and an ethylene bridge is formed.

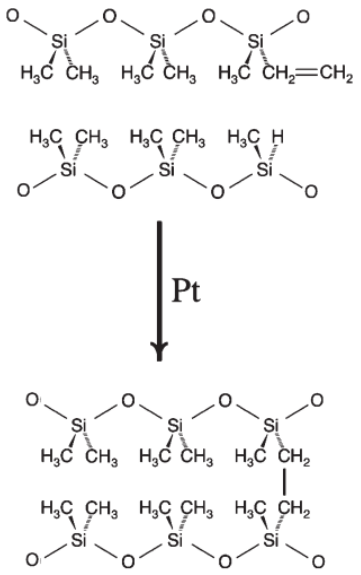

Figure 10 - **PDMS polymerization reaction [127]**. It is a platinum-catalyzed hydrosilylation. Initially, Pt(II) is initially coordinated by two ethylene groups. Pt(ii) is oxidized to Pt(iv) and becomes coordinated to the curing agent instead. At this moment, a hydrogen binds to ethylene group and Pt(iv) is reduced to Pt(ii), and an ethylene bridge is formed.

Therefore, the higher the concentration of the curing agent, higher the extension of the reaction and gel polymerization. Five different formulations with different proportions of PDMS (Sylgar 184) elastomer:curing agent – 10:1, 30:1, 40:1 50:1 and 60:1 - were prepared. Substrates were polymerized on culture plates (Corning Star) and cured during 4 hours at 80 °C - maximum temperature 82 °C on an oven (Memmert).

For rheology characterization, PDMS substrates were polymerized on top of vinyl paper to allow manipulation of the substrate after polymerization and ensure adherence of the system to the rheometer's base.

2.6.1. Functionalization of PDMS substrates

PDMS is hydrophobic, hindering cell-substrate adhesion [128]. Moreover, the elastomer does not provide cells with anchoring points (like ECM proteins) *per se*.

Cells do not adhere to crude PDMS substrates. In order to overcome this, modification of the surface has been proposed by different research groups [105,106]. On the present study, surface was oxidized by the addition of a solution containing water, hydrochloric acid (37%), hydrogen peroxide solution, which forms hydroxyl groups and makes the surface more hydrophilic. For 10:1 and 30:1 PDMS formulations, 3 parts of water, 1 part of hydrochloric acid and 1 part of hydrogen peroxide were mixed; for the other PDMS formulations a solution with 5 parts of water, 1 part of hydrochloric acid and 1 part of hydrogen peroxide was prepared. Oxidation solution was added to PDMS surface for 5 minutes. Secondly, a solution of 10% (v/v) 3-aminopropyltriethoxylsilane (3-APTES) in 96% (v/v) ethanol was prepared and added to the surface for 30 minutes. This solution to generates amine groups on the surface. This step was followed by three 10 minutes washes, shaking, with ddH_2O. Finally, a 3% (v/v) glutaraldehyde in 1x PBS solution was added to PDMS surface for 20 minutes, followed by three 5 minutes washes with ddH_2O. This reagent acts like a crosslinking agent, forming a Schiff's base between aldehyde and amines of 3-APTES [106,129]. Together, these modifications enable proteins to bind covalently to PDMS surface. Functionalization of PDMS surface is resumed on Figure 11. Finally, for PDMS sterilization, functionalized substrates were left for 30 minutes on the flow cabinet under UV light.

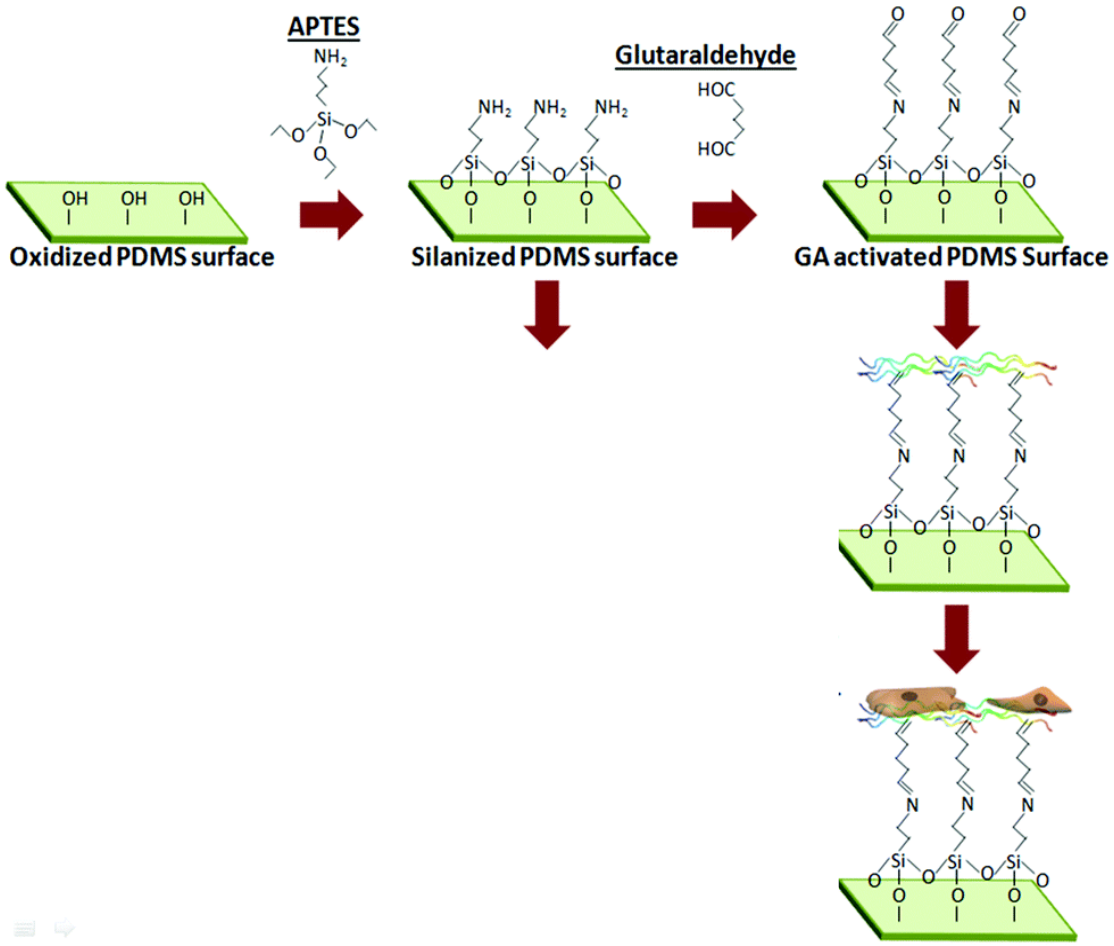

Figure 11 - **PDMS surface functionalization** [106]. First, surface is oxidized with a solution of water, hydrochloric acid and hydrogen peroxide. Addition of 3-APTES solution forms amine groups on the surface that react with glutaraldehyde, forming a Schiff's base. These modifications allow the covalent bonding between coating proteins – fibronectin and collagen type I - and PDMS surface.

After sterilization, a coating solution was prepared. Coating proteins - Human plasma purified Fibronectin (FN) and rat tail type I Collagen (both from Millipore) - were diluted in 1x PBS and added to the surface. The final coating solution contained 1.4 μg of FN and 2.4 μg of collagen I *per* cm² of substrate. Hydrogels were incubated with the coating solution for 4 hours, at 37 °C. Non-ligand proteins were washed twice with sterile 1x PBS and cells were seeded.

2.6.2. Functionalization of glass substrates

Standard protocols use TCPs dishes to culture cells. However, literature does not describe any methodology to effectively functionalize TCPs surface and guaranty that proteins are covalently attached. Therefore, to minimize differences between control and experiment groups, in some experiments TCPs was replaced by glass, since it can be functionalized and stiffness is similar. Functionalization is similar to the one described before for PDMS (section 2.6.1), except for the oxidation step, whereas a 1M NaOH solution is added to the surface during 30 minutes, to hydroxylate glass surface and activate it [130].

2.7. Rheological characterization of PDMS substrate

The rheological characterization of hydrogels was determined by small-strain oscillatory shear tests using a Kinexus Pro rheometer and rSpace sofware Malvern fitted with a parallel plate geometry (stainless steel wrinkled plate). Frequency sweeps were performed from 10 to 0.1 Hz (five reads per decade) with a deformation of 10 millistrain (mε) at 37 °C. A 0.5 N normal force was used to guarantee adherence. The Young's modulus (E) was calculated from the measured viscoelastic shear modulus using the formula $E = 2 \times G' \times (1 + \nu)$ where G′ is the shear storage modulus measured at 1 Hz and ν is Poisson's ratio, assumed to be 0.5 for materials that do not vary its volume upon stretching.

2.8. PDMS thickness assay

Cured 10:1 PDMS substrates were detached from the TCPs plate, since it was the only formulation that could easily be removed. Due to its concavity, the substrate was sliced on the center. Slices were observed on the contrast phase microscope (Axiovert 40C). Thickness of central zone of PDMS was calculated using Axiovision Microscope Software.

2.9. Statistical analysis

Statistical analysis was performed on GraphPad prism 7 software. Non-parametric tests were performed, since the number of repetitions was small. To compare two groups, a Mann-Whitney test was performed. For multiple comparisons, a Kruskal-Wallis test was run to assess statistically significant differences. Additionally, a Dunn's multiple comparison test was performed to analyze which group(s) were diverging. All tests took in consideration that significance level (α) was 0.05. Graphics represent mean and SEM. Additionally, p values are represented: * $p<0.05$; ** $p<0.01$; *** $p<0.001$.

3. Results

3. Results

3.1. PDMS substrates can trigger a mechanical stimulus on MSCs

We first evaluated if substrates stiffness were capable of triggering a mechanical stimulus on MSCs. On the present study, we confirmed that substrate thickness (section 3.1.1) is enough to trigger a mechanical stimulus. Also, we acknowledged that that substrate stiffness is not influencing cell density (section 3.1.2) but it is modulating nucleus area (section 3.1.3) of MSCs.

3.1.1. PDMS substrates are 315 μm thick

The literature indicates that a minimal thickness of the substrate is required so that cells can effectively "sense" substrate stiffness [131]. It was described that cells cultured on thin substrates can "fell" the rigidity of the structure on which the hydrogel was polymerized on top of. Hence, we measured the thickness of 10:1 substrate. For that, we detached the substrate from the culture dish, sliced it on the central zone. Images collected by contrast phase microscopy were analyzed and thickness was measured. This substrate formulation was chosen because it was the only possible to rip out from the plate where PDMS was poured for curing. Since volume is constant in all formulations, we assumed that no significant differences would be found on the final thickness. PDMS hydrogels are 315.5 ± 23.3 μm thick (Figure 12). Substrates need to be thicker than 100 μm to trigger a mechanical stimulus [131]. Accordingly, substrates synthetized are thick enough to initiate a signaling cascade in response to substrate stiffness.

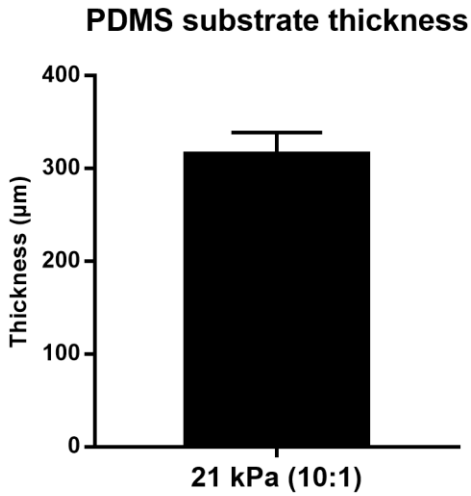

Figure 12 - **Thickness of 10:1 PDMS substrate**. On average, 10:1 PDMS substrate is 315.5 ± 23.3 µm thick (n=5, 26 fragments). Bars represent mean + SEM.

3.1.2. Cells density does not differ between substrates

Mechanical stimulus triggered by a stiff substrate modify cell cytoskeleton, and consequently their shape [70,81]. On a stiff substrate, intracellular tension increases, which stimulates actin polymerization, stress fibers formation and development of FA, which increases cell spreading. MSCs cultured on soft substrate exhibit a poorly define cytoskeleton, are less "anchored" to the substrate and are rounder and smaller (details are described on section 1.2.2). These modifications on cell shape induced by matrix stiffness lead to differences on apparent cell density. Also, when MSCs are transferred from TCPs to a substrate with different stiffness, differences on the rigidity could be associated to cell loss. To investigate if substrate stiffness was significantly influencing cell density, we cultured cells on PDMS substrates with different stiffness and TCPs for 24h. Then, MSCs were stained with DAPI and

observed on a fluorescence microscope (Figure S1). Images were analyzed and the real number of adherent cells was calculated (Figure 13). No significant differences were found between substrates with different stiffness (Kruskal-Wallis test $p>0.05$ and Dunn's multiple comparison test $p>0.05$). Despite cells cultured on soft substrates are smaller, real cell density does not differ between PDMS substrates and TCPs.

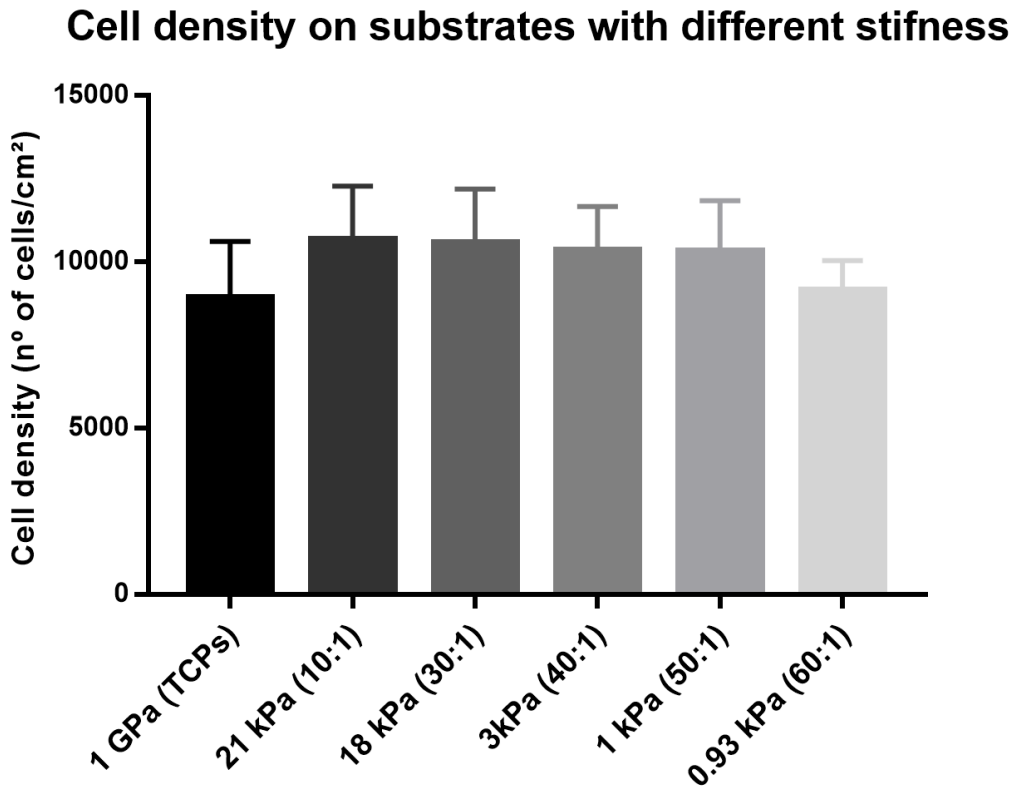

Figure 13 – **Cell density does not differ between substrates**. After 24h, cell density is, on average, 10.000/cm² on all substrates, after 24h. No significant differences on cell density were found between the substrates (n=5) (Kruskal-Wallis test $p>0.05$ and Dunn's multiple comparison test $p>0.05$). Bars represent mean + SEM.

3.1.3. Nucleus area decreases on softer substrates

Intracellular tension increases on cells growing on a stiff substrates [70]. LINC complex connects the nuclear envelope to the cytoskeleton [77]. As a result, intracellular tension can be transmitted to the nucleoskeleton. Modifications on nuclear tension can modulate nucleus area [80]. Similar to what was previously described to the cytoskeleton, nucleus is more flattened on cells cultured on stiff substrate, and consequently its area increases. On soft substrates, nucleus area of MSCs decreases. To be certain that cells were effectively responding to the substrate, we evaluated nucleus area on all PDMS substrates and TCPs. We cultured cells on PDMS substrates with different stiffness and TCPs for 24h. Then, MSCs were stained with DAPI and observed on a fluorescence microscope (Figure S1). Images were analyzed and nucleus area was calculated. After 24h, nucleus area decreased significantly (around 35%) on the 0.931 kPa substrate, when compared to TCPs (Kruskal-Wallis test $p<0.05$ and Dunn's multiple comparison test $p<0.01$) (Figure 14). Additionally, it is possible to see a decreasing tendency of nucleus area along with substrate softening.

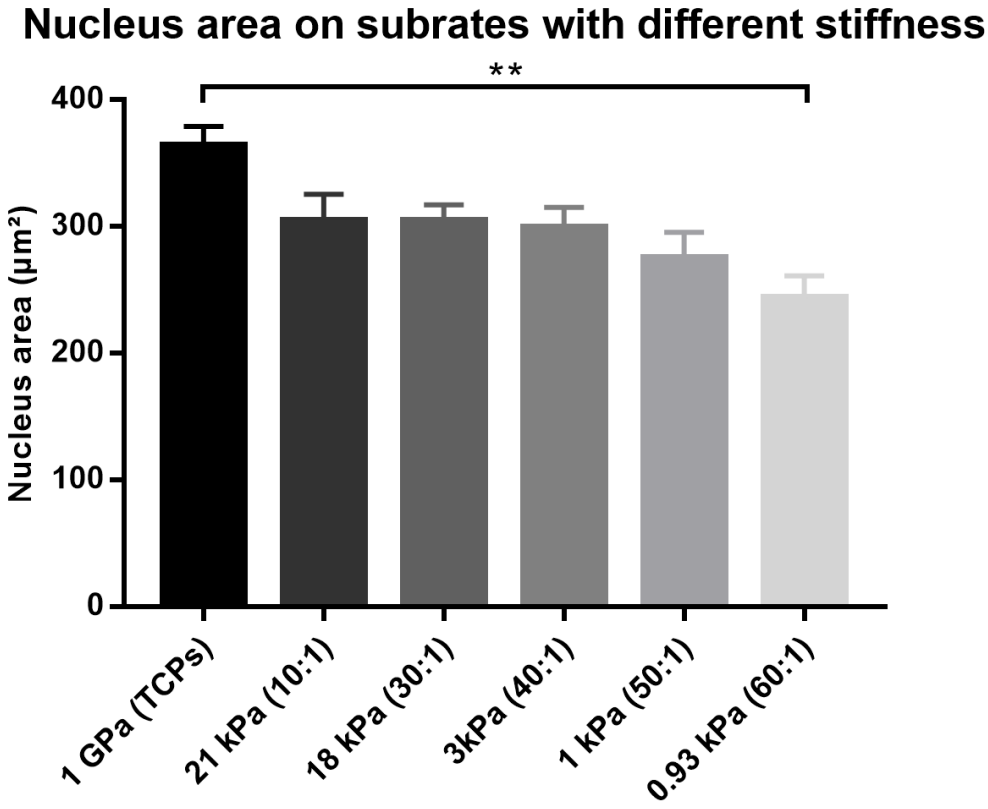

Figure 14 - **Nucleus area on substrates with different stiffness**. Nucleus area of cells cultured on 0.93 kPa substrate is significantly lower than cells cultured on TCPS (n=5) (Kruskal-Wallis test $p<0.05$ and Dunn's multiple comparison test $p<0.01$). After 24h, nucleus area is, in average, 364 ± 33.49 µm² on TCPS, 304.84 ± 46.42 µm² on 21 kPa substrate, 304.42 ± 28.16 µm² on 18 kPa substrate, 299.48 ± 35.22 µm² on 3 kPa substrate, 275.46 µm² ± 44.87on 1 kPa substrate and 243.74 µm² ± 39.05 on 0.931 kPa substrate. Bars represent mean + SEM.

On the present study, we could synthetize hydrogels thick enough to trigger mechanical stimulus. This was corroborated by the declining tendency of the nucleus area observed along with substrate softening. Also, we could confirm that substrate stiffness did not influence the real cell density. Thus, we can conclude that substrate stiffness of synthetized PDMS substrates is modulating MSCs.

3.2. Rheological assessment of viscoelastic properties of PDMS substrates by rheometry

Rheology studies viscoelastic properties of materials. This technique is capable to determine not only storage/elastic modulus - G' - but also loss/viscous modulus – G'' – of materials. G' and G'' are correlated by tan δ: if higher then 1, means that the material is predominantly viscous (for details, see section 1.3.1). To study elastic and viscous properties of different formulations of PDMS substrates, a rheologic analysis was carried out, using a rheometer. Different formulations of PDMS - 10:1, 30:1, 40:1, 50:1 and 60:1 (elastomer:curing agent) – were cured for 4 hours, at 80 °C. Using a rheometer, we performed a frequency sweep test (0.1 – 10 Hz) on all PDMS formulations (Figure 15). Analysis of elastic and viscous modulus behavior on a range of frequencies enables us to infer about viscoelatic properties of PDMS substrates. 10:1 substrate is a completely polymerized hydrogel, since its shear modulus (G' and G'') are independent of the frequency; additionally, tan δ is below 1. For 30:1 and 40:1 substrates, frequency slightly influences G''. Also, tan δ is below 1. This suggests that despite viscous properties also contribute to the hydrogel structure, elastic properties are still dominant for 30:1 and 40:1 formulation. Finally, for 50:1 and 60:1 substrates, G' and G'' are highly frequency dependent. At high frequencies, tan δ is bigger than 1 for 50:1 hydrogel; for 60:1 substrate, tan δ is superior to 1 even at low frequencies, suggesting a major viscous behavior. Therefore, we can conclude that 50:1 and 60:1 viscous properties play a significant role on the structure of this hydrogels. Thus, apart from different stiffness, each PDMS formulation has specific viscous and elastic properties.

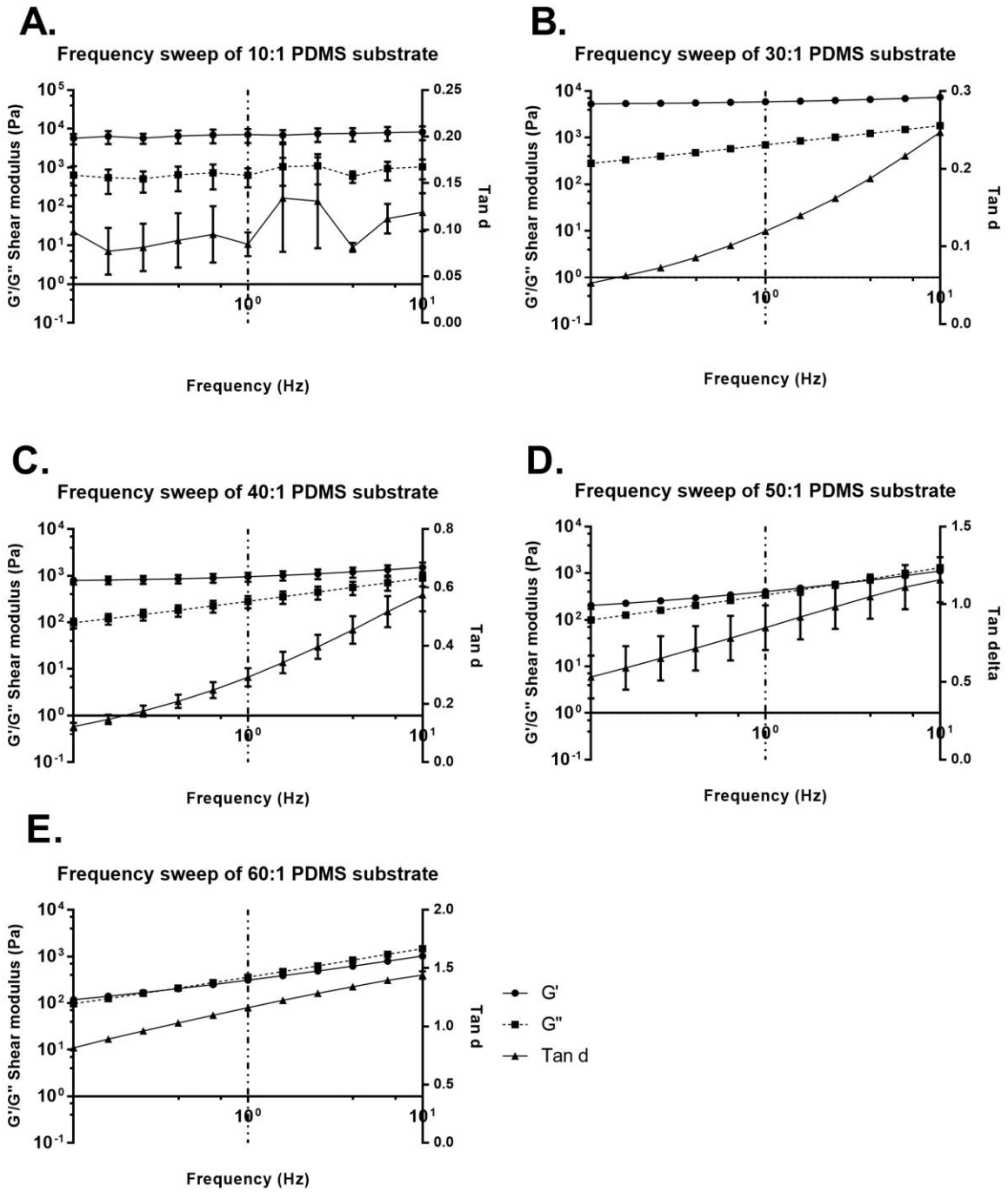

Figure 15 – **Viscoelatic properties of different PDMS formualtions** (n=3). Representative rheological measurements of elastic modulus, G', G'' and tan δ (by rehometry) of five different PDMS formulations, across a frequency sweep (0.1 Hz – 10 Hz) at a constant milistrain (10) at 37 °C. **A:** 10:1 hydrogel is predominantly elastic, since G' and G'' modulus are independent of the frequency. **B:** For 30:1 substrate, G'' is slightly dependent of the frequency, but its elastic properties are still dominant. **C:** 40:1 hydrogel behavior is similar to 30:1 formulation, despite that tan δ is higher. **D:** 50:1 substrate is highly frequency dependent, suggesting a viscous behavior. **E:** 60:1 hydrogel behavior is similar to 50:1 hydrogel, though, tan δ is higher.

We could correlate G' (storage modulus) and Young's Modulus of our substrates through the following formula - $E = 2 \times G' \times (1 + v)$. Young's modulus of PDMS hydrogels vary from 21 kPa to 0.93 kPa, at 1 Hz (Figure 16). Statistical differences were found (Kruskal-Wallis test $p<0.001$) but it was not possible to identify specific groups that diverged (Dunn's multiple comparison test $p>0.05$), suggesting the need for more replicates to validate these results.

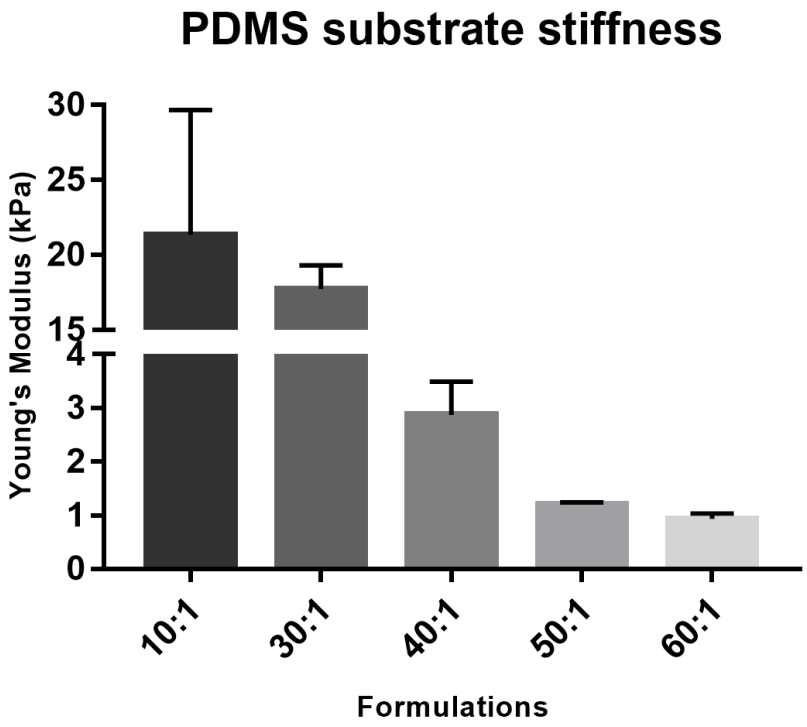

Figure 16 - **Young's modulus of different PDMS substrates formulations**. Young's modulus is 21.362 ± 11.754 Pa (21 kPa) for 10:1 formulation, 17.735 ± 2.234 Pa (18 kPa) for 30:1 formulation, 2.870 ± 1.083 Pa (3 kPa) for 40:1 kPa, 1209 ± 55.21 Pa (1.2 kPa) for 50:1 formulation and 931.8 ± 149.8 Pa for 60:1 formulation. Young's modulus was obtained at 1 Hz (n=3). Statistical differences were found (Kruskal-Wallis test $p<0.001$ and Dunn's multiple comparison test $p>0.05$). Bars represent mean + SEM.

On this present study, we synthetized PDMS hydrogels with a wide range of stiffness – 21 kPa to 0.93 kPa. Also, soft substrates have a major contribution of viscous properties.

3.3. Chondrogenic differentiation of MSCs is modulated by substrate stiffness

MSCs can differentiate into chondrocytes [20]. Protocols commonly used mention that differentiation should last 14 to 21 days [132–134]. On the present study, we reduced this period to 9 days to emphasize the significance of mechanical stimulus on chondrogenic differentiation. MSCs were seeded on different substrates - 21 kPa, 17 kPa, 3 kPa, 1 kPa and 0.93 kPa substrate and glass – and induced to differentiate. At day 9, cells were stained with Safranin O. Safranin O dye has affinity to GAG and it is widely used for cartilage staining [135–137]. To evaluate if cells were synthetizing GAG, differentiated cells (Figure 17) and control cells (Figure 18) were stained with Safranin O and images were collected. On 1 kPa substrate it was possible to see the formation of prominent cellular aggregates, typical of chondrogenesis, in the case of differentiated cells. Also, these agglomerates show a strong red staining, suggesting an intensive GAG synthesis. On other substrates, differentiated cells denoted a tenuous red coloration, implying the beginning of cell condensation; however, this agglomeration was not so mature when compared to 1 kPa substrate. These tenuous staining indicated that GAG were being less expressed. Control groups did not show a red coloration, except for glass substrate, where is possible to see a weak red staining. Robust Safranin O staining and agglomerates formation on 1kPa substrate strongly suggest that this stiffness potentiates chondrogenic differentiation of MSCs.

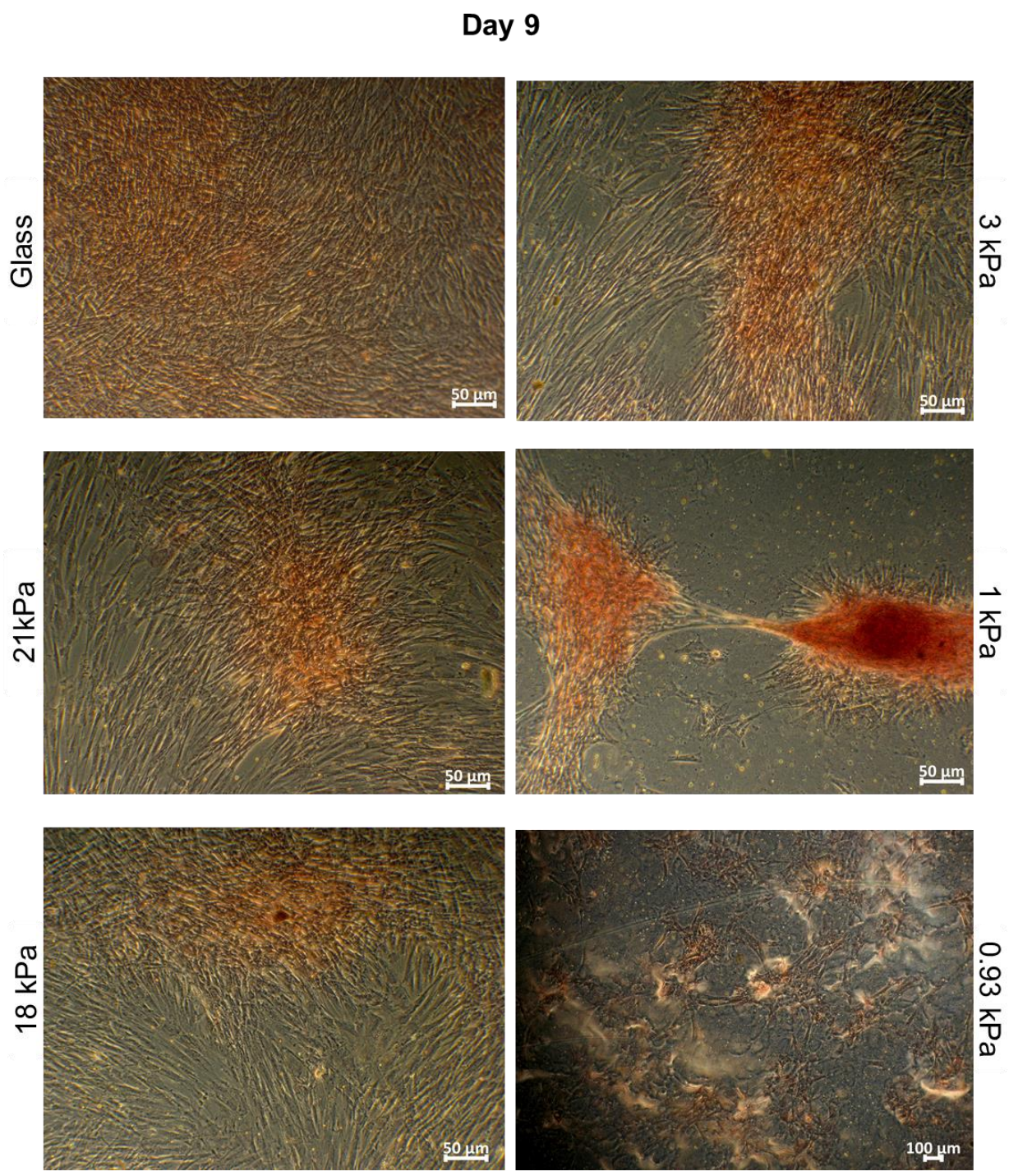

Figure 17 - **Safranin O staining of MSCs cultured with DM for 9 days**. MSCs were cultured different substrates: on the left glass (top), 21 kPa (center) and 17 kPa (bottom); on the right 3 kPa (top), 1 kPa (center) and 0.93 kPa (bottom). At day 9, cells were stained with Safranin O. Images were collected on a contrast phase microscope.

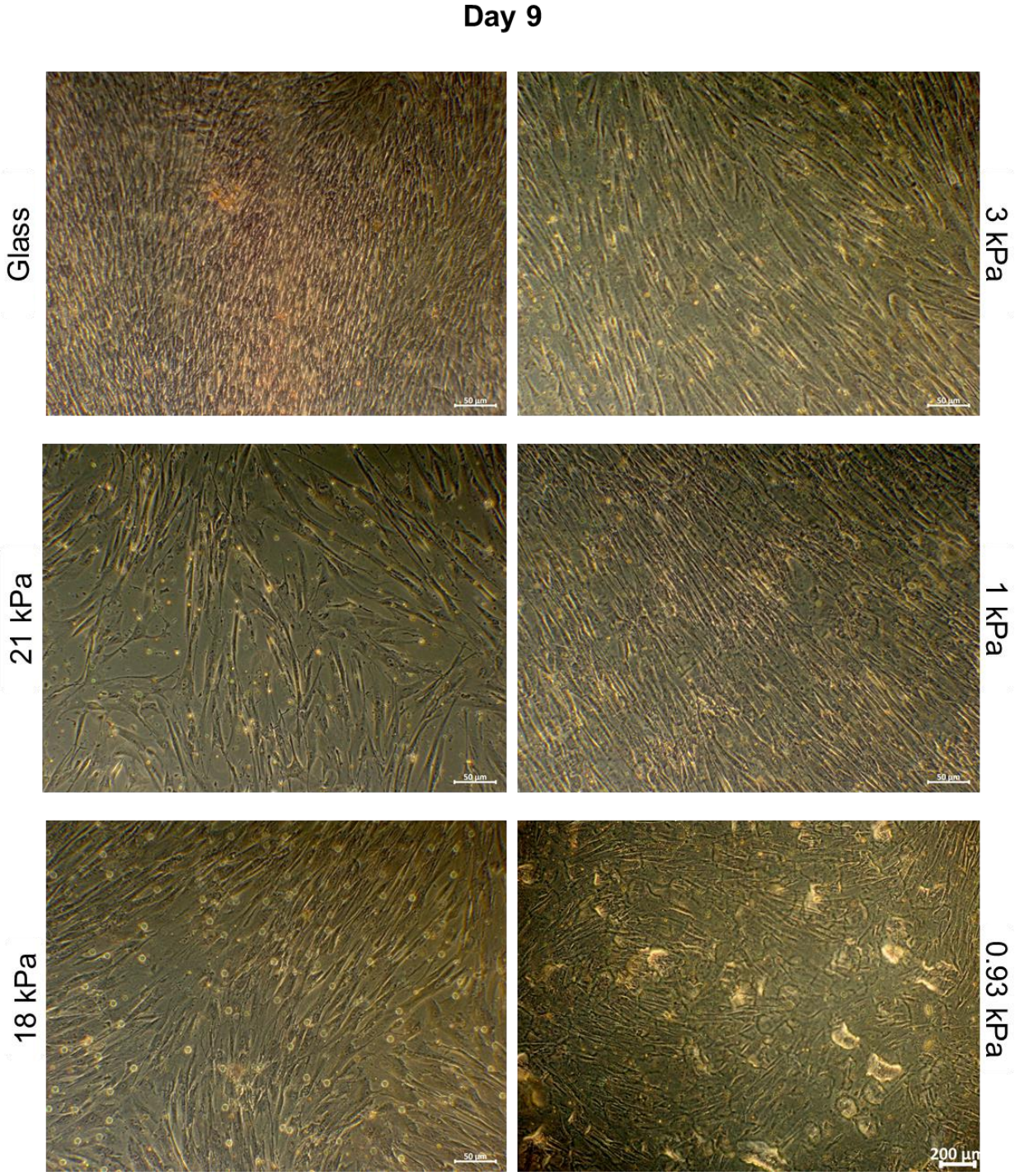

Figure 18 - **Safranin O staining of MSCs cultured with PM.** MSCs were cultured different substrates: on the left glass (top), 21 kPa (center) and 18 kPa (bottom); on the right 3 kPa (top), 1 kPa (center) and 0.93 kPa (bottom). At day 9, cells were stained with Safranin O. Images were collected on a contrast phase microscope.

3.3.1 Establishment of a semi-quantitative assay for chondrogenic differentiation

Literature lacks information about a simple, reliable, and cheap method to quantify chondrogenesis. A research group proposed a methodology that used SO fluorescence to quantify synthetized GAG and infer about chondrogenesis [118]. However, this study normalized SO fluorescence using DAPI fluorescence *per* well. Nevertheless, DAPI staining requires the use of a fluorescence microscope, an expensive equipment. Here, we propose an alternative method to estimate cell number, using Giemsa dye absorbance. Giemsa dye can intercalate with DNA and stain the nucleus [111,112]. It has already been described that Giemsa absorbance (550 nm) is proportional to the number of adherent cells [113]. Since absorbance could not be read directly on culture plates, we evaluated if after extraction this method was still reliable to estimate cell number. For that, we seeded cells at 3.000/cm², 10.000/cm², 20.000/cm² and 30.000/cm². After 24h, MSCs were fixed and stained with Giemsa. We verified that Giemsa OD is proportional to the total number of seeded cells (Figure 19). Therefore, this method is still reliable to estimate about the total number of cells after extraction. Thus, Giemsa absorbance can be used to normalize results.

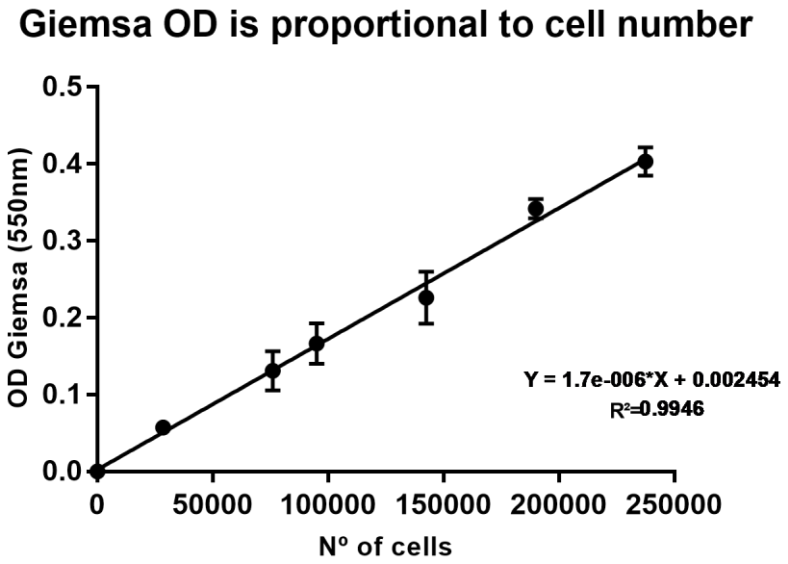

Figure 19 - **Giemsa OD at 550nm is directly proportional to the total of cells seeded on TCPs**. R value ~ 1 shows a strong correlation between extracted Giemsa OD and the total number of cells seeded (n=3).

Safranin O staining is known to be proportional to proteoglycans content [116]. Recently, literature described a semi-quantitative assay for glycosaminoglycans, using Safranin O fluorescence, to infer about chondrogenic differentiation of MSCs [118]. Proteoglycans are a major component of cartilaginous ECM. Hence, an increase of GAG - glycosylated proteoglycans - expression leads to an increase of SO fluorescence, which suggests that cells are differentiating. On the present study, we adapted this method normalizing SO fluoresce to absorbance of extracted Giemsa, regardless of normalizing it to DAPI fluorescence. MSCs were seeded on different substrates - 21 kPa, 17 kPa, 3 kPa, 1 kPa and 0.93 kPa substrate and glass – and induced to differentiate. At day 9, cells were stained with Safranin O. Bounded dye was extracted with ethanol and fluorescence was read. Fluorescence of SO was normalized to Giemsa OD. On the present study we established a cheap, fast and reliable semi-quantitative assay to assess chondrogenic differentiation of MSCs on PDMS and glass substrates (Figure 20). Results indicate that SO fluorescence

increases significantly on differentiated cells cultured on 1 kPa substrate, when compared to its respective control (Figure 20A) (Mann-Whitney test $p<0.05$). Furthermore, we state that the SO fluorescence augments significantly on cells cultured on 1 kPa substrate when compared to cells cultured on glass substrates (Figure 20B) (Dunn's multiple comparison test $p<0.05$). Together, these results suggest that 1 kPa substrate enhances GAG expression. Thus, we can deduce that 1 kPa enhances chondrogenic differentiation of MSCs.

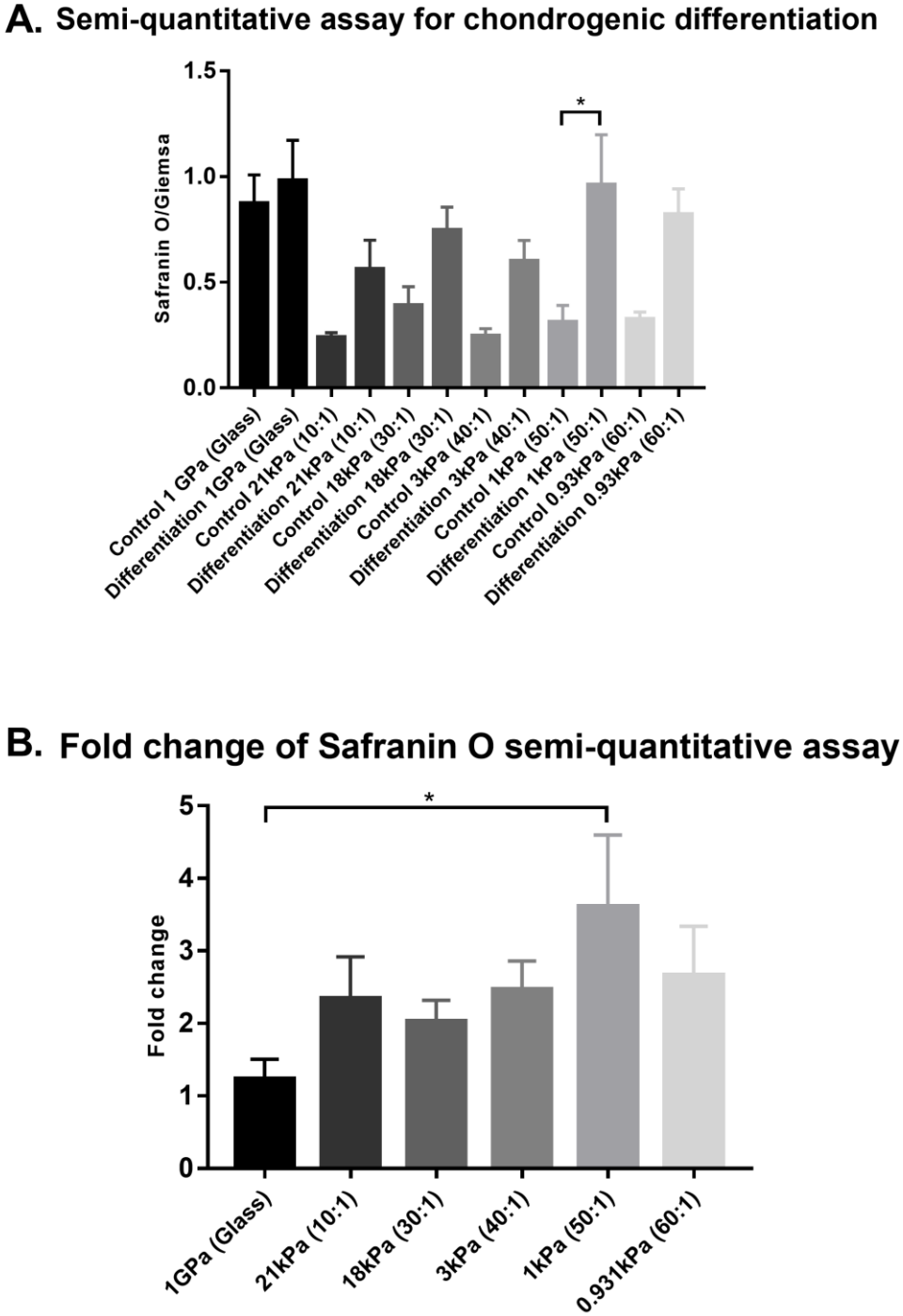

Figure 20 - **Semi-quantitative assay for chondrogenic differentiation.** (n=4) MSCs were induced to differentiate for 9 days. Control groups were cultured with PM for 9 days. **A (top):** GAG semi-quantitative assay. Safranin O fluorescence was normalized to Giemsa OD at 550nm. SO fluorescence increases significantly on 1 kPa substrates, when compared to its respective control (Mann-Whitney $p<0,05$). **B (bottom)**: Fold change of normalized SO fluorescence. SO fluorescence on 1 kPa increases significantly when compared to glass (Dunn's multiple comparisons test $p<0,05$). Together, these data suggest that 1 kPa substrate enhances GAG synthesis, and therefore chondrogenic differentiation. Bars represent mean + SEM.

3.3.2. Assessment of chondrogenic markers expression by RT-PCR

GAG semi-quantitative assay previously described (section 3.3.1) suggested that 1 kPa enhances chondrogenic differentiation. Though, this assay needed to be validated by a well-established molecular biology technique, as RT-PCR. MSCs were seeded on 18 kPa, 1 kPa substrates and glass – and induced to differentiate. At day 9, RNA was isolated and expression of specific chondrogenic markers - Sox9, ACAN and COL II – was investigated on control and differentiated cells. As a negative control, we investigated runx2 (an osteogenic marker) expression. GAPDH was used as a housekeeping gene to normalize results. In general, RT-PCR results show high standard deviations, impairing a precise analysis of the results (Figure 21). No significant differences were found between substrates on chondrogenic or osteogenic markers. Cells cultured on glass and PDMS substrates were expressing both Sox9 (Figure 21A) and runx2 (Figure 21D), suggesting that cells were not naïve as desired [138]. Also, aggrecan was preferentially expressed on glass substrate (Figure 21B). ACAN was not expressed on cells cultured on 17 kPa substrate and it was only expressed on two replicates on cells cultured on 1 kPa. It is not accurate to assess collagen type II expression due to discrepancies between replicates (Figure 21C). Taken together, this data is not enough to validate GAG assay results, that suggested 1 kPa as the optimal stiffness for chondrogenic differentiation of MSCs.

In summary, GAG semi-quantitative assay suggests 1 kPa as the optimal stiffness for chondrogenic differentiation. In the future, these results need to be complemented by RT-PCR results using naïve MSCs.

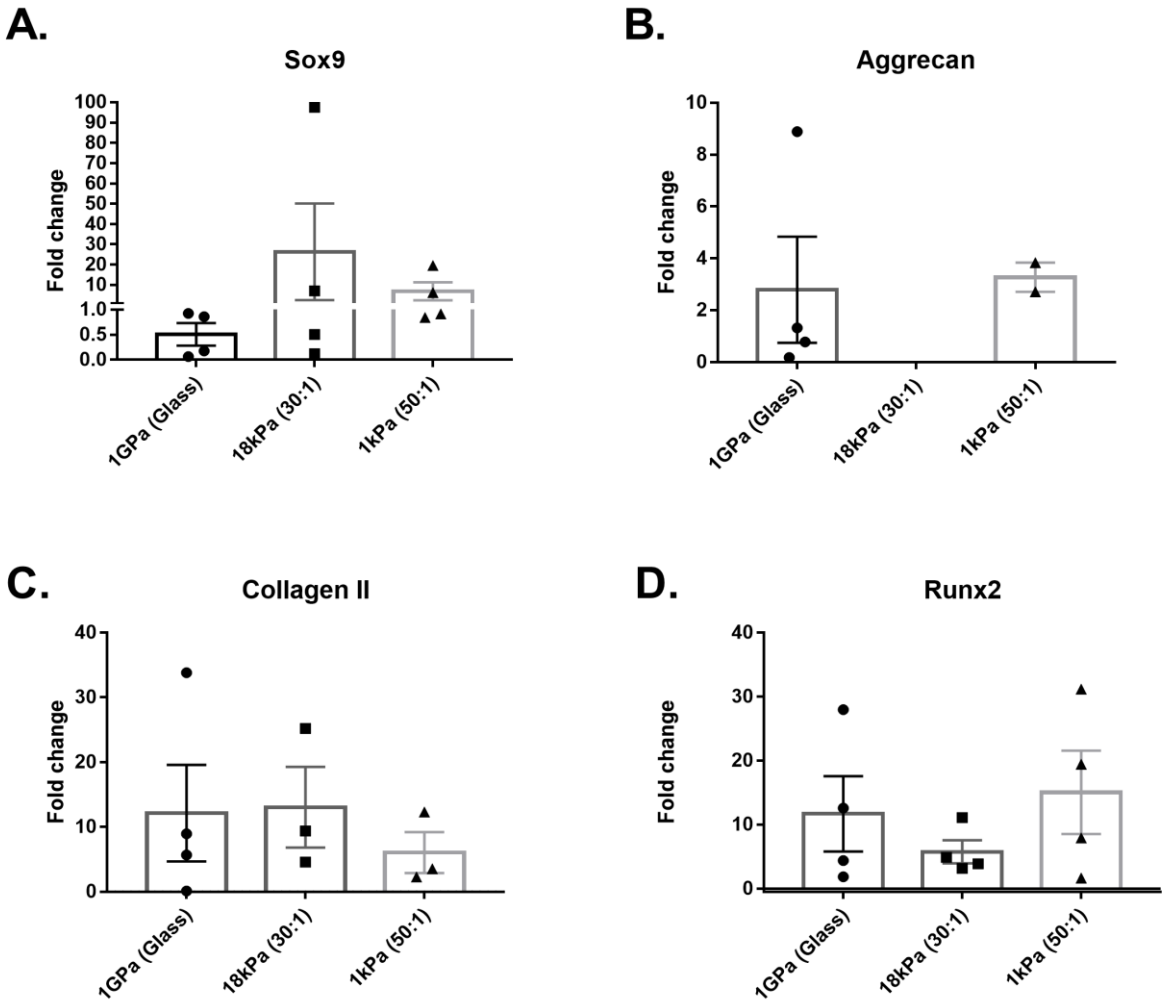

Figure 21 - **Expression of chondrogenic markers and runx2, at day 9**. Sox9 (A), ACAN (B) and Collagen type II (C) expression was analyzed. Runx2 was used as a negative control (D). No significant differences were found on any gene analyzed (Kruskal-Wallis test $p>0.05$ and Dunn's multiple comparisons test $p>0.05$) (n=4). Cells were expressing both Sox9 and runx2, suggesting they are not naïve as desired. Aggrecan was predominantly expressed on glass substrates. Bars represent mean + SEM.

3.4. Proliferation kinetics study of MSCs on PDMS substrates

"Mechanical memory" is an emerging concept [138]. It has been described that if P1 MSCs are maintained more than 10 days on TCPs, YAP and runx2 – an osteogenic marker - move permanently to the nucleus and differentiation is hampered (see details on section 1.2.2.2). Therefore, differentiation on cell lines other than osteogenesis will be biased. We hypothesized that if cells can be proliferated on softer substrates, it would be possible to expand cells and retain YAP and runx2 on the cytoplasm, so that differentiation is not biased. Since cell therapy requires numerous cells, this would be a great achievement [19]. We evaluated kinetics of cell proliferation of 18 kPa and 1 kPa substrate. For that, we expanded MSCs on TCPs, 18 kPa and 1 kPa until passage 6. Results show that proliferation rate of cells growing on PDMS is slower when compared to TCPs (Figure 22). Also, cells cultured on TCPs proliferated extensively until passage 6, while cells expanded on softer substrates are only capable of proliferating until passage 4. Specifically, population doubling decreases significantly on 1 kPa at P3 and on 18 kPa at P6, when compared to TCPs (Kruskal-Wallis test $p<0.05$ and Dunn's multiple comparisons test $p<0.05$) (Figure 22A). Also, generation time was bigger for MSCs proliferated on 18 kPa and 1 kPa substrate, suggesting that they proliferate slower when compared to TCPs (Figure 22B). Additionally, the total number of cells obtained is smaller on PDMS substrates when compared to TCPs (Kruskal-Wallis test $p<0.05$ and Dunn's multiple comparisons test $p<0.05$) (Figure 22C). Specifically, total number of cells is significantly lower on 1kPa at P3, P5 and P6 when comparing to TCPs (Kruskal-Wallis test $p<0.05$ and Dunn's multiple comparisons test $p<0.05$) (Figure 23 C). Comparing 18 kPa and 1 kPa substrate, MSCs cultured on 18 kPa have a more reliable behavior until passage 4 and TNC is slightly higher on 18kPa substrate.

These results suggest 18 kPa substrate as an option to cell proliferation. However, in the future, culture conditions for MSCs proliferation on PDMS need to be optimized.

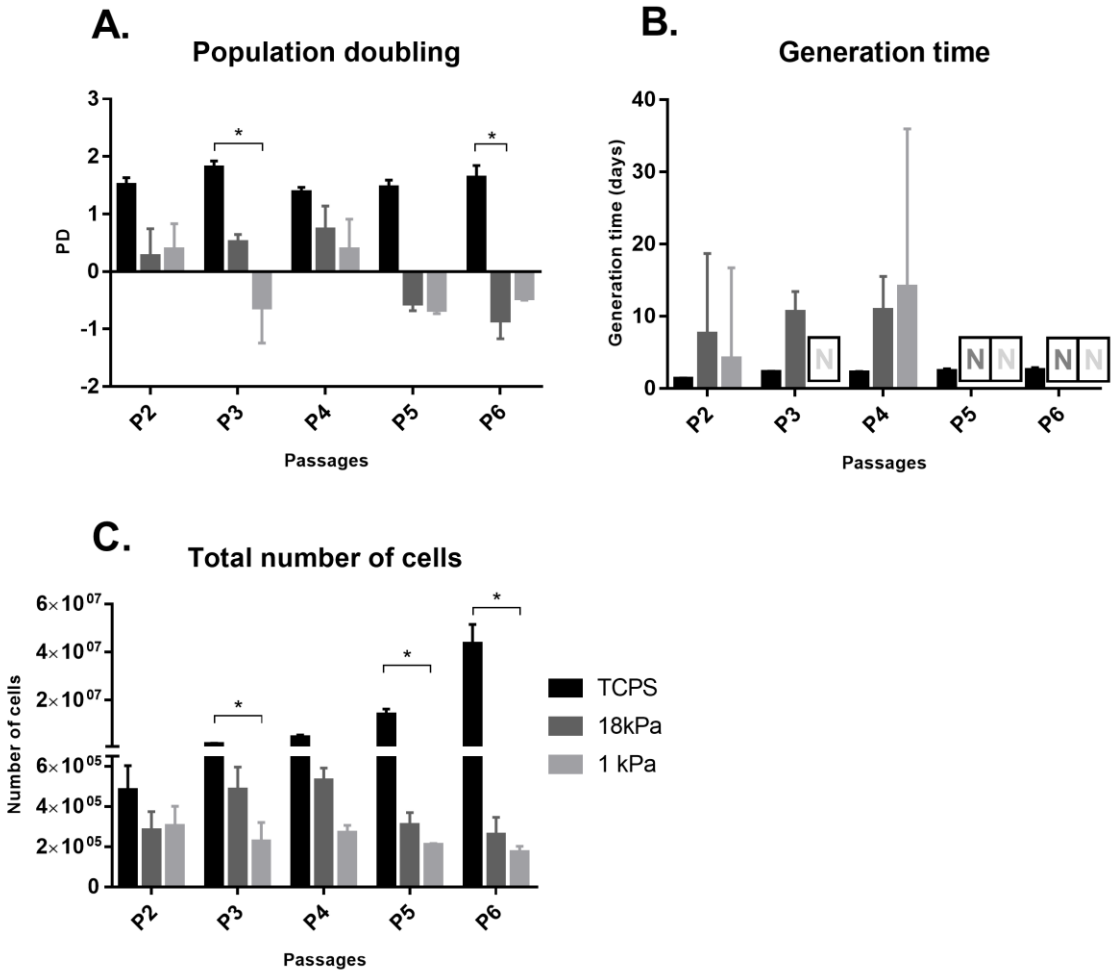

Figure 22 - **Proliferation kinetics of MSCs cultured on TCPs, 18 kPa and 1 kPa substrate.** (A) Population doubling of MSCs cultured on TCPs, 18 kPa and 1 kPa substrate. PD decreases significantly between TCPs and 1 kPa at P3 and between TCPs and 18 kPa at P6 (Kruskal-Wallis test $p<0,05$ and Dunn's multiple comparisons test $p<0,05$). (B) Generation time of MSCs cultured on TCPs, 18 kPa and 1 kPa. In general, generation time is higher for cells cultured on PDMS substrates. GT decreases significantly on 1 kPa substrate at P6, when compared to TCPs P6 (Kruskal-Wallis test $p<0,05$ and Dunn's multiple comparisons test $p<0,05$). (C) Total number of MSCs cultured on TCPs, 18 kPa and 1 kPa substrate. TNC is lower for cells cultured on TCPs. TNC is statistically lower on 1 kPa at P3, P5 and P6, when compared to TCPs P6 (Kruskal-Wallis test $p<0,05$ and Dunn's multiple comparisons test $p<0,05$).

4. Discussion

4. Discussion

It was previously described that MSCs can sense substrate stiffness and modulate their intracellular signaling cascades – mechanotransduction [48,93]. So, in our work, we started by the development of methods for the validation of the experimental conditions, to be sure that substrates prepared were effectively triggering mechanical responses on MSCs. Hence, we evaluated if thickness of the substrate was enough to mechanomodulated intracellular signaling. Literature indicates a range between 20 μm to 100 μm as a minimal thickness required to cells respond effectively to substrate rigidity [131,139,140]. Cells growing on thin gels are able to sense the rigidity of the structure on which the hydrogel was polymerized. In our work, we performed the polymerization of the substrates directly on TCPs plates. If the substrate was not thick enough, MSCs would be responding to 1 GPa. We were able synthetize PDMS substrates with 315 μm (section 3.1.1 – Figure 12). This value was obtained in the central part of the substrate, because after polymerization the hydrogel exhibits a concave form. Concluding, PDMS hydrogels are thick enough to guarantee that MSCs are not "feeling" TCPs stiffness, but hydrogel stiffness.

Despite theoretically thick hydrogels could trigger a mechanical response, we evaluated modifications on nucleus area to be certain that cells were effectively responding to substrate thickness. Cells growing on stiff substrates increase their intracellular tension [70]. Since the nuclear envelope is connected, by LINC complex proteins to the cytoskeleton, tension can be transmitted to the nucleoskeleton [77]. Therefore, nuclear shape is modulated - a "stressed nucleus" is forced by the cytoskeleton to flatten [77,141]. Consequently, these alterations modify nucleus area [80]. Literature indicates that cell spreading is associated with an increase on nucleus area. Additionally, it was shown that nucleus area of cells decreases when cultured

on soft substrates. On this study, we seeded cells on substrates with different stiffness – between 21 kPa and 0.931 kPa – and TCPs and stained MSCs with DAPI. Images, collected by fluorescence microscopy were analyzed and nuclear area was calculated. Nucleus area decreased on cells cultured on soft substrates (section 3.1.3 – Figure 14). Particularly, results indicated that nucleus area is significantly smaller on 0.93 kPa substrate, when compared to TCPs. Also, nucleus area showed a tendency to decline along with substrate softening. This tendency is in accordance to what was previously described [80]. Together, this data suggests that substrate stiffness is capable of modulating intracellular signaling, which conduct to differences on nucleus area. Therefore, we can conclude that the established experimental conditions can mechanomodulate MSCs.

When seeded, cell density was apparently less on soft substrates when compared to TCPs. Additionally, the wanted to guarantee that the transposal of MSCs to softer substrates was not associated to cell loss. To be sure that real cell density was not affected and that functionalization of the substrate was being efficient, we analyzed the DAPI staining images collected by fluorescence microscopy and counted the number of cells attached to the various substrates. No significant differences were found between cell density on the various substrates, evidencing that cell density was not biased (section 3.1.2 – Figure 13). It is known that MSCs are able modulate their actin-myosin cytoskeleton in response to stiffness of their surrounding environment [77]. Consequently, these changes modify cell area and cell spread [139,140,142]. Since spreading decreases on soft substrates, possibly, modifications on the cytoskeleton induced by substrate stiffness lead to a reduction on cell spreading. Consequently, cell area decreases, which resulted on an apparent lower density on soft substrates.

Taken together, this data states that MSCs were effectively responding to mechanical stimulus induced by substrate stiffness. Also, substrate stiffness did not affect cell density.

Due to discrepancies on PDMS substrate stiffness described on the literature (section 1.3 - Table 1), we characterized PDMS substrates by rheology. This technique evaluates not only elastic but also viscous properties of the materials. Results indicate that Young's Modulus of PDMS substrates (section 3.2 - Figure 16) are lower than what was formerly described on the literature, using the same time and temperature [104]. Another study declared that Young's modulus of these hydrogels was higher if cured at 65 °C, overnight [100]. Both studies are concordant, since an increase of the curing time lead to an increase of the Young's Modulus. However, these studies performed a tensile test to calculate Young's Modulus, at RT. It is known that temperature can influence materials behavior. Our rheological assay evaluated elastic properties at 37 °C, the same temperature used for cell culture. Therefore, an increase on the temperature of the assay might modulate PDMS elastic behavior, resulting on a decrease of Young's modulus. This could justify discrepancies between tensile tests and results here shown. Apart from temperature, tensile tests are sensible to the geometry of the structure, which might also lead to inconsistencies on the Young's modulus [143]. However, 10:1 substrate Young's modulus results are not reliable since it was difficult to guarantee adhesion to the surface, hindering the stabilization of the strain applied during the frequency sweep assay, as it is possible to denote on high standard deviations on G'' (section 3-2 - Figure 15A). In the future, stiffness of this formulation needs to be confirmed.

PDMS substrates have already been characterized by rheology [144]. This study described to see the same tendency, - in accordance with our results – namely, increased cross-linking agent concentration leads to the formation of a stiff structure,

with elastic properties (section 3.2 - Figure 15). In contrast, lower concentrations of the crosslinker, leads to lower Young's modulus and more viscous materials. However, results for Young's modulus are lower than results described on the literature [144]. For 10:1 formulations, stiffness is 510 kPa, for 30:1 is 71.6 kPa and 50:1 is 7.6 kPa (measured at 1 Hz). Despite curing temperature is lower than in our study (75 °C), PDMS is left to polymerize overnight, which might lead to longer reaction time, resulting on an increase of stiffness. Also, the assay was performed at 20 °C. As described before, temperature influences elastic behavior of PDMS. This might lead to divergences on the results, since our assay was performed at 37 °C. Rheological characterization of PDMS is scarce, thus no more information can be obtained to discuss our results.

Indentation is a distinct technique to characterize Young's Modulus of substrates. It has been widely used to characterize PDMS, showing discrepant results [102]. This technique is capable of sensing the substrate on a micro scale; contrasting, tensile test and rheology evaluate macro structures [145,146]. Nanoindentation pointed a Young's modulus of 750 kPa for 10:1 formulation and 38 kPa for 50:1 formulation, for substrates cured 1h at 60 °C [102]. These results are not concordant most probably due to the fact that curing time and temperature used were lower and results are like the ones described before. Recently, a study compared macro and micro scale techniques to evaluate elastic properties of PDMS [146]. This study reported differences between techniques when comparing the same PDMS formulations. Particularly on soft substrates, microscale techniques results show a higher Young's Modulus. This same study indicates that macroscale tensile test and compression test are not sensible enough to evaluate soft substrates, possibly because this material is very difficult to handle. Therefore, rheologic test is a sensitive alternative that can give information not only about elasticity but also about viscosity of the substrate.

Unfortunately, it was not possible to characterize PDMS after functionalization, because it was synthetized on top of vinyl paper, impairing the addition of functionalization solutions to the surface. Even though substrates were subjected to UV light for 30 minutes, it is known that surface modification may influence the resulting stiffness [147]. In the future, it is important to try to find another support to the PDMS substrate that enables functionalization.

In summary, there are evidences that softer PDMS substrates have the tendency to be more viscous, while stiffer substrates are predominantly elastic. PDMS hydrogels Young's modulus are 18 kPa for 30:1 formulation, 3 kPa for 40:1 formulation, 1 kPa for 50:1 formulation and 0.93 kPa for 60:1 formulation.

It has been recently shown that not only elastic, but also viscous properties of materials play also an important role on cell culture [148]. A study indicates that for hyaluronic gels, cells are only viable if tan δ is between 0.11 and 0.61 (assay performed at 0.1 Hz at 37 °C). Here, we did not perform any viability assay. However, if these results are transposable to our cells, it could explain why it is difficult to maintain cells on 0.93 kPa substrates, a predominantly viscous substrate. Moreover, it has been described that cells are capable to respond substrate viscosity [149]. Using polyacrylamide gels, with different loss modulus but maintained storage modulus, it was demonstrated that increasing loss modulus increased cell spread but decreased focal adhesion size and maturity. Additionally, adipogenic and myogenic markers also increased on high loss modulus substrates. Literature does not describe the impact of viscosity of the substrate during chondrogenic differentiation. Hence, future work need to clarify if viscous properties of PDMS substrates play an role during chondrogenic differentiation.

Literature is not extensive about easy methods to quantify chondrogenesis. Most of studies evaluate chondrogenesis using molecular biology techniques, as RT-PCR or Western Blots. Despite these techniques are essential to study chondrogenic differentiation, they are not suitable to a fast, day by day, analysis, since they are expensive and time-consuming methods. A semi-quantitative assay for chondrogenic differentiation was established [118]. This method used DAPI staining to normalize SO fluorescence. However, DAPI analysis requires a fluorescence microscope, an expensive equipment not available on all laboratories. In our work, we adapted the previous semi-quantitative assay– using Giemsa absorbance to normalize Safranin O fluorescence, instead of DAPI. A calibration curve for Giemsa OD (section 3.3.1. – Figure 19) was determined. It was possible to denote a strong correlation between the number of cells and Giemsa OD, since R is approximately 1, confirming that this is a suitable parameter to normalize results. Since there was a big discrepancy between SO fluorescence and Giemsa OD units, we normalized the results to a 1 to 10 range, in order to be sure that calculations did not mask the differences.

On the present study SO was normalized to Giemsa OD (section 3.3.1. – Figure 20 A). SO assay results pointed high values of fluorescence for both on undifferentiated and differentiated cells cultured in glass. The semi quantitative assay previously established also showed an increase on SO fluorescence on control group, particularly at day 10 [118]. However, the fold increase is not significant on this substrate (section 3.3.1 – Figure 20 B). These results are confirmed with the images obtained by contrast phase microscopy, since it is possible to see a tenuous red stain, suggesting a more diffuse deposition of GAG both on control (section 3.3. – Figure 18) and differentiated (section 3.3 – Figure 17) groups. Analyzing images of SO staining, 1 kPa substrate stands out from the other substrates. On this substrate, it is possible to see the formation of cell agglomerates, typical of chondrogenesis, on

differentiation group. Also, these agglomerates are strongly stained in red, suggesting an intensive synthesis of GAG. These images are in accordance with the results obtained on the SO assay, since SO fluorescence is high on cells differentiated on 1 kPa. Fluorescence of this dye increases significantly on this substrate, when compared to its respective control (section 3.3.1 – Figure 20). Despite that cells grown in other substrates also show the tendency to form agglomerates, these are not so mature and the staining is not so strong. Additionally, control groups of PDMS substrates do not show any coloration, which is concordant with low SO fluorescence. In summary, images agree with the results obtained on the semi-quantitative assay we established. Cell agglomeration, synthesis of GAG and suggested that chondrogenesis was enhanced on 1 kPa substrate. Taken together, these results point toward 1 kPa as the optimal stiffness for chondrogenic differentiation. However, to validate this assay we evaluated the expression of chondrogenic markers by RT-PCR.

We stained replicates of blank substrates that were previously functionalized and cultured with PM for 9 days. We concluded that SO staining is associated with high background fluorescence, despite it was not possible to observe on the microscope (data not shown). To overcome this issue, we subtracted the mean of background values to SO fluorescence of cultured cells to obtain more accurate values.

To validate the semi-quantitative assay for chondrogenesis, we evaluated expression of chondrogenic markers – Sox9, ACAN and collagen type II – on cells cultured on glass, 17 kPa and 1 kPa substrate, for 9 days. Glass substrate was used to mimic standard conditions of differentiation on TCPs, since both have similar stiffness. Nevertheless, glass can be functionalized.

During chondrogenic differentiation of MSCs for posterior RT-PCR analysis cells did not behave as reported before: cell morphology was similar to its control and there was no formation of cell agglomerates. Since cells did not appear to be different, by microscopy, it is not surprising that chondrogenic markers were not overexpressed on a specific substrate. Also, high divergences between replicates impaired an accurate analysis of RT-PCR results.

Aggrecan is a proteoglycan present on cartilage matrix [4]. Our RT-PCR results also show that ACAN is preferentially expressed by undifferentiated and differentiated cells grown in glass (section 3.3.2 – Figure 21B). SO results are concordant with our RT-PCR, since despite SO fluorescence is higher on glass substrates, there is no significant increment on ACAN expression on this substrate. Surprisingly, ACAN was not expressed on 18 kPa substrate and only twice on 1 kPa substrate. Recently, a study declared that dynamic stretch increased phosphorylated ERK and stimulated aggrecan expression, when compared to control group, where no stretch was applied [150]. Also, inhibition of contractibility decreased aggrecan expression on stretched cells. As described before, a stiff substrate activates RhoA/ROCK pathway, which leads to actin polymerization, formation of stress fibers, modifications on cell contractibility and increases intracellular tension (see details on section 1.2.2.). Most probably, on the present study, glass, a stiff substrate, may change cell contractibility and activate intracellular pathways similar to what was described for dynamical stretching [150]. In summary, both stimulus – stiffness and dynamical stretching – are capable of modulating cell contractility and stimulate aggrecan expression.

A recent study also revealed the relevance of TGFβ autocrine and paracrine stimulation during chondrogenic differentiation of synovial MSCs and chondrocytes culture [151,152]. According to what was previously described, despite real density is the same on all substrates, apparent cell density is different

between PDMS and glass substrate, since cells cultured on soft substrates are less spread and consequently do not touch as it occurs in TCPs/glass (detailed on section 1.2.2). Our hypothesis is that cells close to each other are capable of an effective paracrine signaling, which could favor the expression of chondrogenic markers. Together, these data reveal a new opportunity to study the impact of real cell density on chondrogenic differentiation. A study has documented the relevance of cell density on osteogenic and adipogenic fate [25]. Future studies will need to clarify if cell density plays a key role on chondrogenesis.

RT-PCR results showed that runx2, an osteogenic marker, is being widely expressed on cells on PDMS and glass substrates. Mechanical memory of cells has been studied - if P1 cells are maintained on TCPs for more than 10 days, YAP and runx2 move permanently to the nucleus, even if cells are transposed to a softer substrate (see details on section 1.2.2.2.) [138]. On the present study, MSCs induced to differentiate to subsequent RT-PCR analysis, had already been expanded and frozen at P1. Therefore, we cannot be certain about the proliferating period on TCPs. Runx2 expression (section 3.3.2 – Figure 21D) suggested that these MSCs were kept for longer periods (more than 10 days) in TCPs and suggesting that runx2, and probably YAP, had permanently moved to the nucleus. Moreover, a study acknowledged that expression of neurogenic markers on cells that were first cultured on a stiff substrate and then transferred to a soft substrate were not so remarkable, when compared to cells that were continuously grown on soft substrates [98]. Hypothetically, a similar outcome occurred on MSCs induced to differentiate onto chondrocytes: since cells were maintained for more than 10 days on TCPS, runx2 was permanently expressed. Possibly, this impaired an effective response to the substrate and/or to soluble factors, justifying why cells were not able to express evidently chondrogenic markers.

The process of osteogenic and chondrogenic commitment has been widely studied [153,154]. Literature describes that TGFβ is able to form a complex with Smad3, which recruits histone deacetylases 4 and 5 and is capable of repressing runx2 expression [153]. Also, Sox9 has the ability to repress runx2 to prime cells to chondrogenic fate [154]. In the presence of low expression of runx2 and high expression of Sox9, cells are commited to a permanent chondrogenic fate [155]. Nevertheless, if both genes are co-expressed, chondrocytes acquire a hypertrophic phenotype, characteristic of replacement cartilage, to posterior endochondral ossification. Both persistent or hypertrophic chondrocytes express aggrecan [155]. Results show that cells were expression both Sox9 and runx2 (section 3.3.2 – Figure 21A and 21D). To evaluate if cells were acquiring a hypertrophic phenotype, it would be interesting to complement results obtained by RT-PCR, assessing the expression of hypertrophic markers, as collagen type X and/or BMP6 [155]. Together, these data enhance the relevance of guaranteeing a low runx2 expression to enhance an articular chondrogenic fate.

Despite that Safranin O assay needs further validation, it suggests 1 kPa as the optimal stiffness for chondrogenic differentiation. In accordance, 1 kPa has already been suggested as the optimal stiffness for chondrogenic differentiation [58]. YAP-ROCK2 feedback loop has been characterized – a stiff ECM upregulates ROCK2 leading to an overexpression of YAP [156]. Recently, YAP was shown to be a negative regulator of chondrogenesis [96]. Possibly, due to a decreased intracellular tension, MSCs cultured on 1 kPa substrate can trigger pathways that can relocalize YAP on the cytoplasm and enhance chondrogenic differentiation. Future work using naïve MSCs will help to clarify this hypothesis.

We aim to use MSCs on cell therapy. Though, this treatment requires a high number of cells. If MSCs are expanded for long periods on TCPs, YAP moves

permanently to the nucleus and multipotency might be impaired [138] (details on section 1.2.2.2). Therefore, evaluated kinetics proliferation of MSCs on 18 kPa and 1 kPa PDMS substrates. When compared to TCPs, MSCs on PDMS proliferate less and slower on softer substrates (section 3.4 – Figure 22). Despite MSCs maintain their capacity to proliferate on TCPs until P6, MSCs only proliferate until P6 on PDMS. Also, the number of cells obtained is significantly lower on PDMS substrates. Comparing 18 kPa and 1 kPa substrate, 18 kPa substrate is more suitable to expand MSCs, since behavior of these cells is constant until passage 4. YAP/TAZ are important effectors of the Hippo pathway involved in cell proliferation and apoptosis [157]. YAP/TAZ bind TEAD, and target transcription factors involved on cell proliferation and cell survival [157,158]. Since on soft substrates ROCK activity decreases, YAP/TAZ complex translocation into the nucleus decreases and therefore expression of factors involved on cell proliferation is impaired. Hypothetically, PDMS substrates are reducing RhoA activity, impairing cell proliferation on these substrates. Possibly, RhoA activity is slightly higher on 18 kPa substrate, when compared to 1 kPa. This justifies why proliferation rate on 18 kPa is slightly higher on this substrate.

Future work need to optimize culture conditions for MSCs proliferation on PDMS substrates. As an example, different combinations of coating proteins could enhance MSCs proliferation. It would be interesting to compare the expression of multipotency-specific markers on MSCs expanded on TCPs and a softer substrate, as 18 kPa substrate. Also, chondrogenic potential of MSCs expanded on TCPs and 18 kPa should be evaluated.

5. Conclusion

On the present study, we synthetized PDMS substrates with a wide range of stiffness – 21 kPa to 0.931 kPa. Characterization of viscoelastic properties of these substrates, by rheometry, showed that soft substrates are predominantly viscous, while stiff substrates are mainly elastic. Results show that thickness of synthetized substrates is enough to trigger a mechanical stimulus. This data was corroborated by the declining tendency of the nuclear area of MSCs observed along with substrate softening. Additionally, it was verified that transposal of MSCs to PDMS substrates did not affect cell density.

Slow proliferation rate on 18 kPa suggests that, in the future, culture conditions for MSCs proliferation on PDMS need to be optimized.

Safranin O is a dye that has affinity to GAG, a major component of cartilaginous ECM. Using Safranin O fluorescence, we established an easy, cheap, and rapid methodology to semi-quantify GAG expression and assess chondrogenic differentiation of MSCs. Results suggest that 1 kPa as the optimal stiffness for chondrogenic differentiation of MSCs. Additionally, Safranin O staining emphasizes that 1kPa substrate potentiates cell agglomeration and GAG synthesis. Taken together, this data strongly suggests 1 kPa as the optimal stiffness for chondrogenic differentiation of MSCs. Although, these results need further validation by RT-PCR using naïve cells, namely low runx2 expression MSCs.

6. References

1. Rod R. Seeley, Trent D. Stephens, Philip Tate. Anatomia & Fisiologia. Lusociência; 2011.

2. Sophia Fox AJ, Bedi A, Rodeo SA. The Basic Science of Articular Cartilage: Structure, Composition, and Function. Sports Health Multidiscip. Approach 2009;1:461–8.

3. Mow VC, Ratcliffe A, Poole AR. Cartilage and diarthrodial joints as paradigms for hierarchical materials and structures. Biomaterials 1992;13:67–97.

4. Camarero-Espinosa S, Rothen-Rutishauser B, Foster EJ, Weder C. Articular cartilage: from formation to tissue engineering. Biomater Sci 2016;4:734–67.

5. Hayes AJ, Hall A, Brown L, Tubo R, Caterson B. Macromolecular organization and in vitro growth characteristics of scaffold-free neocartilage grafts. J. Histochem. Cytochem. 2007;55:853–866.

6. Cheng C, Conte E, Pleshko-Camacho N, Hidaka C. Differences in matrix accumulation and hypertrophy in superficial and deep zone chondrocytes are controlled by bone morphogenetic protein. Matrix Biol. 2007;26:541–553.

7. Yang PJ, Temenoff JS. Engineering orthopedic tissue interfaces. Tissue Eng. Part B Rev. 2009;15:127–141.

8. Andrades JA, Motaung SC, Jiménez-Palomo P, Claros S, López-Puerta JM, Becerra J, Schmid TM, Reddi AH. Induction of superficial zone protein (SZP)/lubricin/PRG 4 in muscle-derived mesenchymal stem/progenitor cells by transforming growth factor-β1 and bone morphogenetic protein-7. Arthritis Res. Ther. 2012;14:1.

9. Coates E, Fisher JP. Gene expression of alginate-embedded chondrocyte subpopulations and their response to exogenous IGF-1 delivery. J. Tissue Eng. Regen. Med. 2012;6:179–92.

10. Nguyen LH, Kudva AK, Guckert NL, Linse KD, Roy K. Unique biomaterial compositions direct bone marrow stem cells into specific chondrocytic phenotypes corresponding to the various zones of articular cartilage. Biomaterials 2011;32:1327–38.

11. Hardingham T, Bayliss M. Proteoglycans of articular cartilage: changes in aging and in joint disease. Semin. Arthritis Rheum. 1990;20:12–33.

12. Buckwalter J, Martin J. Osteoarthritis. Adv. Drug Deliv. Rev. 2006;58:150–67.

13. Bottini N, Firestein GS. Duality of fibroblast-like synoviocytes in RA: passive responders and imprinted aggressors. Nat. Rev. Rheumatol. 2012;9:24–33.

14. Smolen JS, Aletaha D, McInnes IB. Rheumatoid arthritis. The Lancet 388:2023–38.

15. Jiang Y, Cai Y, Zhang W, Yin Z, Hu C, Tong T, Lu P, Zhang S, Neculai D, Tuan RS, Ouyang HW. Human Cartilage-Derived Progenitor Cells From Committed Chondrocytes for Efficient Cartilage Repair and Regeneration. Stem Cells Transl. Med. 2016;5:733–44.

16. Ruano-Ravina A, Jato Díaz M. Autologous chondrocyte implantation: a systematic review. Osteoarthritis Cartilage 2006;14:47–51.

17. Ma B, Leijten JCH, Wu L, Kip M, van Blitterswijk CA, Post JN, Karperien M. Gene expression profiling of dedifferentiated human articular chondrocytes in monolayer culture. Osteoarthritis Cartilage 2013;21:599–603.

18. El-Jawhari JJ, El-Sherbiny YM, Jones EA, McGonagle D. Mesenchymal stem cells, autoimmunity and rheumatoid arthritis. QJM 2014;107:505–14.

19. Sierra R, Wyles C, Houdek M, Behfar A. Mesenchymal stem cell therapy for osteoarthritis: current perspectives. Stem Cells Cloning Adv. Appl. 2015;117.

20. Pittenger MF. Multilineage Potential of Adult Human Mesenchymal Stem Cells. Science 1999;284:143–7.

21. Secunda R, Vennila R, Mohanashankar AM, Rajasundari M, Jeswanth S, Surendran R. Isolation, expansion and characterisation of mesenchymal stem cells from human bone marrow, adipose tissue, umbilical cord blood and matrix: a comparative study. Cytotechnology 2015;67:793–807.

22. Bianco P, Robey PG, Simmons PJ. Mesenchymal Stem Cells: Revisiting History, Concepts, and Assays. Cell Stem Cell 2008;2:313–9.

23. Toma C, Pittenger MF, Cahill KS, Byrne BJ, Kessler PD. Human mesenchymal stem cells differentiate to a cardiomyocyte phenotype in the adult murine heart. Circulation 2002;105:93–98.

24. Wu X-B, Tao R. Hepatocyte differentiation of mesenchymal stem cells. Hepatobiliary Pancreat. Dis. Int. 2012;11:360–71.

25. McBeath R, Pirone DM, Nelson CM, Bhadriraju K, Chen CS. Cell shape, cytoskeletal tension, and RhoA regulate stem cell lineage commitment. Dev. Cell 2004;6:483–495.

26. Engler AJ, Sen S, Sweeney HL, Discher DE. Matrix Elasticity Directs Stem Cell Lineage Specification. Cell 2006;126:677–89.

27. Gerhard Krauss. Biochemistry of Signal Transduction and Regulation. Wiley; 2014.

28. Tang QO, Shakib K, Heliotis M, Tsiridis E, Mantalaris A, Ripamonti U, Tsiridis E. TGF-β3: A potential biological therapy for enhancing chondrogenesis. Expert Opin. Biol. Ther. 2009;9:689–701.

29. Kurpinski K, Lam H, Chu J, Wang A, Kim A, Tsay E, Agrawal S, Schaffer DV, Li S. Transforming growth factor-beta and notch signaling mediate stem cell differentiation into smooth muscle cells. Stem Cells Dayt. Ohio 2010;28:734–42.

30. Schmierer B, Hill CS. TGFβ–SMAD signal transduction: molecular specificity and functional flexibility. Nat. Rev. Mol. Cell Biol. 2007;8:970–82.

31. Furumatsu T, Tsuda M, Taniguchi N, Tajima Y, Asahara H. Smad3 Induces Chondrogenesis through the Activation of SOX9 via CREB-binding Protein/p300 Recruitment. J. Biol. Chem. 2005;280:8343–50.

32. Han Y, Lefebvre V. L-Sox5 and Sox6 drive expression of the aggrecan gene in cartilage by securing binding of Sox9 to a far-upstream enhancer. Mol. Cell. Biol. 2008;28:4999–5013.

33. Lefebvre V, Huang W, Harley VR, Goodfellow PN, De Crombrugghe B. SOX9 is a potent activator of the chondrocyte-specific enhancer of the pro alpha1 (II) collagen gene. Mol. Cell. Biol. 1997;17:2336–2346.

34. Cheah KS, Lau ET, Au PK, Tam PP. Expression of the mouse alpha 1 (II) collagen gene is not restricted to cartilage during development. Development 1991;111:945–953.

35. Diederichs S, Gabler J, Autenrieth J, Kynast KL, Merle C, Walles H, Utikal J, Richter W. Differential Regulation of SOX9 Protein During Chondrogenesis of Induced Pluripotent Stem Cells Versus Mesenchymal Stromal Cells: A Shortcoming for Cartilage Formation. Stem Cells Dev. 2016;25:598–609.

36. Tuli R. Transforming Growth Factor- -mediated Chondrogenesis of Human Mesenchymal Progenitor Cells Involves N-cadherin and Mitogen-activated Protein Kinase and Wnt Signaling Cross-talk. J. Biol. Chem. 2003;278:41227–36.

37. McMahon LA, Prendergast PJ, Campbell VA. A comparison of the involvement of p38, ERK1/2 and PI3K in growth factor-induced chondrogenic differentiation of mesenchymal stem cells. Biochem. Biophys. Res. Commun. 2008;368:990–5.

38. Nakajima M, Negishi Y, Tanaka H, Kawashima K. p21Cip-1/SDI-1/WAF-1 expression via the mitogen-activated protein kinase signaling pathway in insulin-induced chondrogenic differentiation of ATDC5 cells. Biochem. Biophys. Res. Commun. 2004;320:1069–75.

39. Huang AH, Farrell MJ, Mauck RL. Mechanics and mechanobiology of mesenchymal stem cell-based engineered cartilage. J. Biomech. 2010;43:128–36.

40. Chen J, Wang Y, Chen C, Lian C, Zhou T, Gao B, Wu Z, Xu C. Exogenous Heparan Sulfate Enhances the TGF- β 3-Induced Chondrogenesis in Human Mesenchymal Stem Cells by Activating TGF- β /Smad Signaling. Stem Cells Int. 2016;2016:1–10.

41. Wang T, Lai JH, Han L-H, Tong X, Yang F. Chondrogenic Differentiation of Adipose-Derived Stromal Cells in Combinatorial Hydrogels Containing Cartilage Matrix Proteins with Decoupled Mechanical Stiffness. Tissue Eng. Part A 2014;20:2131–9.

42. Tang X, Fan L, Pei M, Zeng L, Ge Z. Evolving concepts of chondrogenic differentiation: history, state-of-the-art and future perspectives. Eur Cell Mater 2015;30:12–27.

43. Cigan AD, Nims RJ, Albro MB, Esau JD, Dreyer MP, Vunjak-Novakovic G, Hung CT, Ateshian GA. Insulin, Ascorbate, and Glucose Have a Much Greater Influence Than Transferrin and Selenous Acid on the *In Vitro* Growth of Engineered Cartilage in Chondrogenic Media. Tissue Eng. Part A 2013;19:1941–8.

44. Hatakeyama Y, Tuan RS, Shum L. Distinct functions of BMP4 and GDF5 in the regulation of chondrogenesis. J. Cell. Biochem. 2004;91:1204–17.

45. Qu P, Wang L, Min Y, McKennett L, Keller JR, Lin PC. Vav1 Regulates Mesenchymal Stem Cell Differentiation Decision Between Adipocyte and Chondrocyte via Sirt1. Stem Cells Dayt. Ohio 2016;34:1934–46.

46. Lin X, Wu L, Zhang Z, Yang R, Guan Q, Hou X, Wu Q. MiR-335-5p promotes chondrogenesis in mouse mesenchymal stem cells and is regulated through two positive feedback loops. J. Bone Miner. Res. Off. J. Am. Soc. Bone Miner. Res. 2014;29:1575–85.

47. Frantz C, Stewart KM, Weaver VM. The extracellular matrix at a glance. J. Cell Sci. 2010;123:4195–200.

48. Humphrey JD, Dufresne ER, Schwartz MA. Mechanotransduction and extracellular matrix homeostasis. Nat. Rev. Mol. Cell Biol. 2014;15:802–12.

49. Alberts, Bruce, Johnson, Alexander, Lewis, Julian, Raff,Martin, Roberts, Keith, Walter, Peter. Molecular Biology of the Cell. 4th ed. New York: Garland Sciences; 2002.

50. Rozario T, DeSimone DW. The extracellular matrix in development and morphogenesis: A dynamic view. Dev. Biol. 2010;341:126–40.

51. Panadero JA, Lanceros-Mendez S, Ribelles JLG. Differentiation of mesenchymal stem cells for cartilage tissue engineering: Individual and synergetic effects of three-dimensional environment and mechanical loading. Acta Biomater. 2016;33:1–12.

52. Lee YS, Stott NS, Jiang TX, Widelitz RB, Chuong CM. Early events during precartilage condensation in limb bud micromass cultures. Cells Mater. 1998;8:19–32.

53. Daniels K, Solursh M. Modulation of chondrogenesis by the cytoskeleton and extracellular matrix. J. Cell Sci. 1991;100:249–254.

54. Woods A, Wang G, Beier F. Regulation of chondrocyte differentiation by the actin cytoskeleton and adhesive interactions. J. Cell. Physiol. 2007;213:1–8.

55. Bellas E, Chen CS. Forms, forces, and stem cell fate. Curr. Opin. Cell Biol. 2014;31:92–7.

56. Bershadsky A. Magic touch: how does cell–cell adhesion trigger actin assembly? Trends Cell Biol. 2004;14:589–593.

57. Sonam S, Sathe SR, Yim EKF, Sheetz MP, Lim CT. Cell contractility arising from topography and shear flow determines human mesenchymal stem cell fate. Sci. Rep. 2016;6:20415.

58. Park JS, Chu JS, Tsou AD, Diop R, Tang Z, Wang A, Li S. The effect of matrix stiffness on the differentiation of mesenchymal stem cells in response to TGF-β. Biomaterials 2011;32:3921–30.

59. Gao L, McBeath R, Chen CS. Stem cell shape regulates a chondrogenic versus myogenic fate through Rac1 and. Stem Cells Dayt. Ohio 2010;28:564–72.

60. Price LS, Leng J, Schwartz MA, Bokoch GM. Activation of Rac and Cdc42 by integrins mediates cell spreading. Mol. Biol. Cell 1998;9:1863–1871.

61. Noritake J, Fukata M, Sato K, Nakagawa M, Watanabe T, Izumi N, Wang S, Fukata Y, Kaibuchi K. Positive role of IQGAP1, an effector of Rac1, in actin-meshwork formation at sites of cell-cell contact. Mol. Biol. Cell 2004;15:1065–1076.

62. Goessler UR, Bugert P, Bieback K, Stern-Straeter J, Bran G, Hormann K, Riedel F. Integrin expression in stem cells from bone marrow and adipose tissue during chondrogenic differentiation. Int. J. Mol. Med. 2008;21:271–280.

63. Goessler UR, Bieback K, Bugert P, Heller T, Sadick H, Hormann K, Riedel F. In vitro analysis of integrin expression during chondrogenic differentiation of mesenchymal stem cells and chondrocytes upon dedifferentiation in cell culture. Int. J. Mol. Med. 2006;17:301–308.

64. Raghothaman D, Leong MF, Lim TC, Toh JKC, Wan ACA, Yang Z, Lee EH. Engineering cell matrix interactions in assembled polyelectrolyte fiber hydrogels for mesenchymal stem cell chondrogenesis. Biomaterials 2014;35:2607–16.

65. Provenzano PP, Keely PJ. Mechanical signaling through the cytoskeleton regulates cell proliferation by coordinated focal adhesion and Rho GTPase signaling. J. Cell Sci. 2011;124:1195–205.

66. Mariappan YK, Glaser KJ, Ehman RL. Magnetic resonance elastography: A review. Clin. Anat. 2010;23:497–511.

67. Wang N, Tytell JD, Ingber DE. Mechanotransduction at a distance: mechanically coupling the extracellular matrix with the nucleus. Nat. Rev. Mol. Cell Biol. 2009;10:75–82.

68. Friedland JC, Lee MH, Boettiger D. Mechanically activated integrin switch controls $\alpha 5\beta 1$ function. Science 2009;323:642–644.

69. Bershadsky AD, Balaban NQ, Geiger B. Adhesion-Dependent Cell Mechanosensitivity. Annu. Rev. Cell Dev. Biol. 2003;19:677–95.

70. Lv H, Li L, Sun M, Zhang Y, Chen L, Rong Y, Li Y. Mechanism of regulation of stem cell differentiation by matrix stiffness. Stem Cell Res. Ther. 2015;6:103.

71. del Rio A, Perez-Jimenez R, Liu R, Roca-Cusachs P, Fernandez JM, Sheetz MP. Stretching Single Talin Rod Molecules Activates Vinculin Binding. Science 2009;323:638–41.

72. Hoon J, Tan M, Koh C-G. The Regulation of Cellular Responses to Mechanical Cues by Rho GTPases. Cells 2016;5:17.

73. Gardinier J, Yang W, Madden GR, Kronbergs A, Gangadharan V, Adams E, Czymmek K, Duncan RL. P2Y2 receptors regulate osteoblast mechanosensitivity during fluid flow. AJP Cell Physiol. 2014;306:C1058–67.

74. Totsukawa G, Yamakita Y, Yamashiro S, Hartshorne DJ, Sasaki Y, Matsumura F. Distinct Roles of Rock (Rho-Kinase) and Mlck in Spatial Regulation of Mlc Phosphorylation for Assembly of Stress Fibers and Focal Adhesions in 3t3 Fibroblasts. J. Cell Biol. 2000;150:797–806.

75. Lessey EC, Guilluy C, Burridge K. From Mechanical Force to RhoA Activation. Biochemistry (Mosc.) 2012;51:7420–32.

76. Geiger B, Spatz JP, Bershadsky AD. Environmental sensing through focal adhesions. Nat. Rev. Mol. Cell Biol. 2009;10:21–33.

77. Cho S, Irianto J, Discher DE. Mechanosensing by the nucleus: From pathways to scaling relationships. J. Cell Biol. 2017;216:305–15.

78. Crisp M, Liu Q, Roux K, Rattner JB, Shanahan C, Burke B, Stahl PD, Hodzic D. Coupling of the nucleus and cytoplasm: role of the LINC complex. J. Cell Biol. 2006;172:41–53.

79. Buxboim A, Swift J, Irianto J, Spinler K, Dingal PC ?Dave?P., Athirasala A, Kao Y-R, Cho S, Harada T, Shin J-W, Discher D. Matrix Elasticity Regulates Lamin-A,C Phosphorylation and Turnover with Feedback to Actomyosin. Curr. Biol. 2014;24:1909–17.

80. Swift J, Ivanovska IL, Buxboim A, Harada T, Dingal PCDP, Pinter J, Pajerowski JD, Spinler KR, Shin J-W, Tewari M, Rehfeldt F, Speicher DW, Discher DE. Nuclear Lamin-A Scales with Tissue Stiffness and Enhances Matrix-Directed Differentiation. Science 2013;341:1240104–1240104.

81. Huang C, Dai J, Zhang XA. Environmental physical cues determine the lineage specification of mesenchymal stem cells. Biochim. Biophys. Acta BBA - Gen. Subj. 2015;1850:1261–6.

82. Fu J, Wang Y-K, Yang MT, Desai RA, Yu X, Liu Z, Chen CS. Mechanical regulation of cell function with geometrically modulated elastomeric substrates. Nat. Methods 2010;7:733–6.

83. Du J, Chen X, Liang X, Zhang G, Xu J, He L, Zhan Q, Feng X-Q, Chien S, Yang C. Integrin activation and internalization on soft ECM as a mechanism of induction of stem cell differentiation by ECM elasticity. Proc. Natl. Acad. Sci. 2011;108:9466–71.

84. Sefat F, Youseffi M, Khaghani SA, Soon CF, Javid F. Effect of transforming growth factor-β3 on mono and multilayer chondrocytes. Cytokine 2016;83:118–26.

85. Allen JL, Cooke ME, Alliston T. ECM stiffness primes the TGFbeta pathway to promote chondrocyte differentiation. Mol. Biol. Cell 2012;23:3731–42.

86. Li D, Zhou J, Chowdhury F, Cheng J, Wang N, Wang F. Role of mechanical factors in fate decisions of stem cells. Regen. Med. 2011;6:229–40.

87. Joon Kwon H. Chondrogenesis on sulfonate-coated hydrogels is regulated by their mechanical properties. J. Mech. Behav. Biomed. Mater. 2013;17:337–46.

88. Bian L, Hou C, Tous E, Rai R, Mauck RL, Burdick JA. The influence of hyaluronic acid hydrogel crosslinking density and macromolecular diffusivity on human MSC chondrogenesis and hypertrophy. Biomaterials 2013;34:413–21.

89. Moeinzadeh S, Pajoum Shariati SR, Jabbari E. Comparative effect of physicomechanical and biomolecular cues on zone-specific chondrogenic differentiation of mesenchymal stem cells. Biomaterials 2016;92:57–70.

90. Woods A, Beier F. RhoA/ROCK Signaling Regulates Chondrogenesis in a Context-dependent Manner. J. Biol. Chem. 2006;281:13134–40.

91. Takahashi I, Onodera K, Sasano Y, Mizoguchi I, Bae J-W, Mitani H, Kagayama M, Mitani H. Effect of stretching on gene expression of β1 integrin and focal adhesion kinase and on chondrogenesis through cell-extracellular matrix interactions. Eur. J. Cell Biol. 2003;82:182–192.

92. Zhang T, Wen F, Wu Y, Goh GSH, Ge Z, Tan LP, Hui JHP, Yang Z. Cross-talk between TGF-beta/SMAD and integrin signaling pathways in regulating hypertrophy of mesenchymal stem cell chondrogenesis under deferral dynamic compression. Biomaterials 2015;38:72–85.

93. Dupont S, Morsut L, Aragona M, Enzo E, Giulitti S, Cordenonsi M, Zanconato F, Le Digabel J, Forcato M, Bicciato S, Elvassore N, Piccolo S. Role of YAP/TAZ in mechanotransduction. Nature 2011;474:179–83.

94. Sorrentino G, Ruggeri N, Specchia V, Cordenonsi M, Mano M, Dupont S, Manfrin A, Ingallina E, Sommaggio R, Piazza S, Rosato A, Piccolo S, Del Sal G. Metabolic control of YAP and TAZ by the mevalonate pathway. Nat. Cell Biol. 2014;16:357–66.

95. Halder G, Dupont S, Piccolo S. Transduction of mechanical and cytoskeletal cues by YAP and TAZ. Nat. Rev. Mol. Cell Biol. 2012;13:591.

96. Karystinou A, Roelofs AJ, Neve A, Cantatore FP, Wackerhage H, De Bari C. Yes-associated protein (YAP) is a negative regulator of chondrogenesis in mesenchymal stem cells. Arthritis Res. Ther. 2015;17:147.

97. Yang C, Tibbitt MW, Basta L, Anseth KS. Mechanical memory and dosing influence stem cell fate. Nat. Mater. 2014;13:645–52.

98. Lee J, Abdeen AA, Kilian KA. Rewiring mesenchymal stem cell lineage specification by switching the biophysical microenvironment. 2014;4:5188.

99. Zhao B, Tumaneng K, Guan K-L. The Hippo pathway in organ size control, tissue regeneration and stem cell self-renewal. Nat. Cell Biol. 2011;13:877–83.

100. Brown XQ, Ookawa K, Wong JY. Evaluation of polydimethylsiloxane scaffolds with physiologically-relevant elastic moduli: interplay of substrate mechanics and surface chemistry effects on vascular smooth muscle cell response. Biomaterials 2005;26:3123–9.

101. Park JY, Yoo SJ, Lee E-J, Lee DH, Kim JY, Lee S-H. Increased poly(dimethylsiloxane) stiffness improves viability and morphology of mouse fibroblast cells. BioChip J. 2010;4:230–6.

102. Teixeira AI, Ilkhanizadeh S, Wigenius JA, Duckworth JK, Inganäs O, Hermanson O. The promotion of neuronal maturation on soft substrates. Biomaterials 2009;30:4567–72.

103. Wang Z, Volinsky AA, Gallant ND. Crosslinking effect on polydimethylsiloxane elastic modulus measured by custom-built compression instrument. J. Appl. Polym. Sci. 2014;131:n/a-n/a.

104. Ochsner M, Dusseiller MR, Grandin HM, Luna-Morris S, Textor M, Vogel V, Smith ML. Micro-well arrays for 3D shape control and high resolution analysis of single cells. Lab. Chip 2007;7:1074.

105. Diaz Blanco C, Ortner A, Dimitrov R, Navarro A, Mendoza E, Tzanov T. Building an Antifouling Zwitterionic Coating on Urinary Catheters Using an Enzymatically Triggered Bottom-Up Approach. ACS Appl. Mater. Interfaces 2014;6:11385–93.

106. Yu L, Li CM, Liu Y, Gao J, Wang W, Gan Y. Flow-through functionalized PDMS microfluidic channels with dextran derivative for ELISAs. Lab. Chip 2009;9:1243.

107. Janmey PA, Georges PC, Hvidt S. Basic Rheology for Biologists. Cell Mech. 2007;83:1–27.

108. Johnston ID, McCluskey DK, Tan CKL, Tracey MC. Mechanical characterization of bulk Sylgard 184 for microfluidics and microengineering. J. Micromechanics Microengineering 2014;24:035017.

109. Rosales AM, Anseth KS. The design of reversible hydrogels to capture extracellular matrix dynamics. Nat. Rev. Mater. 2016;1:15012.

110. Choi D-W, Chang Y-H. Steady and Dynamic Shear Rheological Properties of Buckwheat Starch-galactomannan Mixtures. Prev. Nutr. Food Sci. 2012;17:192–6.

111. Zipfel E, Grezes JR, Naujok A, Seiffert W, Wittekind DH, Zimmermann HW. [Romanowsky dyes and the Romanowsky-Giemsa effect. 3. Microspectrophotometric studies of Romanowsky-Giemsa staining. Spectroscopic evidence of a DNA-azure. Histochemistry 1984;81:337–51.

112. Osipov A, Arkhangelskaya E, Vinokurov A, Smetanina N, Zhavoronkov A, Klokov D. DNA Comet Giemsa Staining for Conventional Bright-Field Microscopy. Int. J. Mol. Sci. 2014;15:6086–95.

113. Waltz DA, Natkin LR, Fujita RM, Wei Y, Chapman HA. Plasmin and plasminogen activator inhibitor type 1 promote cellular motility by regulating the interaction between the urokinase receptor and vitronectin. J. Clin. Invest. 1997;100:58.

114. Bulstra SK, Drukker J, Kuijer R, Buurman WA, Linden A van der. Thionin staining of paraffin and plastic embedded sections of cartilage. Biotech. Histochem. 1993;68:20–28.

115. Kiviranta I, Jurvelin J, Säämänen A-M, Helminen HJ. Microspectrophotometric quantitation of glycosaminoglycans in articular cartilage sections stained with Safranin O. Histochem. Cell Biol. 1985;82:249–255.

116. Camplejohn KL, Allard SA. Limitations of safranin "O" staining in proteoglycan-depleted cartilage demonstrated with monoclonal antibodies. Histochemistry 1988;89:185–8.

117. Zaia J. On-line separations combined with MS for analysis of glycosaminoglycans. Mass Spectrom. Rev. 2009;28:254–72.

118. Yen C-Y, Wu Y-W, Hsiung C-N, Yeh M-I, Lin Y-M, Lee S-Y. Cell-based semiquantitative assay for sulfated glycosaminoglycans facilitating the identification of chondrogenesis. Anal. Biochem. 2015;486:41–3.

119. Commonwealth Secretariat. Updating and augmenting the economic vulnerability index [Internet]. Organisation for Economic Co-operation and Development; 2010. page 5–15.Available from: http://www.thecommonwealth-ilibrary.org/content/chapter/9781848590878-3-en

120. Hughes, Andrew. Amino Acids, Peptides and Proteins in Organic Chemistry, Analysis and Function of Amino Acids and Peptides. WILEY-VCH. 2011.

121. Lee H-H, Chang C-C, Shieh M-J, Wang J-P, Chen Y-T, Young T-H, Hung S-C. Hypoxia enhances chondrogenesis and prevents terminal differentiation through PI3K/Akt/FoxO dependent anti-apoptotic effect. Sci. Rep. 2013;3:2683.

122. Schmittgen TD, Livak KJ. Analyzing real-time PCR data by the comparative CT method. Nat. Protoc. 2008;3:1101–8.

123. Tanious FA, Veal JM, Buczak H, Ratmeyer LS, Wilson WD. DAPI (4',6-diamidino-2-phenylindole) binds differently to DNA and RNA: minor-groove binding at AT sites and intercalation at AU sites. Biochemistry (Mosc.) 1992;31:3103–12.

124. Bieback K, Hecker A, Kocaomer A, Lannert H, Schallmoser K, Strunk D, Kluter H. Human alternatives to fetal bovine serum for the expansion of mesenchymal stromal cells from bone marrow. Stem Cells Dayt. Ohio 2009;27:2331–41.

125. Leite C, Silva NT, Mendes S, Ribeiro A, de Faria JP, Lourenço T, dos Santos F, Andrade PZ, Cardoso CMP, Vieira M, Paiva A, da Silva CL, Cabral JMS, Relvas JB, Grãos M. Differentiation of Human Umbilical Cord Matrix Mesenchymal Stem Cells into Neural-Like Progenitor Cells and Maturation into an Oligodendroglial-Like Lineage. PLoS ONE 2014;9:e111059.

126. Lifeng, Chi. Nanotechnology: Nanostructured Surfaces. 1st edition. Wiley-VCH;

127. Zheng P, McCarthy TJ. Rediscovering Silicones: Molecularly Smooth, Low Surface Energy, Unfilled, UV/Vis-Transparent, Extremely Cross-Linked, Thermally Stable, Hard, Elastic PDMS. Langmuir 2010;26:18585–90.

128. Bodas D, Khan-Malek C. Hydrophilization and hydrophobic recovery of PDMS by oxygen plasma and chemical treatment—An SEM investigation. Sens. Actuators B Chem. 2007;123:368–73.

129. Payne JW. Polymerization of proteins with glutaraldehyde. Soluble molecular-weight markers. Biochem. J. 1973;135:867–873.

130. Canfarotta F, Poma A, Guerreiro A, Piletsky S. Solid-phase synthesis of molecularly imprinted nanoparticles. Nat. Protoc. 2016;11:443–55.

131. Buxboim A, Ivanovska IL, Discher DE. Matrix elasticity, cytoskeletal forces and physics of the nucleus: how deeply do cells "feel" outside and in? J. Cell Sci. 2010;123:297–308.

132. StemPro® Chondrogenesis Differentiation Kit - A10071-01 [Internet]. [cited 2017 May 29];Available from: https://tools.thermofisher.com/content/sfs/manuals/stempro_chondro_diff_man.pdf

133. Zhao Y-H, Lv X, Liu Y-L, Zhao Y, Li Q, Chen Y-J, Zhang M. Hydrostatic pressure promotes the proliferation and osteogenic/chondrogenic differentiation of mesenchymal stem cells: The roles of RhoA and Rac1. Stem Cell Res. 2015;14:283–96.

134. Maturavongsadit P, Luckanagul JA, Metavarayuth K, Zhao X, Chen L, Lin Y, Wang Q. Promotion of In Vitro Chondrogenesis of Mesenchymal Stem Cells Using In Situ Hyaluronic Hydrogel Functionalized with Rod-Like Viral Nanoparticles. Biomacromolecules 2016;17:1930–8.

135. Pauli C, Grogan SP, Patil S, Otsuki S, Hasegawa A, Koziol J, Lotz MK, D'Lima DD. Macroscopic and histopathologic analysis of human knee menisci in aging and osteoarthritis. Osteoarthritis Cartilage 2011;19:1132–41.

136. Yui N, Yoshioka H, Fujiya H, Musha H, Beppu M, Karasawa R, Yudoh K. The DNA Repair Enzyme Apurinic/Apyrimidinic Endonuclease (Apex Nuclease) 2 Has the Potential to Protect against Down-Regulation of Chondrocyte Activity in Osteoarthritis. Int. J. Mol. Sci. 2014;15:14921–34.

137. Schmitz N, Laverty S, Kraus VB, Aigner T. Basic methods in histopathology of joint tissues. Osteoarthritis Cartilage 2010;18:S113–6.

138. Yang C, Tibbitt MW, Basta L, Anseth KS. Mechanical memory and dosing influence stem cell fate. Nat. Mater. 2014;13:645–52.

139. Lin Y-C, Tambe DT, Park CY, Wasserman MR, Trepat X, Krishnan R, Lenormand G, Fredberg JJ, Butler JP. Mechanosensing of substrate thickness. Phys. Rev. E 2010;82:041918.

140. Vichare S, Sen S, Inamdar MM. Cellular mechanoadaptation to substrate mechanical properties: contributions of substrate stiffness and thickness to cell stiffness measurements using AFM. Soft Matter 2014;10:1174.

141. Lozoya OA, Gilchrist CL, Guilak F. Universally Conserved Relationships between Nuclear Shape and Cytoplasmic Mechanical Properties in Human Stem Cells. Sci. Rep. 2016;6:23047.

142. Chaudhuri O, Gu L, Darnell M, Klumpers D, Bencherif SA, Weaver JC, Huebsch N, Mooney DJ. Substrate stress relaxation regulates cell spreading. Nat. Commun. 2015;6:6365.

143. Pardini LC, Manhani LGB. Influence of the testing gage length on the strength, Young's modulus and Weibull modulus of carbon fibres and glass fibres. Mater. Res. 2002;5:411–420.

144. Chen L, Bonaccurso E, Deng P, Zhang H. Droplet impact on soft viscoelastic surfaces. Phys. Rev. E 2016;94:063117.

145. Wang X, Li Y, Hodgson P, Wen C. Nano-and macro-scale characterisation of the mechanical properties of bovine bone. In: Materials forum. Institute of Materials Engineering Australasia; 2007. page 156–159.

146. Comparison of three different scales techniques for the dynamic mechanical characterization of two polymers (PDMS and SU8). Eur. Phys. J. Appl. Phys. 2010;48:1–14.

147. Genchi GG, Ciofani G, Liakos I, Ricotti L, Ceseracciu L, Athanassiou A, Mazzolai B, Menciassi A, Mattoli V. Bio/non-bio interfaces: A straightforward method for obtaining long term PDMS/muscle cell biohybrid constructs. Colloids Surf. B Biointerfaces 2013;105:144–51.

148. Eddhahak A, Zidi M. Influence of viscoelastic properties of an hyaluronic acid-based hydrogel on viability of mesenchymal stem cells. Biomed. Mater. Eng. 2015;26:103–114.

149. Cameron AR, Frith JE, Cooper-White JJ. The influence of substrate creep on mesenchymal stem cell behaviour and phenotype. Biomaterials 2011;32:5979–93.

150. Driscoll TP, Cosgrove BD, Heo S-J, Shurden ZE, Mauck RL. Cytoskeletal to Nuclear Strain Transfer Regulates YAP Signaling in Mesenchymal Stem Cells. Biophys. J. 2015;108:2783–93.

151. Kubosch EJ, Heidt E, Bernstein A, Bottiger K, Schmal H. The trans-well coculture of human synovial mesenchymal stem cells with chondrocytes leads to self-organization, chondrogenic differentiation, and secretion of TGFbeta. Stem Cell Res. Ther. 2016;7:64.

152. Tekari A, Luginbuehl R, Hofstetter W, Egli RJ. Transforming growth factor beta signaling is essential for the autonomous formation of cartilage-like tissue by expanded chondrocytes. PLoS One 2015;10:e0120857.

153. Kang JS, Alliston T, Delston R, Derynck R. Repression of Runx2 function by TGF-β through recruitment of class II histone deacetylases by Smad3. EMBO J. 2005;24:2543–2555.

154. Zhou G, Zheng Q, Engin F, Munivez E, Chen Y, Sebald E, Krakow D, Lee B. Dominance of SOX9 function over RUNX2 during skeletogenesis. Proc. Natl. Acad. Sci. 2006;103:19004–19009.

155. Eames BF, Sharpe PT, Helms JA. Hierarchy revealed in the specification of three skeletal fates by Sox9 and Runx2. Dev. Biol. 2004;274:188–200.

156. Sugimoto W, Itoh K, Mitsui Y, Ebata T, Fujita H, Hirata H, Kawauchi K. Substrate rigidity-dependent positive feedback regulation between YAP and ROCK2. Cell Adhes. Migr. 2017;00–00.

157. Varelas X. The Hippo pathway effectors TAZ and YAP in development, homeostasis and disease. Development 2014;141:1614–26.

158. Moroishi T, Park HW, Qin B, Chen Q, Meng Z, Plouffe SW, Taniguchi K, Yu F-X, Karin M, Pan D, others. A YAP/TAZ-induced feedback mechanism regulates Hippo pathway homeostasis. Genes Dev. 2015;29:1271–1284.

7.Supplementary Data

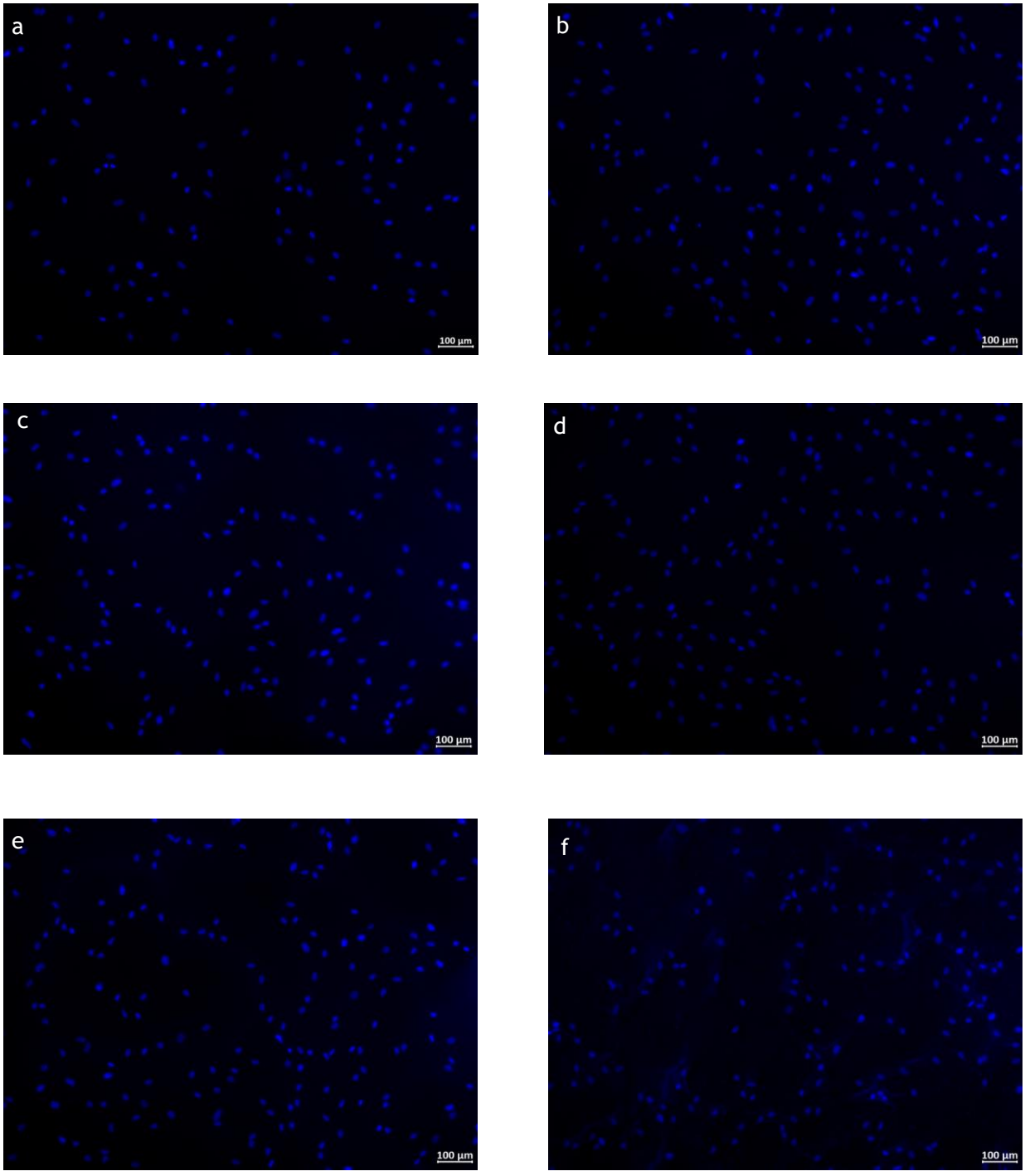

Figure S 1 - **DAPI staining of nucleus on different PDMS substrates**. Cells cultured for 24h in PM were stained with DAPI on different substrates: (a) TCPs (b) 21 kPa substrate (c) 18 kPa substrate (d) 3 kPa substrate (e) 1 kPa substrate (f) 0,931 kPa substrate. Images were collected on a fluorescence microscope.

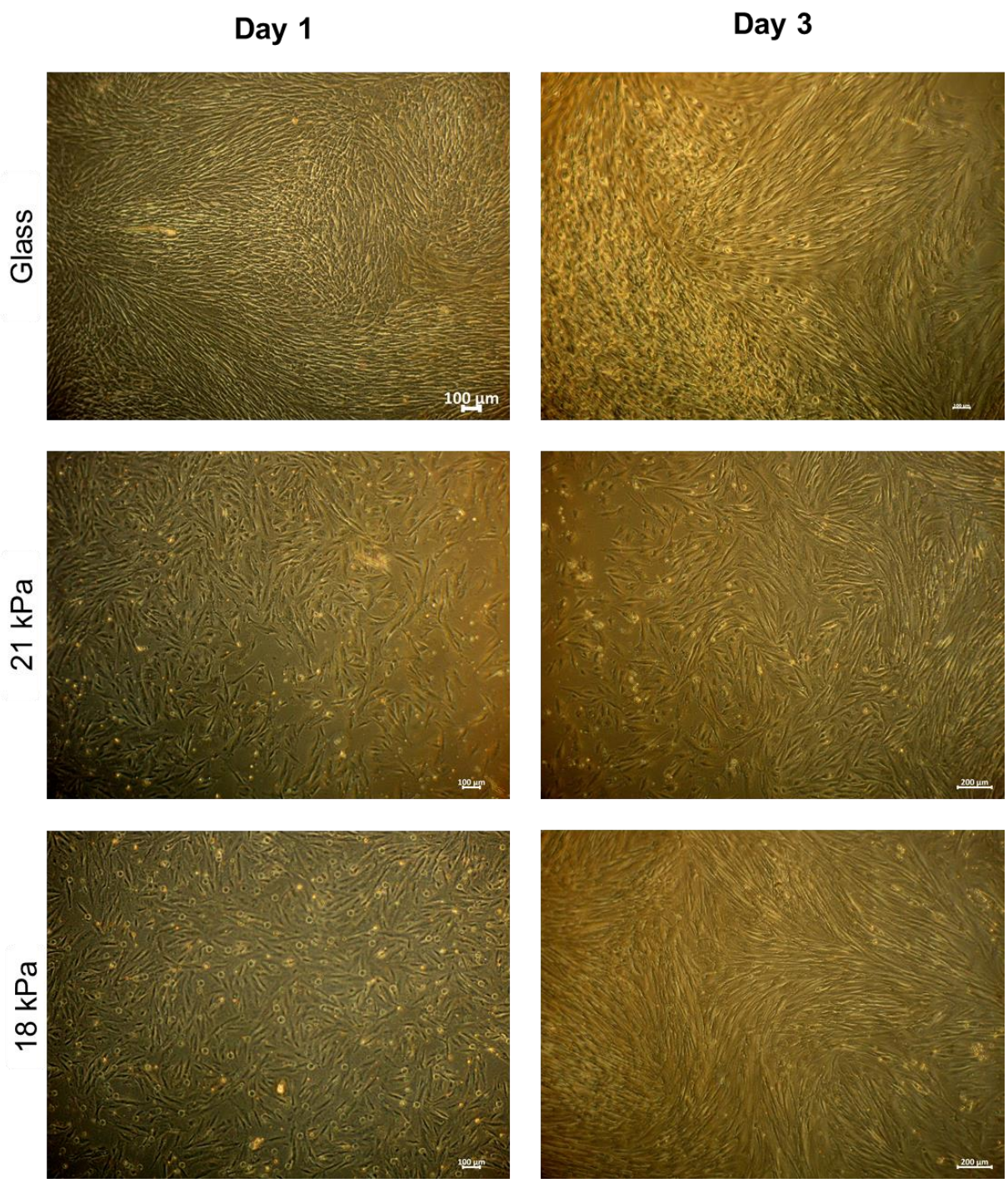

Figure S 2 - **MSCs were cultured with DM, for 1 (left) and 3 (right) days**. MSCs were cultured on different substrates: glass (top), 21 kPa substrate (center) and 18 kPa substrate (bottom). Images were collected on a contrast phase microscope.

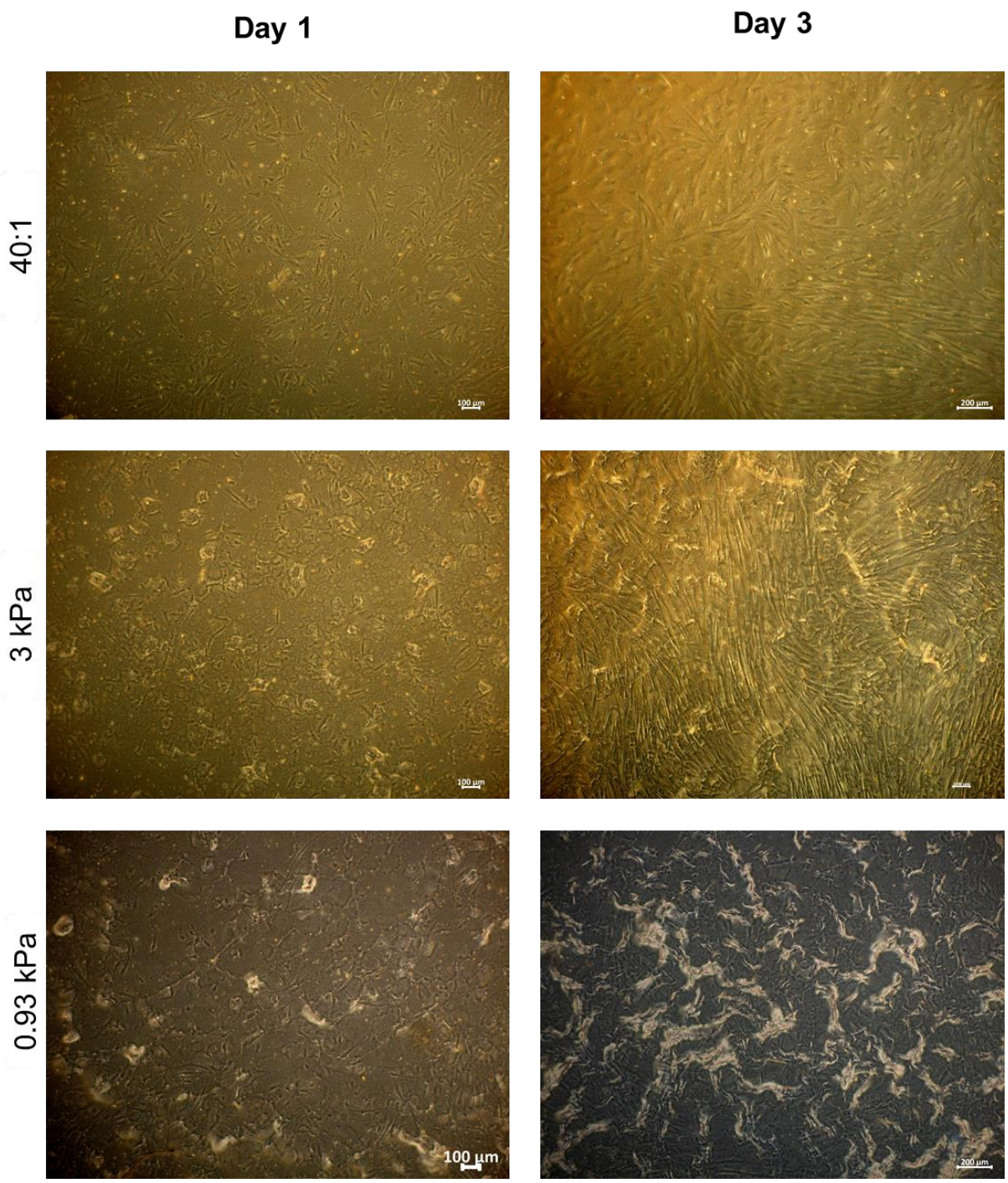

Figure S 3 - **MSCs were cultured with DM, for 1 (left) and 3 (right) days**. MSCs were cultured on different substrates: 3 kPa (top), 1 kPa substrate (center) and 0.93 kPa substrate (bottom). Images were collected on contrast phase microscopy.

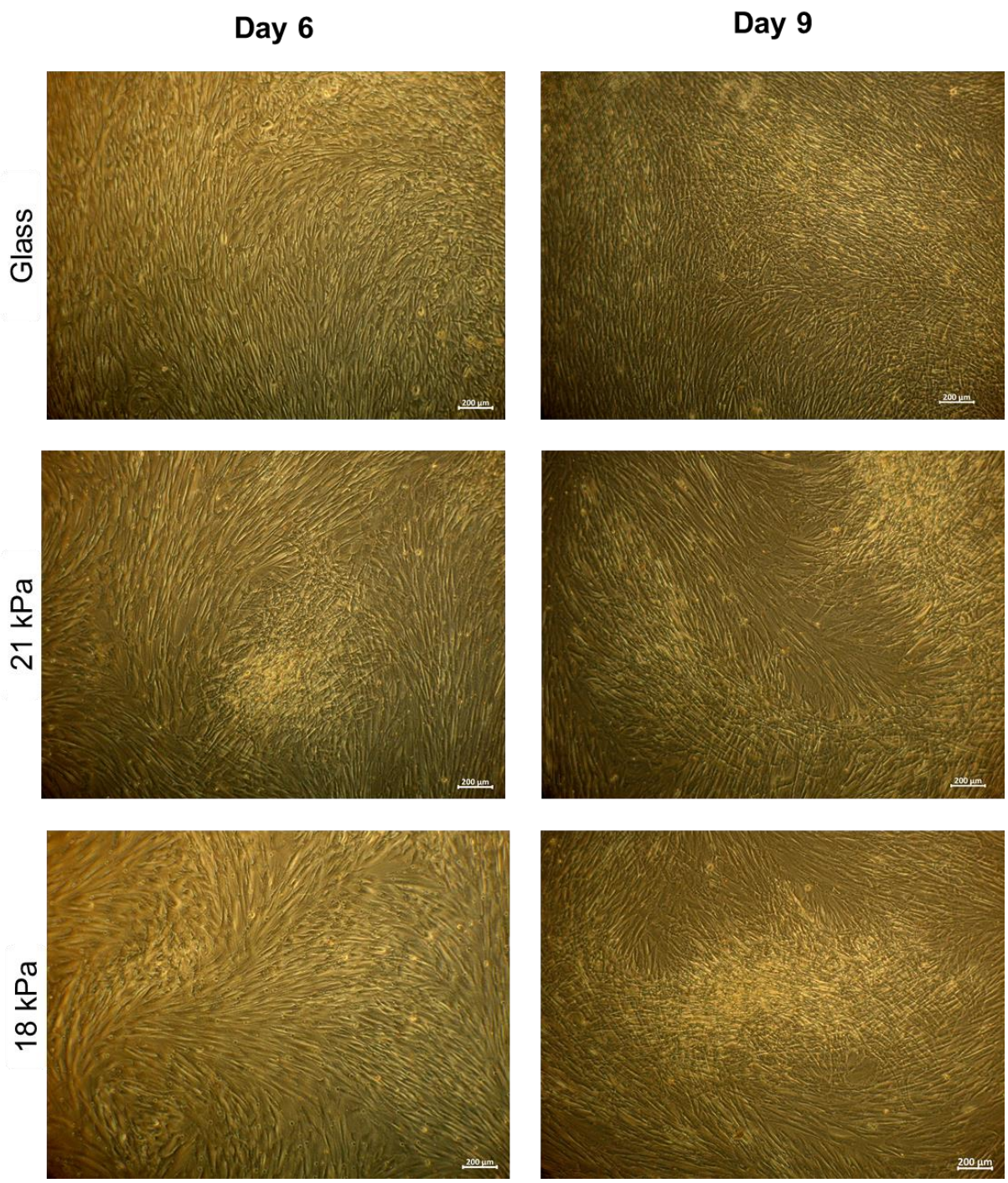

Figure S 4 - **MSCs cultured with DM, for 6 (left) and 9 (right) days.** MSCs were cultured on different substrates: glass (top), 21 kPa substrate (center) and 18 kPa substrate (bottom). Images were collected on a contrast phase microscope.

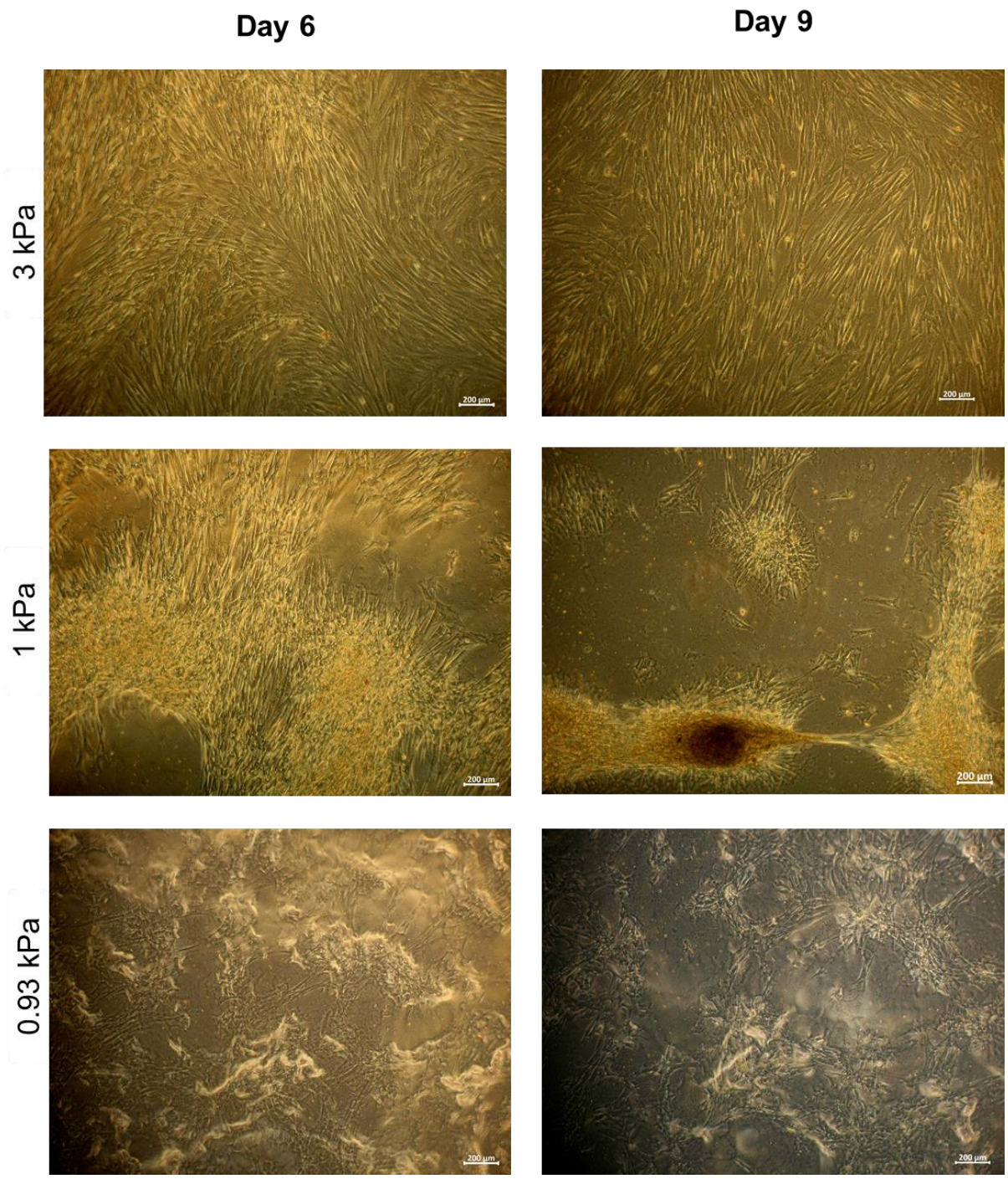

Figure S 5 **- MSCs cultured with DM, for 6 (left) and 9 (right) day**. MSCs were cultured on different substrates: 3 kPa (top), 1 kPa substrate (center) and 0.93 kPa substrate (bottom). Images were collected on a contrast phase microscope.

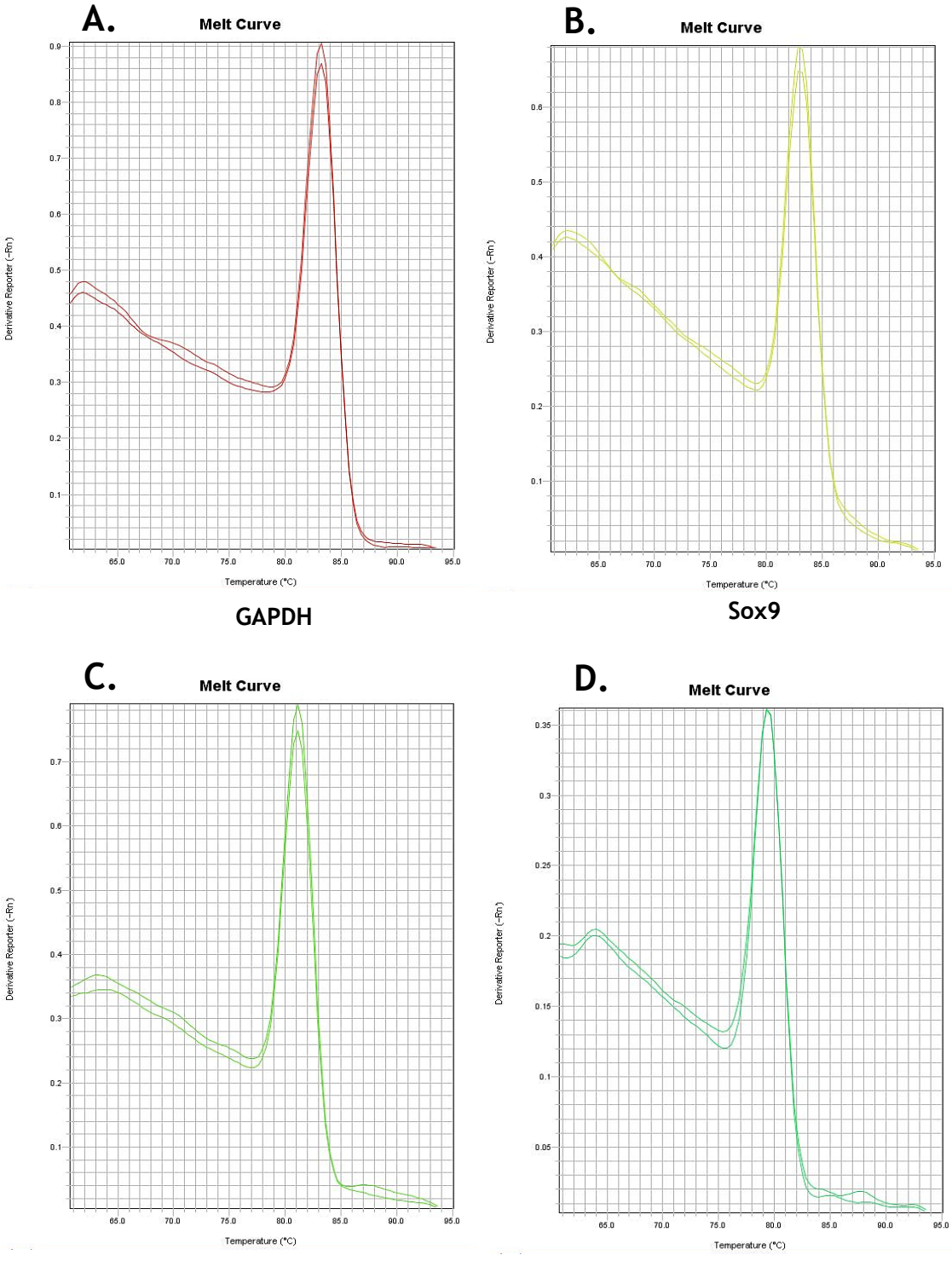

Figure S 6 – **Melting curves of chondrogenic markers obtained by RT-PCR**. GAPDH is a housekeeping gene. Sox9, ACAN and collagen type II were used as chondrogenic markers. For each gene, melting curves are overlapping, suggesting that specific products are being amplified. No primers dimers were detected since there is no amplification at lower temperatures. Concentrations of primers were optimized: **A.** F primer – 50 nM; R primer – 900 nM; **B:** F primer – 50 nM; R primer – 300 nM; **C:** F primer – 50 nM; R primer – 50 nM; **D:** F primer – 50 nM; R primer – 50 nM.

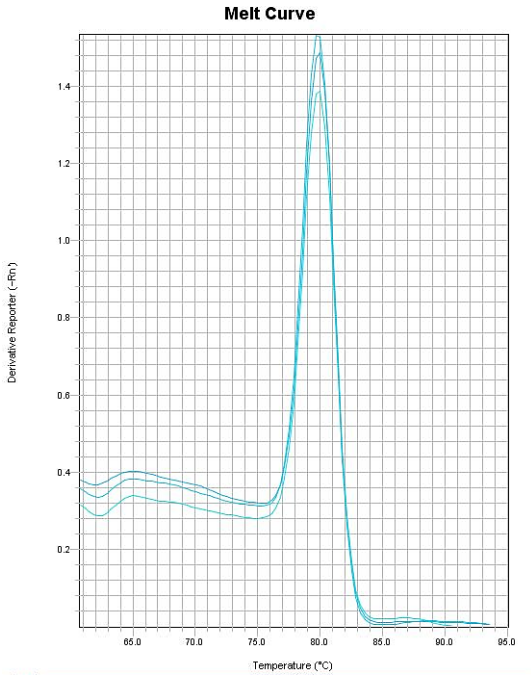

Runx2

Figure S 7 - **Melting curves of runx2 obtained by RT-PCR.** Melting curves are overlapping, suggesting that specific products are being amplified. No primers dimers were detected since there is no amplification at lower temperatures. Concentrations of primers were optimized: F primer – 300 nM; R primer – 300 nM